TU WIEN

TECHNISCHE UNIVERSITÄT WIEN

DISSERTATION

Modelling Synthesis of Lattice Gas Cellular Automata and of Random Walk and Application to Gluing of Bulk Material

Ausgeführt zum Zwecke der Erlangung des akademischen Grades einer
Doktorin der technischen Wissenschaften
unter der Leitung von

Ao.Univ.Prof. Dipl.-Ing. Dr.techn. Felix Breitenecker

E101
Institut für Analysis und Scientific Computing

und Dipl.-Ing. (FH) Dr.nat.techn. Martin Riegler als Zweitbetreuer

eingereicht an der Technischen Universität Wien
Fakultät für Mathematik und Geoinformation

von

Dipl.-Ing. Carina Rößler, BSc

00726726
Kugelgasse 5/3
3100 St. Pölten
Österreich

Wien, am 8. Dezember 2019

Kurzfassung

In dieser Doktorarbeit wurde ein mathematisches Modell zur Beschreibung der Bewegung sowie der Kollisionen von Holzspänen und Klebstofftropfen, welche im Zuge der Herstellung einer Spanplatte auftreten, erstellt. Dieser Vorgang wird Beleimung genannt und im Labormaßstab mithilfe eines Pflugscharmischers durchgeführt. Die Holzspäne befinden sich in einem Mischer und werden mit Hilfe der Mischarme bewegt, d.h., die Holzspäne unterliegen durch die Lage im Mischer einer Randbedingung. Ihre Bewegung ist lokal beschränkt (Späne liegen tendenziell am Boden des Mischers), außer sie werden vom Mischarm nach oben transportiert. Von oben wird Klebstoff mittels einer Düse in den Mischer eingesprüht, wodurch die dabei gebildeten Klebstofftropfen auf die bewegten Späne treffen. Die dabei auftretenden Typen von Kollisionen und deren zugrundeliegenden Regeln müssen definiert werden. Bei einer Kollision von Holzspan und Leimtropfen dringt ein Teil des Leimtropfens in den Span ein und der Rest des Leimtropfens bleibt an der Spanoberfläche haften. Durch Kollisionen von beleimten Holzspänen mit anderen Holzspänen wird ein Teil des Leimtropfens, der an der Spanoberfläche haftet, auf die anderen Holzspäne übertragen. Darüber hinaus muss berücksichtigt werden, dass sich die Größe des Leimtropfens aufgrund von Kollisionen mit anderen Leimtropfen und Holzspänen über die Zeit verändert.

Ziel der Arbeit war es, die Partikelbewegung, d.h. die Bewegung der Partikel im Mischer, sowie Kollisionen zwischen Leimtropfen und Holzspänen in einem mathematischen Modell zu beschreiben. Hierfür mussten geeignete Geometrien für die Leimtropfen und Holzspäne gewählt werden. Im Zuge der Modellbildung ergaben sich einige Fragestellungen: Zuerst war es notwendig die für die Modellbildung relevanten Eigenschaften und Vorgänge des realen Prozesses zu ermitteln. Außerdem musste der Detaillierungsgrad, welcher notwendig ist um die Beleimung mittels des Modells beschreiben zu können, bestimmt werden. Anschließend musste untersucht werden, welche Modellierungsmethoden für den vorliegenden Sachverhalt verwendet werden können. Hierbei war auch wichtig, wie verschiedene Detaillierungsgrade in ein bestehendes Modell miteinbezogen werden können. Um ein möglichst gutes Simulationsergebnis zu erhalten, müssen die Werte der im Modell verwendeten Eingangsparameter möglichst realistisch gewählt werden. Die hierfür verwendeten Daten und deren Qualität sind ebenfalls entscheidend für die Qualität der Simulationsergebnisse. Zur Eingrenzung der Arbeit wurden keine chemischen Reaktionen und Vorgänge auf molekularer Ebene berücksichtigt.

Zur Vereinfachung wurde in einem ersten Schritt ein zweidimensionales Modell für den Querschnitt des Pflugscharmischers orthogonal zur Längsachse erstellt. Für die Modellierung der Beleimung wurden die Modellierungsmethoden Lattice Gas Cellular Automata (LGCA) und Random Walk verwendet. Der zweidimensionale Querschnitt des Mischers wurde mit einem Kreis approximiert. Auf diesem Kreis wurde ein hexagonales Gitter, welches für den LGCA notwendig ist, definiert. Die Bewegung der Holzspäne wurde mit LGCA modelliert. Als Grundlage hierfür wurden die klassischen HPP LGCA (entwickelt von Hardy, de Pazzis und Pomeau) und FHP LGCA (entwickelt von Frisch, Hasslacher

und Pomeau) formal definiert. Die Bewegung der Leimtropfen wurde mit einem Random Walk auf dem hexagonalen Gitter modelliert. Daher war es notwendig, die Synthese der verwendeten Modellierungsmethoden zu definieren, d.h., der LGCA wurde gemeinsam mit dem Random Walk auf dem Gitter des LGCA definiert. Der LGCA besitzt in seiner Evolution systeminhärent die Detektion von Kollisionen und die Durchführung von Kollisionsregeln. Daher ist das Auftreten von Kollisionen zwischen Holzspänen bereits im Modell abgedeckt. Allerdings ist hierbei zu beachten, dass entsprechend der Gitterweite und der Spandimensionen ein Holzspan mehrere Gitterpunkte besetzen kann. Es wurden Simulationen von verschiedenen Szenarien durchgeführt um den Effekt von unterschiedlichen Modellteilen zu untersuchen. Im Rahmen einer qualitativen Validierung wurden die Ergebnisse dieser Szenarien verglichen und interpretiert.

Anschließend wurde überprüft, ob das für zwei Dimensionen entwickelte Modell auf den dreidimensionalen Fall angewandt werden kann. Für die Erstellung eines Modells in drei Dimensionen wurde die longitudinale Achse (Längsachse) ebenfalls diskretisiert. An jedem Gitterpunkt der longitudinalen Achse entsteht ein Kreis, für welchen das zweidimensionale Modell angewendet wird. Somit wurden für die Modellierung in drei Dimensionen simultan mehrere zweidimensionale Modelle ausgeführt. Die Holzspäne können durch die Bewegung der Mischarme von einem zweidimensionalen Modell in ein benachbartes transportiert werden. Dieser Transport von einem zweidimensionalen Modell in ein anderes wurde als zusätzlicher Schritt im Modell implementiert. Die Leimtropfen können sich entsprechend ihrer Position ebenfalls von einem zweidimensionalen Modell in ein benachbartes bewegen.

Im Zuge dieser Arbeit wurde ein mathematisches Modell erstellt und die Anwendbarkeit auf den präsentierten Anwendungsfall gezeigt. Eine ausführliche Validierung des Modells wurde nicht durchgeführt und ist Teil von weiterführenden Arbeiten.

Abstract

In this thesis, a mathematical model for the description of the movement as well as the collisions of wood particles and adhesive droplets occurring during particleboard production has been developed. This process is called gluing. For gluing in laboratory scale a resinating mixer is used. The wood particles are located in a mixer and moved by the mixing arms. Due to the location within the mixer, the wood particles are subject to a boundary condition. Their movement is locally limited (the wood particles tend to lie at the bottom of the mixer), except when they are transported upwards by the mixing arms. The adhesive is sprayed into the mixer by a nozzle from the top of the mixer. Thus, the adhesive droplets hit the moving wood particles. The different types of collision and their underlying collision rules have to be defined. When a collision of a wood particle and an adhesive droplet occurs, a part of the adhesive droplet penetrates into the wood particle, and the rest of the adhesive droplet sticks to the surface of the wood particle. By collision of glued wood particles with other wood particles, a part of the adhesive droplet that sticks to the wood surface is transferred to the other wood particle. In addition, it should be taken into account that the sizes of the adhesive droplets change over time due to collisions of one adhesive droplet with another one or collisions of an adhesive droplet with a wood particle.

The goal of the thesis was to describe the movement of the wood particles and adhesive droplets as well as the collisions between adhesive droplets and wood particles using a mathematical model. Therefore, suitable geometries for the adhesive droplets and wood particles had to be selected. Within the framework of modelling, some questions arose: First, for modelling it was necessary to determine the relevant properties and characteristics of the real process. Further, for describing the gluing process the necessary level of detail had to be determined. Subsequently, an investigation regarding the suitable modelling methods for the present case was carried out. Therefore, it was of importance how different levels of detail can be included in an existing model. In order to obtain good simulation results, the values of the input parameters used in the model have to be determined as accurately and realistically as possible. The used data and their quality are also crucial for the quality of the simulation results. In order to limit the scope of this thesis, no chemical reactions and processes at molecular level were considered.

To simplify the modelling, a two-dimensional model for the cross section of the resinating mixer that is orthogonal to the longitudinal axis has been developed in the first step. For modelling of the gluing process, the mathematical modelling methods lattice gas cellular automata (LGCA) and random walk were used. The two-dimensional cross section of the mixer was approximated by a circle. For the LGCA it is necessary to create a grid. Thus, a hexagonal grid on the circle was defined. The movement of the wood particles was modelled by using LGCA. In this context, there was the need for a formal definition of the classical HPP LGCA (developed by Hardy, de Pazzis and Pomeau) and FHP LGCA (developed by Frisch, Hasslacher and Pomeau). The movement of the adhesive droplets was modelled with a random walk on the hexagonal grid of the LGCA. Therefore, it

was necessary to define the synthesis of the used modelling methods, i.e. the LGCA together with the random walk on the grid of the LGCA. Due to the definition of the LGCA, the detection of collisions and the implementation of collision rules are included in the evolution of the LGCA. Therefore, the collision of wood particles is contained within the LGCA. However, due to the grid width and the dimensions of the wood particles, it is possible that a wood particle occupies several grid points. Simulations of different scenarios were carried out for the investigation of the effects of different parts of the model. The results of the different scenarios were compared and interpreted in the course of a qualitative validation.

Afterwards, a proof of concept for assuring that the model developed for two dimensions can be applied to three dimensions was carried out. For developing the model in three dimensions, the longitudinal axis was also discretised. At each grid point of the longitudinal axis is a circle where the two-dimensional model is applied. Thus, for modelling in three dimensions, several two-dimensional models were executed simultaneously. The wood particles can be transported from one two-dimensional model to a neighbouring one by the mixing arms. Transport from one two-dimensional model to another was implemented as an extra step in the model. Similarly, the adhesive droplets can move according to their position from one two-dimensional model to a neighbouring one.

In the course of this work a mathematical model was developed and it was shown that this model can be applied to the presented use case. A detailed validation of the model was not carried out and is part of future work.

Danksagung

Mein herzlicher Dank gilt

- Prof. Felix Breitenecker für die Übernahme der Betreuung und die gute Zusammenarbeit. Die zahlreichen Diskussionen und dabei entstandenen Ideen waren mir eine große Hilfe bei der Erstellung dieser Dissertation.

- Martin Riegler für die Hilfe bei der Themenfindung und der Definition der Forschungsfragen, sowie die Anmerkungen zur Arbeit und die zahlreichen Diskussionen, die zur stetigen Verbesserung meiner Arbeit beigetragen haben.

- der Kompetenzzentrum Holz GmbH, insbesondere Martin Riegler und Christian Hansmann für die Anstellung und die Möglichkeit im Zuge dieser Anstellung eine Dissertation zu schreiben.

- all meinen Kolleginnen und Kollegen der Kompetenzzentrum Holz GmbH für ihre Unterstützung. Besonderer Dank gebührt dabei meiner ehemaligen Büronachbarin Sabine Dworak und meinem aktuellen Büronachbarn Christian Pfeffer. Außerdem möchte ich mich speziell bei Sarah Ritter bedanken, die mich immer unterstützt hat und eine gute Freundin geworden ist.

- Sarah Ritter, Birger Bartuska, Hendrikus W.G. van Herwijnen, Xenia Descovich, Nina Brauner und Irene Hafner für die vielen Anmerkungen und Korrekturen.

- Arlene Jo Neukirchner für ihre Unterstützung als Native-Speakerin und die hilfreichen Korrekturen.

- Sarah Ritter, Birger Bartuska, Stefan Pinkl, Elfriede Hogger und Lukas Malzl für die Durchführung von Versuchen und Experimenten im Labor und Technikum sowie Johannes Wallisch für die Aufbereitung von Materialien.

- Elisabeth Time für die Erstellung einer Grafik.

- meiner Familie, insbesondere meinen Eltern und Schwiegereltern, für ihre Hilfe und Unterstützung.

- meinem Mann Matthias für seine Unterstützung, Geduld, die vielen Diskussionen und Anmerkungen und seine aufbauenden Worte.

Contents

vi

1

Introduction

For producing a particleboard wood particles are mixed with an adhesive and then pressed under application of pressure and high temperature. Particleboards are used e.g. in the production of furniture. The quality of the produced particleboard depends on the raw material as well as on the various processing steps. The final product has to fulfil certain minimum requirements to meet the corresponding standards. In the course of the manufacturing process, there is an interaction between raw materials, machining, and the quality of the final board. To ensure constant product qualities, raw material characteristics and process parameters need to be controlled on a knowledge-basis. On the one hand, the flexibility of using different raw materials is very limited due to availability. On the other hand, interventions within the manufacturing process in the area of machining have a great potential to purposefully control the process. During the entire manufacturing process, the different processing steps can be controlled by a wide variety of process parameters. These parameters have to be continuously adapted to guarantee high quality of the final product and to optimize the use of energy and other resources. By adapting the process parameters, it is possible to compensate fluctuations in the available raw material.

The industrial manufacturing process of particleboards consists of several consecutive sub-processes. Due to the complex and extensive manufacturing process, it was not possible to investigate the entire production process within the scope of this thesis. For selecting a process for a detailed study, the optimisation potential regarding certain criteria of the decisive sub-processes was estimated. This selection was accomplished by using a procedure similar to a value benefit analysis. Based on these results, the process of gluing was selected.

In order to study the selected process, mathematical modelling and simulation were used. Therefore, first the term "mathematical model" is explained. Dym (2004) describes a mathematical model as "a representation in mathematical terms of the behaviour of real devices and objects".
Next, the purpose and usage of mathematical modelling and simulation is described.

Cellier & Kofman (2006) state: "The whole purpose of the mathematical model is to provide the human user of the modelling and simulation environment with a means to represent knowledge about the physical system to be simulated in a way that is as convenient to him or her as possible. [...] Once the mathematical model has been formulated, the modelling and simulation environment can make use of that model to perform simulations, and produce simulation results."

Dym (2004) formulates the principles of mathematical modelling using the following questions:

- Why?
  What are we looking for? Identify the need for the model.

- Find?
  What do we want to know? List the data we are seeking.

- Given?
  What do we know? Identify the available relevant data.

- Assume?
  What can we assume? Identify the circumstances that apply.

- How?
  How should we look at this model? Identify the governing physical principles.

- Predict?
  What will our model predict? Identify the equations that will be used, the calculations that will be made, and the answers that will result.

- Valid?
  Are the predictions valid? Identify tests that can be made to validate the model, i.e., is it consistent with its principles and assumptions?

- Verified?
  Are the predictions good? Identify tests that can be made to verify the model, i.e., is it useful in terms of the initial reason it was done?

- Improve?
  Can we improve the model? Identify parameter values that are not adequately known, variables that should have been included, and/or assumptions/restrictions that could be lifted. Implement the iterative loop that we can call "model-validate-verify-improve-predict".

- Use?
  How will we exercise the model? What will we do with the model?

These questions should be used as guidance during the process of mathematical modelling and simulation. In Figure 1.1 the principles of mathematical modelling are shown in relation to the development of the mathematical model according to Dym (2004).

```
                    ┌─────────────────────┐
                    │    OBJECT/SYSTEM     │
                    └─────────────────────┘
            Why?  │ Find?
What are we looking for? │ What do we want to know?
                    ┌─────────────────────┐
                    │       MODEL          │
                    │ VARIABLES, PARAMETERS │
                    └─────────────────────┘

         Given?              How?
    What do we know?   How should we look at this model?
         Assume?          Predict?
   What can we assume?  What will our model predict?

                              Improve?
                         How can we improve the model?

                                 Valid?
                          Are the predictions valid?
     ┌──────────────────┐                          ┌──────────┐
     │ MODEL PREDICTIONS │                          │   TEST   │
     └──────────────────┘  Verified?                └──────────┘
                          Are the predictions good?

     ┌─────────────────────────────────┐
     │  VALID, ACCEPTED PREDICTIONS     │
     └─────────────────────────────────┘
          Use?
     How will we exercise the model?
```
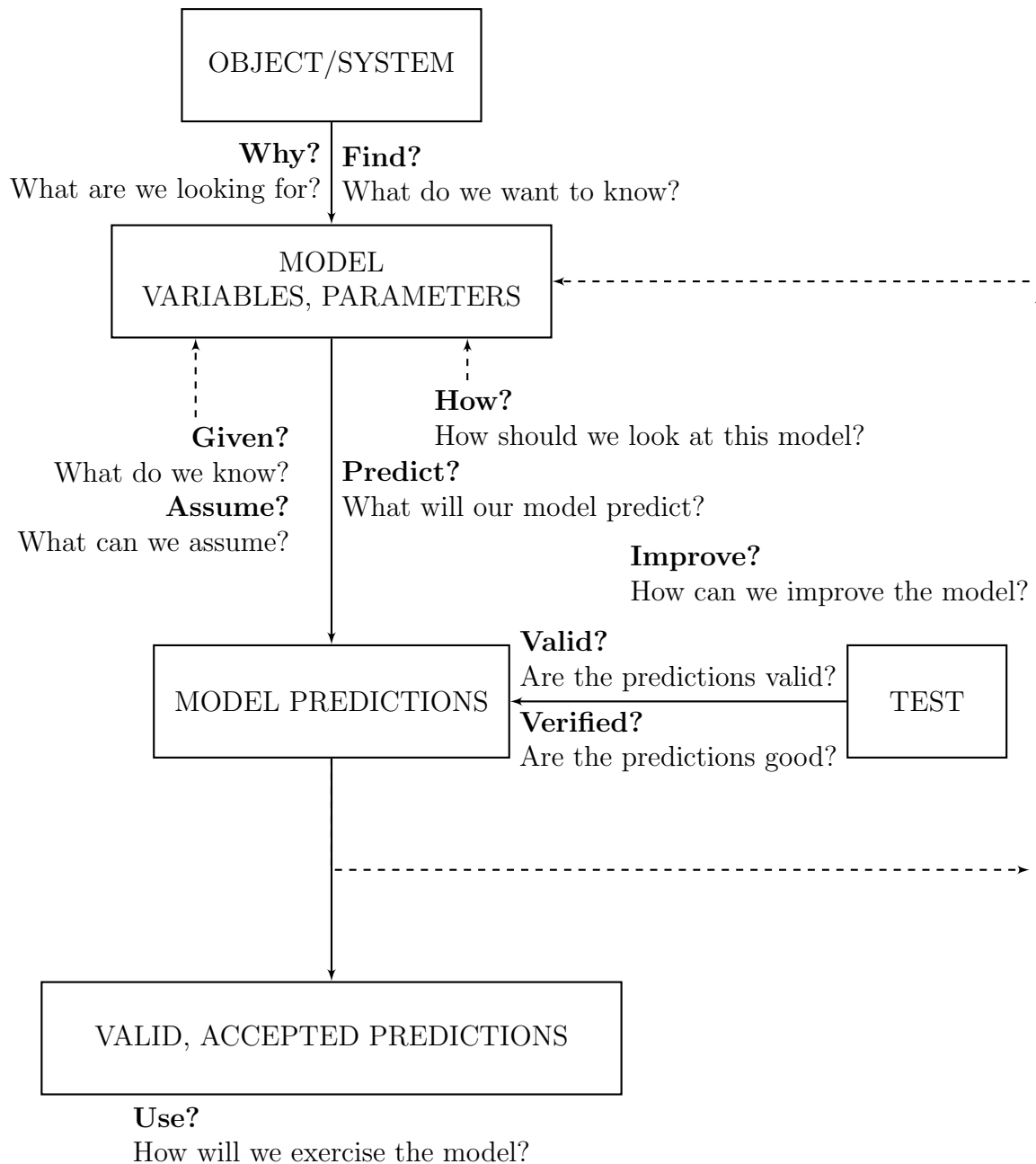
Figure 1.1: Principles and development of mathematical modelling according to Dym (2004)

In literature a wide variety of methods for mathematical modelling is available. Possible methods for modelling the gluing process are described in Chapter 4.

1.1 Motivation

Based on a value benefit analysis the gluing process of the manufacturing process of particleboards was selected for modelling. During gluing, wood particles are mixed with a synthetic adhesive. One reason for the high optimisation potential of this process is the reduction of the amount of synthetic adhesive. In 2008 approximately 35 million m^3 of particleboards were produced in Europe according to van Herwijnen et al. (2010). For this amount of particleboards approximately 2 million tons of adhesive were used, which corresponds to about 650 million € under the assumption of adhesive costs of about 320 €/t (calculation described in Chapter 3). Therefore, a reduction of the amount of adhesive has a strong impact on the production costs and the ecological footprint.

The aim of the modelling was to obtain a better understanding of the gluing process. At the end of this sub-process, there are typically no properties or characteristics that are measured. In other words, there is no characterisation method that provides real-time information about the quality of gluing. However, several topics for investigations arose:

- How do the wood particles and adhesive droplets behave during gluing?

- How is the adhesive distributed across the surface of the wood particles?

The second question is a central issue since the adhesive distribution is crucial for the bonding of the particles within the final particleboard. As these questions are hard to answer by experiments, mathematical modelling and simulation are suitable tools. Subsequently, the impact of potential measures for improvement can be predicted by simulations. The implementation of reliable measures should increase the efficiency (resources, energy, costs etc.) of the manufacturing process of particleboards.

During gluing wood particles are moving within a mixer and adhesive droplets are sprayed by a nozzle. Using certain criteria adequate modelling techniques for the gluing process were chosen. For describing the movement of the wood particles a lattice gas cellular automaton was used. The movement of the adhesive droplets was described by a random walk. Therefore, a novel modelling method "synthesis of lattice gas cellular automaton and random walk" was introduced. This novel modelling method is based on a lattice gas cellular automaton and a random walk is included within the method. Based on the description of the single modelling methods lattice gas cellular automata and random walk (Chapter 4) the new method was developed. First, two important lattice gas cellular automata were defined formally. The novelty of the formal definition of these lattice gas cellular automata was to define local and global operators for collision, neighbouring nodes and streaming. Based on these formal definitions the novel modelling method was defined. Within the new method an additional step is carried out. This step allows to include movement according to a random walk. For developing the modelling method "synthesis of lattice gas cellular automaton and random walk", a local and global operator "inclusion of random walk" was introduced.

1.2 Objective of the Thesis

The objective of this thesis was to develop a mathematical model for the movement and collisions of wood particles and adhesive droplets in the course of the gluing process. The gluing process is a sub-process of the manufacturing process of particleboards. By using the developed model a better understanding of this process should be obtained. The model was implemented using MATLAB, whereas various scenarios with different parameter sets were simulated. In the course of this thesis the following research questions arose:

- *Which aspects of the process are relevant for modelling?*
  It is necessary to understand the real process for developing a mathematical model. A model represents a simplification of the real world. In order to create a mathematical model, the essential behaviour of the real process has to be identified.

- *Which level of detail is necessary for a model of the process?*
  On the one hand the model should be as detailed as necessary, but on the other hand as simple as possible.

- *Which modelling approaches are suitable for creating a model of the process?*
  A huge amount of mathematical modelling methods are available. It is necessary to determine the methods that can be used for creating a model of the process and also the methods that are not suitable.

- *How can different levels of detail be included in the model?*
  Considering a model in a certain level of detail, it is necessary to investigate the possibility to modify the developed model towards a model with another level of detail.

- *How can the models be parametrised?*
  For obtaining a realistic simulation result it is necessary that the values of the input parameters of the model can be determined or measured in accordance with reality.

- *Which measures regarding data acquisition, data quality, and validation are necessary for applying the model?*
  In order to ensure a good quality of the simulation results, the availability and quality of the data is decisive. This is necessary for comparing the model with the real process.

The research questions are answered within the thesis and in Chapter 9 the answers of all these questions are presented.

1.3 Outline of the Thesis

First, a motivation for the investigation of the topic of this thesis is given. The motivation is followed by the objective and the research questions. Further, an outline of the thesis is presented at the end of Chapter 1.

The focus of Chapter 2 is on the production of particleboards. A short overview of the history of particleboard production is outlined. Next, the used raw materials and the manufacturing process of particleboards are described. Then a brief overview of production volumes and the significance of particleboard production for the Austrian economy is shown. Due to the extensive and complex manufacturing process of particleboards one process of the whole production was considered within the scope of this thesis. The selection of this process is described at the end of Chapter 2.

Chapter 3 describes the gluing process in detail. First, basics of bonding are summarised. Next, the interaction of wood particles and adhesive droplets is discussed. Afterwards, the resinating mixer (laboratory scale) and its functioning are presented. Furthermore, the numbers of wood particles and adhesive droplets are estimated. These estimations are used for the decision of the modelling method.

In the following Chapter 4 an overview of mathematical modelling methods that can be used for modelling the gluing process is presented. Further, the selection of the used modelling methods is explained. Lattice gas cellular automata and random walk are chosen as modelling methods. The selected modelling methods are described based on literature.

In Chapter 5 formal definitions of the selected modelling methods of Chapter 4 are given. Next, the modelling methods are modified regarding the usage for the system that will be modelled. Further, the different modelling methods have to be combined for developing the model for the gluing process.

Chapter 6 uses the theory developed in Chapter 5 for creating a mathematical model for the gluing process. For simplification, the movement of the particles was considered in two dimensions. For the movement of wood particles and adhesive droplets as modelling technique a synthesis of a lattice gas cellular automaton and a random walk was used. The lattice gas cellular automaton was used for describing the movement of the wood particles and the random walk was used for describing the movement of the adhesive droplets.

In Chapter 7 the simulation results of the model developed in Chapter 6 are presented. The model was implemented in MATLAB. Different scenarios for the parameters of the model were used for simulation. At the end of this Chapter a qualitative validation of the simulation results for the scenarios is presented.

In Chapter 8 a proof of concept for the three-dimensional case is presented. The longi-

tudinal axis was discretised and for each grid point a two-dimensional model was used. Thus, for the three-dimensional case the model of the two-dimensional case was applied.

Finally, a brief summary, answers to the research questions, a conclusion, and an outlook are given in Chapter 9.

2

Particleboard Production

In this Chapter a short introduction to the production of particleboards is provided. First, the origins and motivation of the invention of "particleboards" are outlined. Next, the manufacturing process of particleboards is described briefly. Afterwards, the economic importance of particleboard production in Austria is shown. Finally, a sub-process of particleboard production is selected for modelling and simulation. The selection procedure is described at the end of this Chapter.

2.1 History

As mentioned in Fahrni (1957), Hubbard proposed to create "artificial wood" from sawdust and blood albumin under pressure and heat in a publication in 1887. As stated in Winter & Svehla (2013), theoretical experiments with particleboards are described before 1900, but the industrial manufacturing of particleboards began in the forties of the 20th century. According to Fahrni (1957), the first plant producing particleboards was constructed in 1941 in Bremen-Hemelingen. However Jägersberg (2004) states that Max Himmelheber invented the particleboard at the beginning of the fifties of the 20th century. The idea was to create a stable, cheap and durable product from waste wood.

2.2 Manufacturing Process

According to Rowell (2012), there are three major properties that define the particleboard:

- Type of particles

- Synthetic adhesive for bonding

- High pressure and temperature during pressing

In Figure 2.1 a schematic depiction of the manufacturing process of particleboards, which consists of several sub-processes, based on Wagenführ & Scholz (2012) and Rowell (2012) is shown. The sub-processes are described in Section 2.2.2.
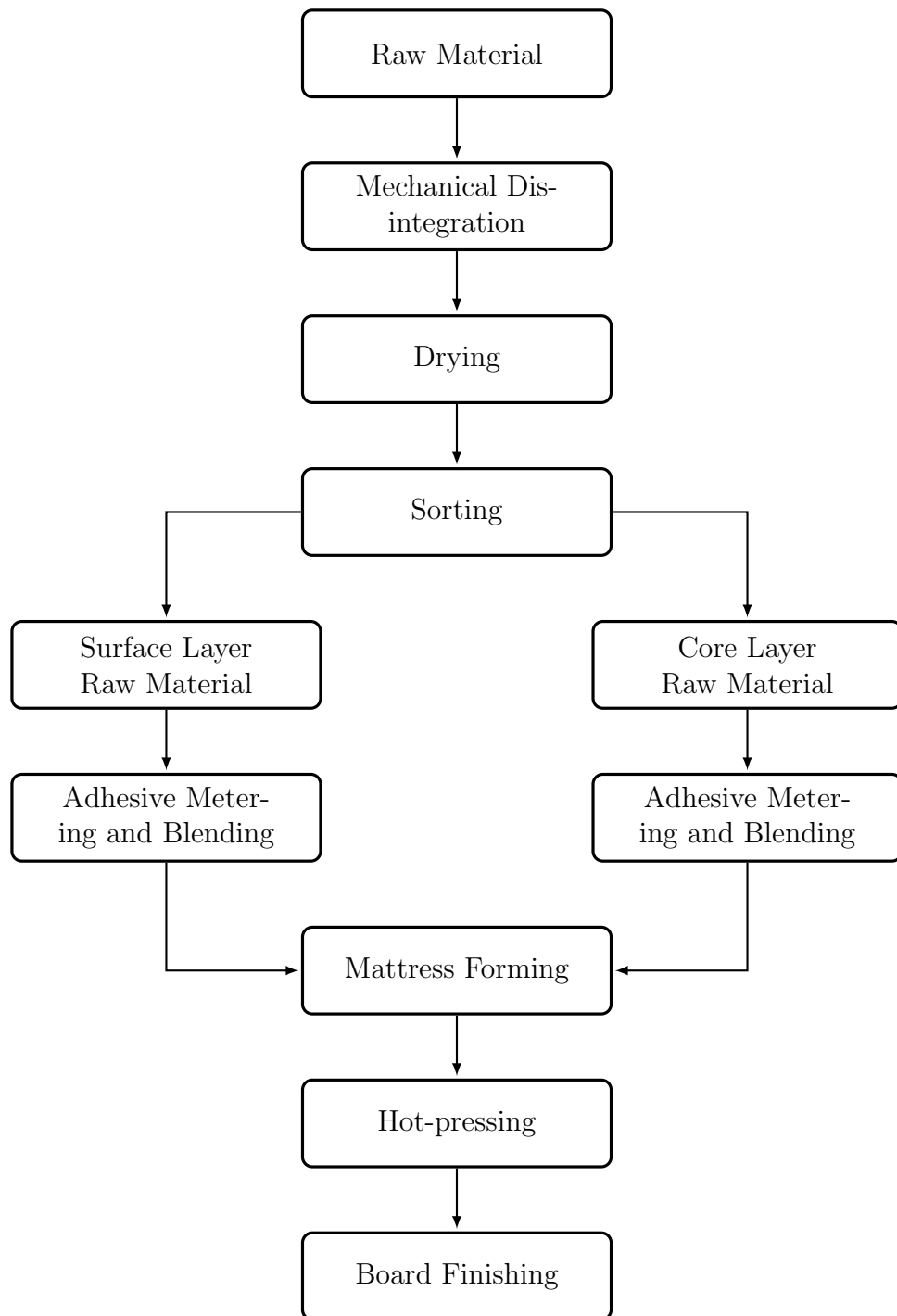
Figure 2.1: Process steps of the manufacturing process of particleboards based on Wagenführ & Scholz (2012) and Rowell (2012)

First, wood particles are produced and dried. For the surface layers and the core layer different types of particles are used, whereby the fine particles are used for the surface layers in order to obtain a high surface quality. Therefore, the dried particles have to be sorted. During adhesive metering and blending the particles are mixed with an adhesive formulation. The glued particles are formed into a mattress, which is pressed under heat and pressure.

2.2.1 Raw Material

In the following, the two main raw materials used for particleboard production, adhesive and wood, are described based on Rowell (2012), Wagenführ & Scholz (2012), Dunky & Niemz (2002), and Deppe & Ernst (2000).

Adhesive

In general, the adhesive needs to fulfil two important requirements:

- The adhesive must not cure before the hot-pressing.

- In the press the adhesive has to cure fast.

According to Rowell (2012), for particleboard production the most commonly used adhesive is urea formaldehyde (UF). In Mantanis et al. (2018) it is stated that in the European particleboard industry about 90 % of the used adhesive is UF. UF is cheap and provides good properties (white or clear bondline, good dry strength) for particleboard production. The disadvantages are that it is not weather resistant and that it releases formaldehyde. Melamine formaldehyde (MF) is also used for particleboard production. As stated in Wagenführ & Scholz (2012) MF resins are used to obtain better properties of the particleboards. MF resins are significantly more expensive than UF resins. Adding melamine to an UF adhesive yields a melamine-urea formaldehyde (MUF) adhesive. MUF adhesives have a improved moisture resistance compared to UF adhesives.

Wood

The used raw material for particleboards consists of wood (approximately 95 %) and seasonal crops (e.g. flax, bagasse, cereal straw) according to Rowell (2012). As stated in Rowell (2012), softwoods are preferred to hardwoods for particleboard production. For particleboard production the three major types of wood as raw material are described in the following according to Rowell (2012):

- Round wood:
  The advantage of using round wood is that particle size, shape, surface quality, and the usage of bark can be controlled. The disadvantage of this raw material is the cost.

- Wood residues:
  Sawmill residues (e.g. slabs, edge trimmings), residues from joinery (e.g. shavings, sawdust), and plywood mill veneer cores are used. The sawdust can be used in the surface layer for producing particleboards with a hard, smooth, dense surface.

- Recovered wood (recycled wood):
  Recovered wood (e.g. old furniture, pallets) is cheap, but it is often contaminated by stones, concrete, metals, plastics, rubber etc. Therefore, it is necessary to remove these contaminants, which means that cleaning systems have to be used.

Figure 2.2 shows the development of the raw materials used for particleboard production according to Dix & Marutzky (1997) and Deppe & Ernst (2000). The amount of round wood is decreasing, while the use of wood residues and recycled wood is increasing.
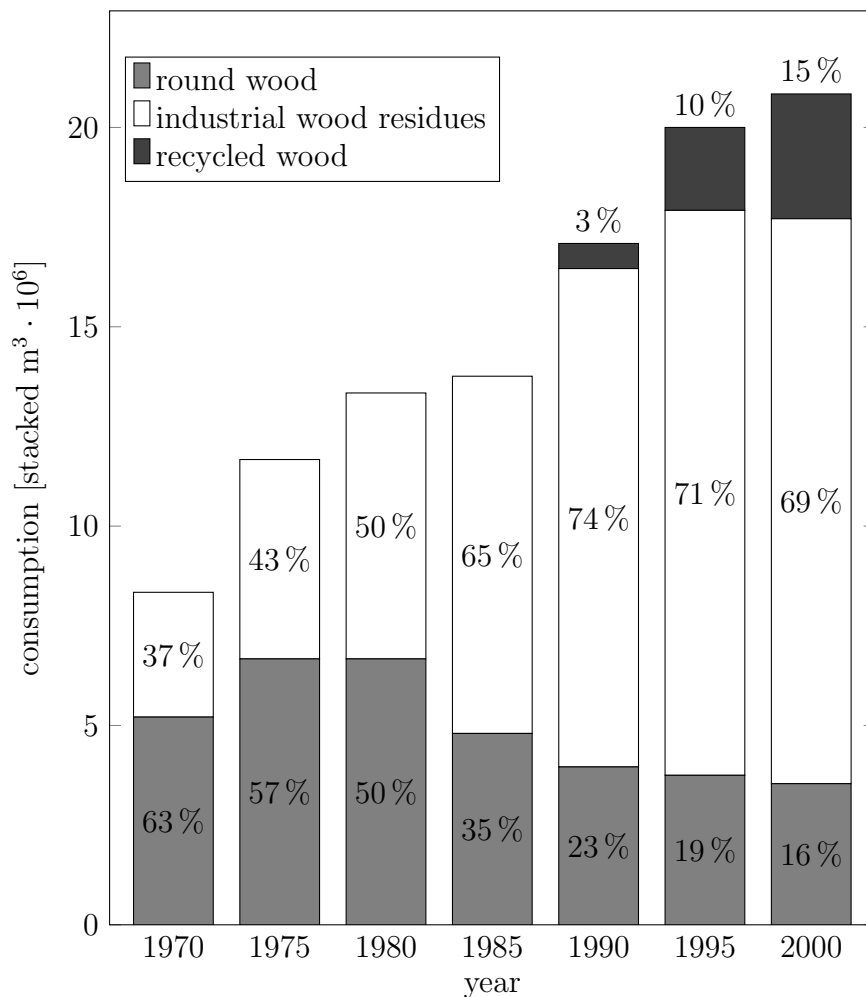

Figure 2.2: Development of the raw materials used for particleboard production in the Federal Republic of Germany according to Dix & Marutzky (1997) for 1970-1995 (1995 estimated) and Deppe & Ernst (2000) for 2000

In Table 2.1 some characteristics of particles used for particleboard production composed by Niemz in Dunky & Niemz (2002) are shown.

Table 2.1: Characteristics of wood particles (guide values) for usual particleboards composed by Niemz in Dunky & Niemz (2002)

particle type	length (L) [mm]	width (W) [mm]	thickness (T) [mm]	bulk density [kg/m^3]
surface layer				
standard particles	5 - 10	-	0.2 - 0.3	60 - 120
fine particles	3 - 6	-	0.1 - 0.25	120 - 180
core layer				
standard particles	8 - 15	1.5 - 3.5	0.25 - 0.4	40 - 140
cutting particles	8 - 15	2.0 - 4.0	0.4 - 0.6	48 - 180
impact particles	8 - 15	1.5 - 3.5	0.5 - 2.0	100 - 180
waste particles				
milling particles, wood shavings	5 - 15	2.5 - 5	0.25 - 0.8	50 - 130
gang saw particles	2 - 5	1.0 - 2	0.4 - 1	120 - 180
other particles				
sanding dust	0.4 - 0.6	-	-	160 - 200

Guide values of the raw density, pH-value, properties of produced particleboards (board density: 640 - 650 kg/m^3) and wood consumption using different wood species are given in Table 2.2 according to Kehr in Wagenführ & Scholz (2012).

Table 2.2: Guide values for properties of raw material and particleboards using different wood species according to Kehr in Wagenführ & Scholz (2012)

	poplar	spruce	pine	oak	common beech
raw density [kg/m^3]	390	430	490	650	680
pH-value	6.1 - 8.1	5.3 - 5.7	4.7 - 5.1	3.9 - 4.6	5.5 - 5.9
bending strength [N/mm^2]	27.0 - 32.0	27.0 - 30.0	29.0 - 32.0	19.0 - 23.0	18.0 - 22.0
transversal internal bond strength [N/mm^2]	0.30 - 0.60	0.55 - 0.65	0.60 - 0.75	0.50 - 0.70	0.80 - 1.10
wood consumption per m^3 of particleboard [solid m^3]	2.0 - 2.2	1.6 - 1.8	1.5 - 1.7	1.1 - 1.4	1.1 - 1.3

2.2.2 Sub-Processes

In the following the main sub-processes of the manufacturing process are described briefly based on Rowell (2012), Wagenführ & Scholz (2012), Dunky & Niemz (2002), and Deppe & Ernst (2000).

Mechanical Disintegration

For mechanical disintegration cutter block chippers (e.g. for round wood) and knife ring flakers (e.g. for chips) are used. Secondary crushing is performed using mills (e.g. hammer mills). The geometry of the particles influences the quality of the final particleboard. According to Wagenführ & Scholz (2012), particles with a high slenderness ratio lead to a high bending strength, whereas for a high transversal internal bond strength cubic particles should be used. For a high surface quality very thin particles should be used.

Drying

The goal is to achieve a specific moisture content of the wood particles of 2 - 8 % according to Rowell (2012). The desired moisture content is depending on the adhesive used. According to Kehr in Wagenführ & Scholz (2012) the reference values are stated as 1 - 8 % for the surface layers and 4 - 6 % for the core layer. As described in Rowell (2012), it is necessary to dry to low moisture contents so that during pressing there is not too much steam due to too high moisture contents. Based on a team of authors in Dunky & Niemz (2002) it is mentioned that the moisture content after drying affects the bending strength and transversal internal bond strength of the finished particleboard.

Sorting

During sorting the coarse and fine particles are removed. In literature reference values for the limits are given. Mechanical sieves and air classifiers can be used for sorting. Sorting is necessary for separation into surface and core layer particles.

Adhesive Metering and Blending (Gluing)

The adhesives used are water-based solutions, which consist of about 65 % solids for UF resins. There are specific recipes for the adhesive formulations, whereby the adhesive is mixed with water and additives (e.g. hardeners, fire retardants, preservatives) before gluing. Hardeners are used as catalyst for the adhesive curing. For the surface and core layers of the particleboard different recipes can be applied. The adhesive formulation is sprayed by nozzles onto the wood particles during blending. At the end of this sub-process the adhesive droplets should be equally distributed across the surface of the wooden particles. In the following this sub-process is called gluing.

Mattress Forming

The aim is to uniformly distribute the glued wood particles across the length and width. This is important due to the fact that the density of the board influences its properties.

The density profile across the thickness has to be symmetrical regarding the centre of the board. For obtaining similar strength in length and width of the final product, the goal of mattress forming is to randomly orientate the wooden particles.

Hot-Pressing

During hot-pressing heat and pressure are applied to the mattress for curing of the adhesive and consolidation of the mattress. There are several factors (e.g. pressing temperature, moisture content of the wood particles, closing speed) that influence the properties of the final board. In industrial scale the most commonly used systems are continuous presses. In Figure 2.3 a schematic illustration of a continuous press according to Thömen & Humphrey (2007) is shown. The mattress is moved by rolling elements in feed direction. Temperature is applied by steel belts heated by heating platens.
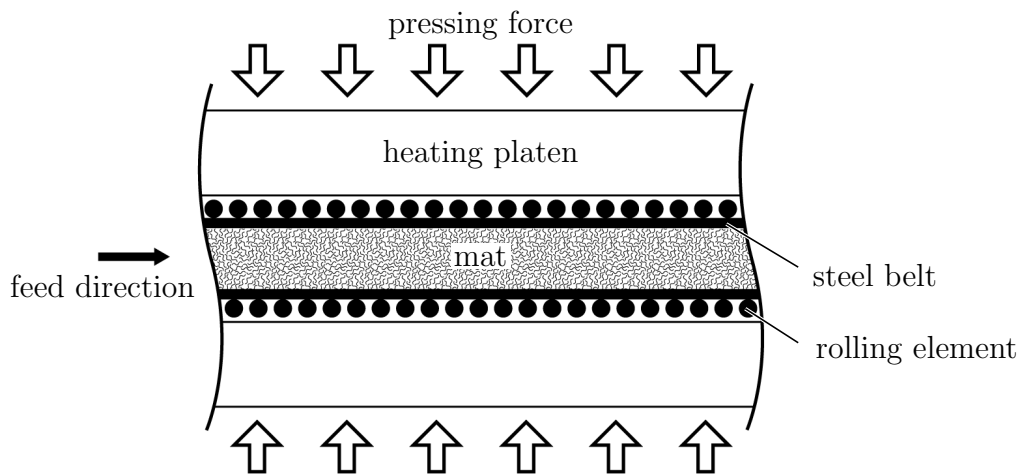
Figure 2.3: Schematic illustration of hot-pressing using a continuous press according to Thömen & Humphrey (2007)

Board Finishing

There are several processing steps for board finishing. The boards have to be cooled, conditioned, cut according to the specified dimensions, and sanded. In Figure 2.4 a part of a cross section of a three-layered particleboard is shown.

Figure 2.4: Part of a cross section of a three-layered particleboard

14

2.3 Economy

The production volume of particleboards in Europe is shown in Figure 2.5 based on Deppe & Ernst (2000) and van Herwijnen et al. (2010).
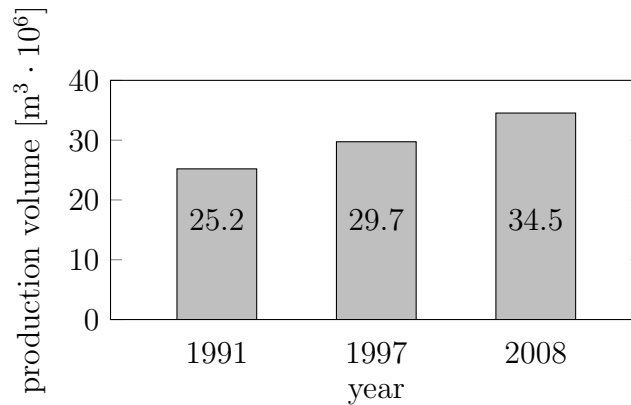

Figure 2.5: Production volume of particleboards in Europe according to Deppe & Ernst (2000) and van Herwijnen et al. (2010)

In the following, the significance of particleboard production for the Austrian economy is outlined. In Figure 2.6 the quantity of production, export, and import of particleboards for Austria is shown from 1995 to 2016 based on the Food and Agriculture Organization of the United Nations (2018). Due to the economic crisis, there is a slump in 2008 and 2009. The export quantity increased by about 85 % from 1995 to 2016.
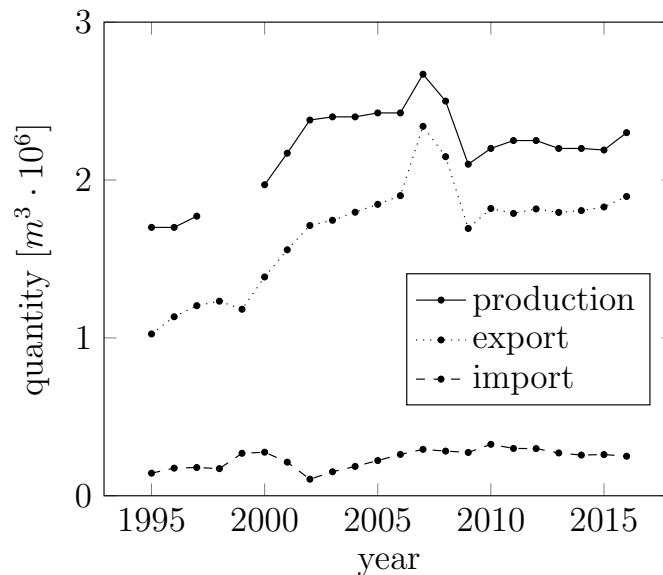
Figure 2.6: Development of particleboard production, export, and import in Austria according to the Food and Agriculture Organization of the United Nations (2018)

According to the Food and Agriculture Organization of the United Nations (2018), in Figure 2.7 the export and import value of particleboards for Austria is shown. Due to the economic crisis, there is a slump in 2009. The export value increased by about 92 % from 1995 to 2016.
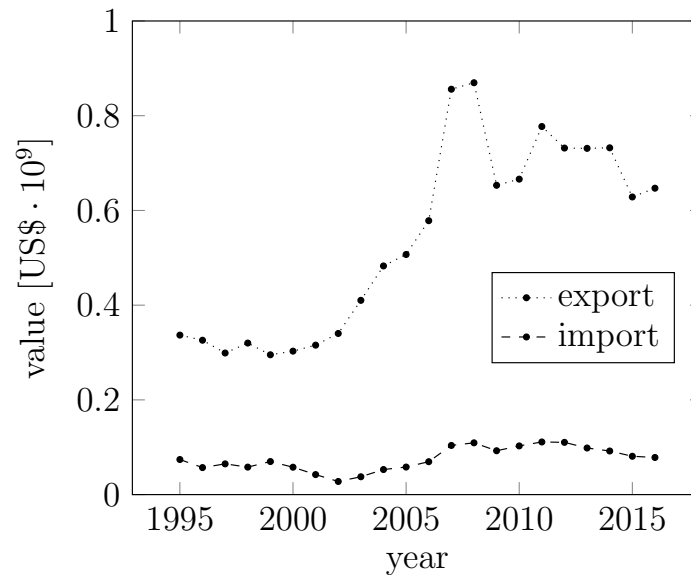

Figure 2.7: Development of the value of particleboard export and import in Austria according to the Food and Agriculture Organization of the United Nations (2018)

2.4 Selection of Sub-Process for Modelling

Modelling the entire manufacturing process of particleboards in the desired level of detail is very extensive and would have gone beyond the scope of the current thesis. Therefore, the sub-process with the highest potential for gaining new insights was identified and chosen for detailed modelling.

In order to choose a sub-process, a procedure similar to a value benefit analysis was applied. In the following, the methodology of a value benefit analysis is described shortly. According to Verein Deutscher Ingenieure (1993), different criteria for the evaluation of the proposed solutions are necessary. For each proposed solution the degree of fulfilment for each criteria is determined. The sum of all values for one solution is the utility value for this solution. The optimal solution is the one with the highest utility value. The procedure for a value benefit analysis is described based on Thormählen (1977):

- Setting up a table: In the first column the criteria are listed. Each of the other columns represents a proposed solution.

- For each criterion the utility value is determined by a subjective rating.

- The column sums are the total utility values of the proposed solutions.

- The total utility values represent a ranking of the proposed solutions.

According to the overview of the production process of particleboards in Section 2.2, the significant sub-processes have been selected. These are mechanical disintegration, drying, gluing, mattress forming, and hot-pressing. The sub-processes were used as the proposed solutions of the value benefit analysis. For selecting a sub-process, the optimization potential of these sub-processes was estimated using the following factors which represent the criteria of the value benefit analysis:

- Cost:
  If the cost of the sub-process is low, the optimization potential is low.

- Lack of knowledge:
  If the process is well understood and a lot of data are recorded, the optimization potential is low.

- Control capabilities:
  If there are no possibilities for changing process parameters, the optimization potential is low.

- Variation of end product:
  If there is little variation of the end product of the sub-process (e.g. deviation from setpoint), the optimization potential is low.

- Influence of raw material:
  If the raw material has no influence on the sub-process, the optimization potential is low.

- Complexity:
  If the sub-process is not complex, the benefit of a model and thus the optimization potential is low.

- Process operation:
  If the process operation shows low variation, the optimization potential is low.

- Applicability:
  It is advantageous if the developed model is applicable to other production processes.

For each sub-process all factors were rated from 1 (low) to 5 (high) by experts in wood technology. The optimization potential was obtained by adding up the ratings for each column. The results are shown in Table 2.3.

Table 2.3: Estimation of the optimization potential of the sub-processes

Sub-process Criteria	Mechanical disintegration	Drying	Gluing	Mattress forming	Hot-pressing
Cost	2	4	5	1	3
Lack of knowledge	3	4	4	2	1
Control capabilities	4	4	4	2	5
Variation of end product	5	2	4	3	1
Influence of raw material	5	5	2	1	3
Complexity	3	2	4	1	5
Process operation	3	3	4	2	1
Applicability	2	5	3	2	3
Optimization potential	27	29	30	14	22

The sub-process mattress forming had the lowest rating. Therefore, this process was not chosen. Due to the detailed models which already exist for the hot-pressing (e.g. Thömen (2010)), this sub-process was also not selected. The processes mechanical disintegration, drying, and gluing had similar ratings. Thus, a criterion for choosing one of these processes was necessary. For each sub-process possible research topics and resulting benefits of modelling and simulation were collected:

- Mechanical disintegration:
  For mechanical disintegration a possible research topic would be the investigation of the fracture behaviour including the dynamics during cutting.

- Drying:
  An interesting topic would be the time dependent development of moisture inside of wood particles. Another possible topic would be a model for the energy consumption for the drying process.

- Gluing:
  Possible research areas would be the movement (including collisions) of the wooden particles and the adhesive droplets during blending. Within this setting it occurs that a wood particle with adhesive on its surface collides with another wood particle and thus, a part of the adhesive is transferred to the other wood particle (transfer of adhesive). Furthermore, the distribution of the adhesive droplets on the surface of the wood particles could be investigated.

Based on the possible research topics the gluing process seemed to be the most promising for modelling. Smith (2007) states that previous research did not focus on the behaviour of strands in blenders and undertook experiments where strands were filmed during tumbling. According to the ratings in Table 2.3 and the previously mentioned circumstances, the gluing process has been selected for further studies. This process will be described in more detail in Chapter 3.

3
Gluing Process

In this Chapter the gluing process is considered in more detail. In general, gluing consists of four steps, as described in Dunky & Niemz (2002):

- Preparation of the adhesive formulation: the adhesive is mixed with water and additives.

- Amount of wood particles.

- Amount of adhesive formulation.

- Application and mixing of the wood particles and the adhesive formulation.

In 2008 the production volume of particleboards in Europe was 34.5 million m^3 according to van Herwijnen et al. (2010). The amount of adhesive used for production is 2 - 10 % of wood weight depending on the type of adhesive used as stated in Rowell (2012). Türk (2014) quotes a price of 0.32 €/kg for UF resin, while Metzger (2007) quotes a price of 0.30 - 0.32 €/kg.

To get an idea of the amount of adhesive used for this volume of production an approximation is calculated. With an assumed density of 650 kg/m^3 this volume corresponds to about 22.4 million tons of particleboards in that year. Further, assuming the amount of adhesive used is 10 % of wood weight, about 9.1 % of the amount of particleboards is adhesive. Thus, about 2 million tons of adhesive were used for particleboard production in Europe in 2008, which corresponds to about 650 million € under the assumption of adhesive costs of about 320 €/t (quoted by Türk (2014)). According to Diem et al. (2010), in 2004 in total (not only particleboard production) about 5.5 million tons of UF and MUF resins were used in Europe.

The adhesive cost account for about 15 - 25 % according to Rowell (2012). In Schöpper (2006) it is stated that the adhesive costs can account for up to 20 % of the total production costs, while Metzger (2007) states a percentage of about 27 %. Therefore, changes in the amount of adhesive used can influence the total production costs decisively.

3.1 Basics of Bonding

Based on Habenicht (1986) the strength of bonding is achieved by:

- Strength of the parts to be bonded.

- Strength of the bondline (cohesion).

- Strength of the interface layer of the wooden surface and the adhesive layer (adhesion).

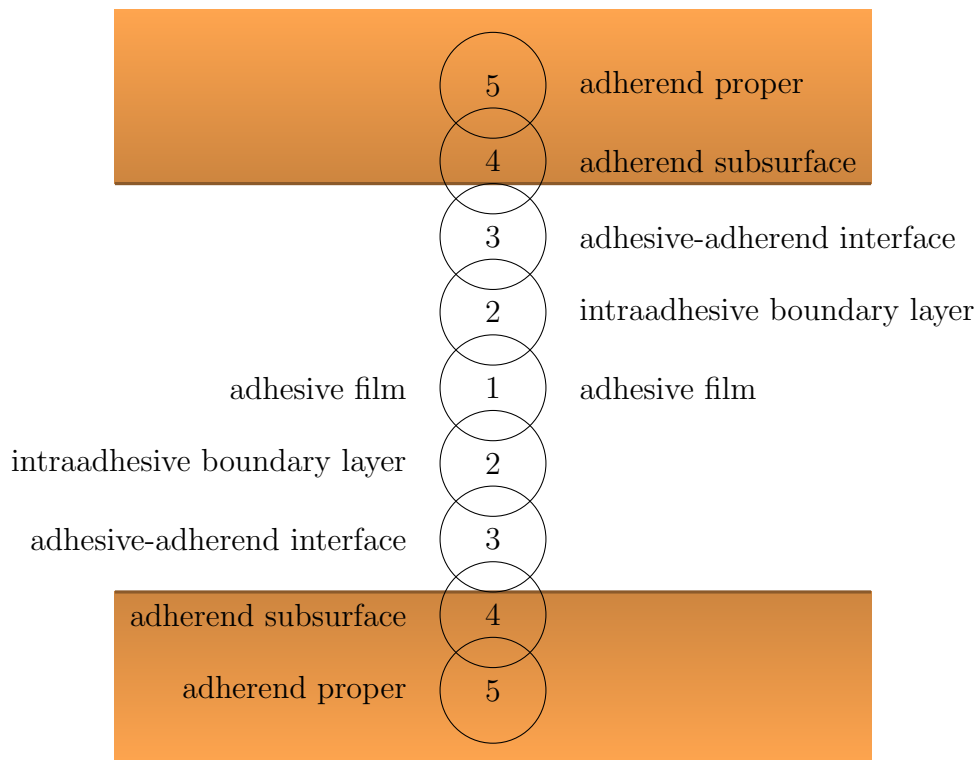In Figure 3.1 a model for the bonding of wood is represented according to Marra (1992).

Figure 3.1: Model for bonding of wood according to Marra (1992): 1 adhesive film; 2 intraadhesive boundary layer; 3 adhesive-adherend interface; 4 adherend subsurface; 5 adherend proper

3.2 Interaction of Wood Particles and Adhesive Droplets

According to Dunky & Niemz (2002), the adhesive formulation has to be uniformly applied onto the surface of the wood particles. For the application of the adhesive formulation a mixer is used. Within this mixer the adhesive formulation is sprayed onto the wood particles. The adhesive formulation on the surface of wood particles is distributed through wiping off a part of the adhesive formulation by friction with other wood particles (transfer of adhesive). The transfer of adhesive is depicted in Figure 3.2.
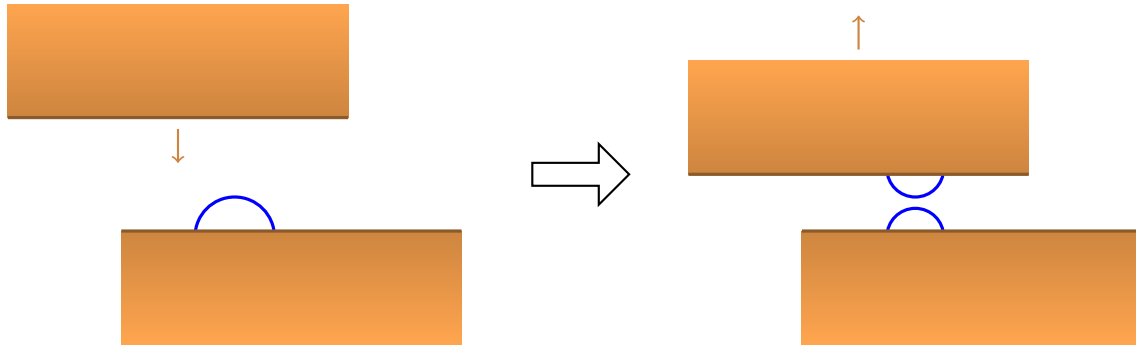
Figure 3.2: Schematic depiction of transfer of adhesive (brown: wood particle; blue: adhesive droplet)

According to Dunky & Niemz (2002), a prerequisite for bonding two wooden parts is the wettability of the wooden surface by the adhesive. Further, a good wettability is necessary to obtain high adhesive forces in the interface layer of the wooden surface and the glueline.

3.2.1 Formation of Contact Angle

The contact angle is the angle between the adhesive droplet and the wooden surface. In Figure 3.3 the contact angle θ is depicted schematically. The contact angle can be used as a measure for evaluating the wettability. Small contact angles ($\theta < 45°$) indicate a good wettability of the surface.
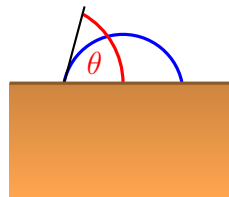
Figure 3.3: Schematic depiction of contact angle θ

The following processes play a significant role in the formation of the contact angle:

- Spreading of the adhesive formulation:
  The adhesive droplet spreads over the surface of the wood particle over time. In Figure 3.4 the spreading of the adhesive droplet is depicted schematically. $\theta = 0°$ means that the liquid is completely spreading across the surface.
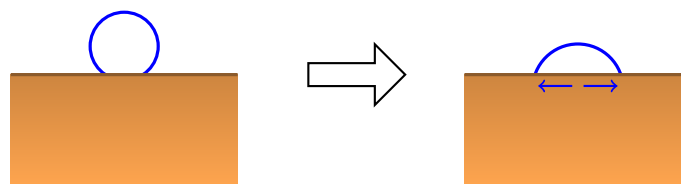
Figure 3.4: Schematic depiction of spreading of adhesive droplet

- Penetration of the adhesive formulation into the wood particle:
  The adhesive droplet penetrates into the porous wood structure over time. In Figure 3.5 the penetration of the adhesive droplet into the wood particle is depicted schematically.
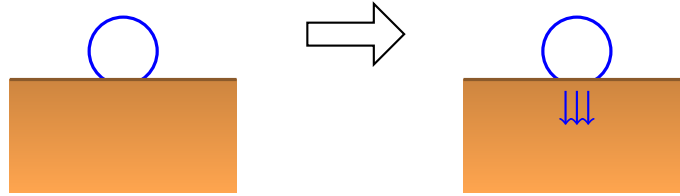

Figure 3.5: Schematic depiciton of penetration of adhesive droplet into wood particle

3.2.2 Adhesive Distribution

In Mahrdt et al. (2015) thin cross sectional specimens of particleboards (laboratory scale) have been investigated regarding the adhesive distribution. As described in this publication, the specimens were cut in very thin cross sections and stained with two dyes (a visible and a fluorescent dye). These specimens were viewed under a microscope in visible light for the wooden particles and fluorescent light for the adhesive. In Figure 3.6 an image of such a section is shown, whereby the purple areas are parts of wood particles (visible light image) and the bright areas represent the adhesive (fluorescent light image).
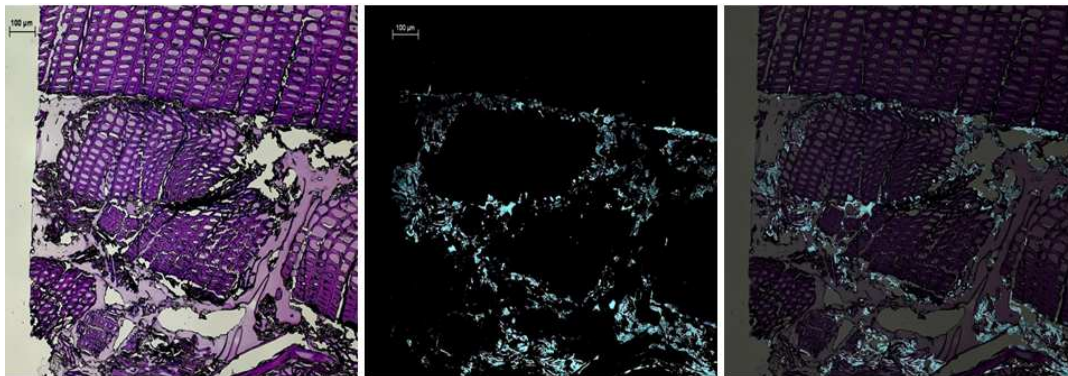
Figure 3.6: Cross sectional specimen of a particleboard: image in visible light (left), in fluorescent light (middle) and combined image (right) according to Mahrdt et al. (2015)

Mahrdt et al. (2015) considered three different types of location of the adhesive:

- Bondline:
  Adhesive that contributes to the bonding.

- Penetration:
  Adhesive that penetrates too deeply into the wood particle does not contribute to

the bonding.

- Excess:
  This category corresponds to adhesive that is not located in the bondline nor penetrated into the wood particles.

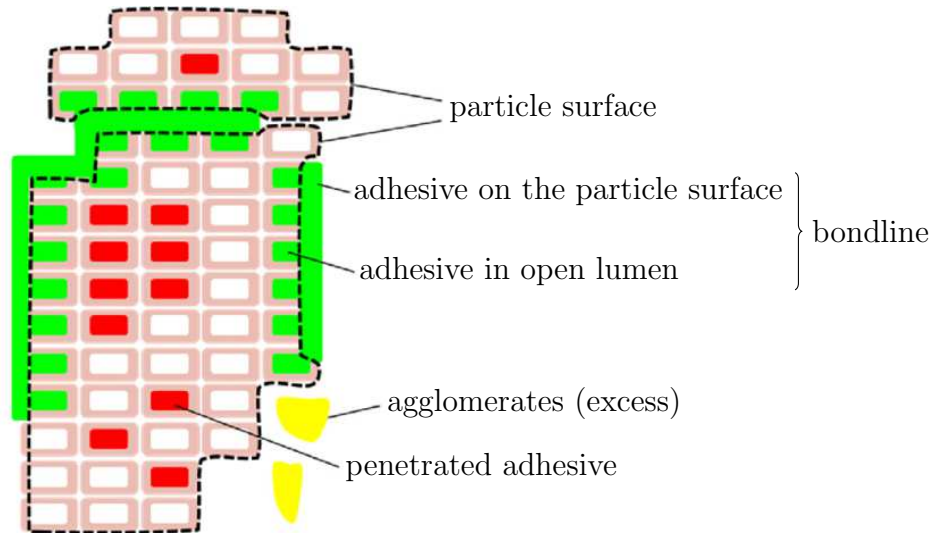According to Mahrdt et al. (2015), the different locations of the adhesive are shown in Figure 3.7.

Figure 3.7: Cross sectional model of wood particles and the different adhesive locations according to Mahrdt et al. (2015)

The bondline and the boundaries for each part of a wooden particle have to be drawn in manually on digital images. By using the information of the different images (wood particles, adhesive, boundaries) an evaluation of the adhesive distribution can be performed. The whole procedure is time-consuming and therefore only a limited number of specimens can be analysed.

3.3 Description of the Modelled System

In laboratory scale a resinating mixer is typically used for the gluing process. For setting up the framework for the mathematical model in the present thesis, a mixer from Gebrüder Lödige Maschinenbau GmbH (type: FM 50 E / 1 MZ, year of construction: 1976) was used. In the following, this mixer is described in detail. The mixing tank is of cylindrical shape. In the centre is a shaft, where the mixing arms called ploughshares are fixed. Four mixing arms of two different types are used within this mixer. The adhesive droplets are sprayed into the mixer from above with a spray gun of SATA GmbH & Co. KG (type: SATA spray master RP 2.0 mm, SATAjet 1000 B RP). Further, there is a knife head in the mixer. In Figure 3.8 the inside of this resinating mixer is shown.

Figure 3.8: Resinating mixer

First, the wood particles are put inside through the opening at the top. Thus, the wood particles are lying at the bottom of the mixer. By movement of the mixing arms the wood particles are moved within the mixer. The adhesive formulation is sprayed into the mixer while the mixing arms are moving the wood particles. Due to the mixing arms possible agglomerations of wood particles are separated, which is important for a homogeneous distribution of the adhesive on the wooden surface.

3.3.1 Description of the Resinating Mixer

For a better understanding of the resinating mixer some dimensions and pictures are listed below. The measured dimensions are only approximate measurements due to the complex geometries of the elements. Two cross sectional areas of the resinating mixer including the positions of the ploughshares and the knife head are depicted schematically in Figure 3.9.
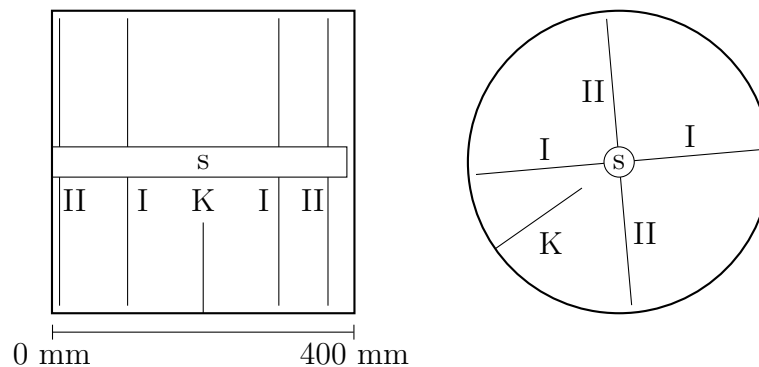
Figure 3.9: Schematic depiction of positions of shaft (s), ploughshares type I (I) and type II (II), and knife head (K)

24

Mixing Tank

The mixing tank is approximately cylindrical. In the centre is a shaft. In Table 3.1 the dimensions of the mixing tank are listed.

<div align="center">

Table 3.1: Dimensions of mixing tank

axial inner length of tank [mm]	≈ 400
inner diameter of tank [mm]	≈ 400
diameter of shaft [mm]	≈ 40

</div>

Ploughshare Type I

Within the mixing tank there are two ploughshares of type I, which are attached to the shaft. In Table 3.2 the dimensions are listed and in Figure 3.10 a ploughshare of type I is shown. The dimensions of the mixing arm given in Table 3.2 are marked red in Figure 3.10.

Table 3.2: Dimensions of mixing arm type I

position on shaft [mm]	≈ 100
position on shaft [mm]	≈ 300
base of isosceles triangle [mm]	≈ 100
legs of isosceles triangle [mm]	≈ 200
maximum height of mixing arm [mm]	≈ 70

Figure 3.10: Mixing arm type I of resinating mixer

Ploughshare Type II

Within the mixing tank there are two ploughshares of type II, which are attached to the shaft. In Table 3.3 the dimensions are listed and in Figure 3.11 a ploughshare of type II is shown. The dimensions of the mixing arm given in Table 3.3 are marked red in Figure 3.11.

Table 3.3: Dimensions of mixing arm type II

position on shaft [mm]	≈ 10
position on shaft [mm]	≈ 365
maximum length [mm]	≈ 190
maximum width [mm]	≈ 70

Figure 3.11: Mixing arm type II of resinating mixer

Knife Head

Within the mixing tank there is one knife head. The knife head can additionally be used for mixing. In Table 3.4 the dimensions of the knife head are listed.

Table 3.4: Dimensions of knife head

axial position in the mixer [mm]	≈ 200
height [mm]	≈ 140
maximum diameter [mm]	≈ 180

Figure 3.12: Knife head of resinating mixer

3.3.2 Raw Materials for Particleboard Production in Laboratory Scale

In Table 3.5 typical raw materials used for the production of a particleboard in laboratory scale (amount of applied adhesive 8 % ([g] solid adhesive to [g] absolute dry wood), target density 600 kg/m³, size 43 cm × 50 cm) are listed. The raw materials and amounts in Table 3.5 are according to the recipe for one particleboard produced in laboratory scale at Kompetenzzentrum Holz GmbH.

Table 3.5: Amount of raw materials for particleboard production in laboratory scale

raw material	amount
wood particles [kg]	≈ 1.7
adhesive (UF resin) [kg]	≈ 0.20
hardener [kg]	≈ 0.0065
additional water [kg]	≈ 0.084

3.3.3 Estimation of the Number of Wood Particles and Adhesive Droplets

In the following, the number of wood particles and adhesive droplets within the mixing tank were approximately estimated using the amount of raw materials given in Table 3.5. According to the cylindrical shape of the mixing tank (radius 20 cm, height 40 cm), the volume was calculated to be $\approx 50\,265$ cm³. First, models for a cross section of the resinating mixer that is orthogonal to the longitudinal axis were considered. Therefore, the area of this cross section was calculated as a circle (radius 20 cm) to be $\approx 1\,257$ cm². To approximately calculate the numbers of wood particles and adhesive droplets, the raw densities are necessary. The raw density of different wood species is listed in Table 2.2. According to Dunky & Niemz (2002), the density of an adhesive (UF resin), which consists of about 66 % solids, is between 1.28 and 1.30 g/cm³. As stated in Rowell (2012), the droplet size varies between 30 and 100 μm. Meinecke & Klauditz (1962)

state a range of 8 - 110 μm for the diameter of the adhesive droplets. In Lehmann (1965) diameters up to 200 μm are stated. For the calculations it was assumed that the properties of all wood particles are the same, and for all adhesive particles as well, i.e. a characteristic wood particle and a characteristic adhesive particle were used. In the following, ρ denotes the density, V the volume and M the mass.

Number of Wood Particles
The total mass of wood particles is given in Table 3.5. For calculating an approximate number of wood particles selected properties of wood particles are listed in Table 3.6.

Table 3.6: Properties of wood particles for calculation of an approximate number of wood particles

length [mm]	10
width [mm]	3
thickness [mm]	1
raw density [kg/m^3]	500

- **3D**
  The geometry of the wood particle was assumed to be a cuboid. Thus, the volume is 0.03 cm^3. Based on the mass and density of wood particles the volume of all wood particles could be calculated using the relation $M/\rho = V$ as

$$\frac{1.7}{500} = 0.0034\,\mathrm{m}^3 = 3\,400\,\mathrm{cm}^3. \tag{3.1}$$

  By using the total volume of the wood particles and the volume of one wood particle the number of wood particles could be estimated as

$$\frac{3\,400}{0.03} \approx 113 \cdot 10^3. \tag{3.2}$$

  The ratio of the total volume of wood particles to the volume of the mixing tank is 6.76 %.

- **2D**
  As explained above, an estimation of the number of wood particles in two dimensions is necessary.
  The area of a wood particle, which was assumed to be a rectangle, is according to its dimensions (length, width) 0.3 cm^2. Using the area of a cross section of the resinating mixer that is orthogonal to the longitudinal axis (1 257 cm^2) and the ratio of the volumes in three dimensions, the area that is covered by wood particles was calculated as

$$1\,257 \cdot 6.76\% \approx 85\,\mathrm{cm}^2. \tag{3.3}$$

The estimated number of wood particles in two dimensions was calculated as

$$\frac{85}{0.3} \approx 280. \tag{3.4}$$

To sum up, the number of wood particles was estimated to be about $113 \cdot 10^3$ in three dimensions and to be about 280 in two dimensions.

Number of Adhesive Droplets

The total mass of adhesive is given in Table 3.5. According to Table 3.5, a mixture of three liquids (adhesive, additional water, hardener) is used as the adhesive formulation. Due to the small amount of hardener, the hardener is not considered for the following calculations. Furthermore, the amount of water is also not considered due to the fact that it is unknown how the properties of the mixture would change compared with the two single liquids. As raw density of the adhesive 1.3 g/cm^3 was used for the calculations. The properties of the adhesive droplets of the mixture are listed in Table 3.7.

Table 3.7: Properties of adhesive droplets for calculation of an approximate number of adhesive droplets

diameter [μm]	200
raw density [g/cm^3]	≈ 1.3

- **3D**

  The geometry of the adhesive droplet was assumed to be a sphere. Thus, the volume is $\approx 4.189 \cdot 10^{-6}$ cm^3. Based on the mass and density of the adhesive the volume of all adhesive droplets could be calculated using the relation $M/\rho = V$ as

  $$\frac{200}{1.3} \approx 154 \, \text{cm}^3. \tag{3.5}$$

  By using the total volume of the adhesive droplets and the volume of one adhesive droplet the number of adhesive droplets could be estimated as

  $$\frac{154}{4.189 \cdot 10^{-6}} \approx 37 \cdot 10^6. \tag{3.6}$$

  The ratio of the total volume of adhesive droplets to the volume of the mixing tank is 0.31 %.

- **2D**

  As explained above, an estimation of the number of adhesive droplets in two dimensions was necessary.

  The area of an adhesive droplet, which was assumed to be a circle, is according to its dimension (diameter) $\approx 3.142 \cdot 10^{-4}$ cm^2. Using the area of a cross section of the resinating mixer that is orthogonal to the longitudinal axis (1 257 cm^2) and

the ratio of the volumes in three dimensions, the area that is covered by adhesive droplets was calculated as

$$1\,257 \cdot 0.31\% \approx 3.8\,\text{cm}^2. \tag{3.7}$$

The estimated number of adhesive droplets in two dimensions was calculated as

$$\frac{3.8}{3.142 \cdot 10^{-4}} \approx 12 \cdot 10^3. \tag{3.8}$$

To sum up, the number of adhesive droplets was estimated to be about $37 \cdot 10^6$ in three dimensions and to be about $12 \cdot 10^3$ in two dimensions.

<div align="right">*4*</div>

Mathematical Modelling Methods

A brief overview of possible modelling techniques for the particle movement during gluing is given below. To simplify the modelling, a two-dimensional model for the cross section of the resinating mixer that is orthogonal to the longitudinal axis was developed first. According to the assumed properties of wood particles and adhesive droplets of Chapter 3 and the amount of raw material of Table 3.5, there are about 280 wood particles and $12 \cdot 10^3$ adhesive droplets for the two-dimensional case. Among others, the high numbers of wood particles and adhesive droplets were an essential criterion for choosing adequate modelling techniques. Criteria for choosing adequate modelling techniques are:

- Can the relevant aspects of the real process be covered with the modelling technique?

- Can changes of the level of detail be included in the model?

- Can changes of parameters (e.g. adding new parameters) be included in the model?

- Is the modelling technique able to cover the numbers of wood particles and adhesive droplets?

- Is it possible to transfer the model from two dimensions to three dimensions?

Next, possible modelling techniques for the gluing process in two dimensions and their properties regarding the criteria mentioned above are presented:

- Ordinary Differential Equations (ODE)
  Ordinary differential equations are used for modelling the motion of particles, see for example Cellier & Greifeneder (1991) or Breitenecker et al. (1993). For wood particles as well as for adhesive droplets ODE systems can be used for describing the motion. The relevant aspects of the real process can be included within the ODE system, but each event (e.g. a collision) requires a stop and restart of the ODE solver. Changes of the level of detail can be included within the model, but a change can cause a change of the properties of the ODE and thus their solubility

is influenced. An inclusion of changes regarding the parameters in general can change the solubility and during simulation it requires a stop and restart of the ODE solver. A transfer from two dimensions to three dimensions is possible using the ODE system in three dimensions. Due to the number of particles, a system of ordinary differential equations for modelling the motion of the particles is not manageable.

- Discrete Element Method
  Discrete element method can be used for modelling the motion of particles (rigid bodies) of granular media under consideration of collisions between the particles, see for example Cundall & Strack (1979) or Džiugys & Peters (2001). For the adhesive droplets this method is not suitable due to the high number of droplets and their behaviour during collision. This method can theoretically be used for modelling the wood particles, but for the complex geometry of the wood particles and their high number in three dimensions this method is very complex. Changes of the level of detail and of parameters can change the underlying equations. A transfer from two dimensions to three dimensions is possible.

- Lattice Gas Cellular Automata
  In general, lattice gas cellular automata are used for simulation of fluid flows, see for example Wolf-Gladrow (2004). This method cannot be used for modelling the movement of the adhesive droplets because the behaviour during spraying cannot be modelled appropriately. As wood particles are a bulk material and their movement is caused by mixing arms their motion is similar to a fluid flow, i.e. the motion of wood particles can be described using lattice gas cellular automata. Changes of the level of detail and of parameters can be included. The number of wood particles can be covered. A transfer from two dimensions to three dimensions is possible using a three-dimensional lattice.

- Agent Based Modelling
  Agent based models consist of agents, their relationships and an environment, see for example Macal & North (2005). Agents are autonomous, independent, and have individual properties. In contrast to LGCA, no lattice is needed and the agents can have individual properties. The motion of wood particles and adhesive droplets can be modelled using this method. Changes of the level of detail and of parameters can be included. The number of wood particles and adhesive droplets can be covered, but using individual properties for each agent would result in a huge system. A transfer from two dimensions to three dimensions is possible.

- Random Walk
  For diffusion a random walk can be used to create a mathematical model, see for example Spitzer (1976). The motion of adhesive droplets can be described using random walk. For the motion of the wood particles a random walk is not useful due to the given direction of the mixing arms. Changes of the level of detail and of parameters can be included. The number of adhesive droplets can

be covered. A transfer from two dimensions to three dimensions is possible using a three-dimensional lattice.

In the following some publications regarding mathematical models for the gluing process of wood composites are summarised.

- In Meinecke & Klauditz (1962) a simple model for the gluing process was described. Within this research report a probabilistic model is described. Two areas are described in this model: the mixing area where the wood particles are mixed and a gluing area where a part of the wood particles is put and is getting glued. Using certain probabilities the wood particles selected for gluing and the wood particles selected for staying in the mixing area are chosen. This procedure is carried out for several steps.

- Dai et al. (2007) developed a mathematical model for the spatial adhesive distribution on the surface of the constituent elements of specific wood composites. The developed model is probabilistic where adhesive spots are randomly distributed on the strand surface. The experimental tests were performed with phenolformaldehyde (PF) resin and commercial aspen strands. Using image analysis the experimental adhesive distribution was evaluated.

- In Sundin (2007) the blow line of an industrial production plant for medium density fibreboards (MDF) was considered. The goal was to design a blow line injector for the adhesive such that the adhesive consumption is reduced. Within this thesis a computational fluid dynamics (CFD) simulation regarding the variation of drop size in a blow line was carried out. As a fluid water was used and the blow line was assumed to be empty, i.e. without fibres.

For modelling the movement of the wood particles and adhesive droplets different methods can be used. Within this thesis a lattice gas cellular automaton was used for modelling the movement of the wood particles and random walk was used for modelling the movement of the adhesive droplets. The lattice gas cellular automaton was chosen because it is a trade-off between totally individual and aggregated number, i.e. some individual properties can be included whereas some properties are the same for all wood particles. The choice of using random walk was made because it is a practicable and fast method for describing the real behaviour. In the following, the modelling techniques used for the mathematical model, which is presented in Chapter 6, are described.

4.1 Cellular Automata

As introduction to cellular automata an example is given. Depending on the context the abbreviation CA stands for cellular automaton or cellular automata.

Example 4.1. A one-dimensional cellular automaton is described according to Wolfram (1983) and Martin et al. (1984). This means that a row of a specific number of cells, which is shown in Figure 4.1, is observed.
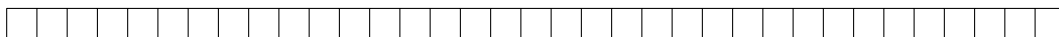

Figure 4.1: Illustration of a row of 35 cells

The cells have either the value 0 or the value 1. In Figure 4.2 a setting of the values of the cells is shown, whereby value 0 is represented by a white square and value 1 by a black square. This setting can be interpreted as starting point $t = 0$ of an evolution over time.

Figure 4.2: Illustration of the cells and their values at time $t = 0$

The value of each cell is updated by a specific rule. The used update rule is defined as

$$a_i^{(t)} = \left(a_{i-1}^{(t-1)} + a_{i+1}^{(t-1)} \right) \mod 2, \tag{4.1}$$

where $a_i^{(t)}$ denotes the value of cell i at time t. Thus, the value of each cell at time $t = 1$ can be calculated, which is shown in Figure 4.3.

Figure 4.3: Illustration at time $t = 1$

An arbitrary number of time steps of the evolution can be calculated and visualised by putting the row of the new time step below the others. In Figure 4.4 16 time steps of the evolution are shown.
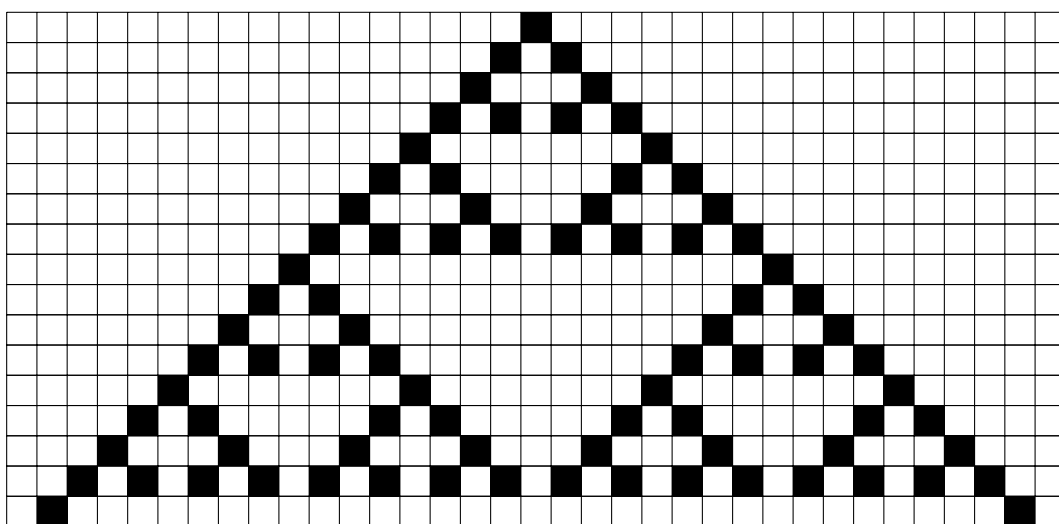
Figure 4.4: Illustration of the evolution over 16 time steps

The following definition of CA follows Kutrib et al. (1997) and Wolf-Gladrow (2004).

Definition 4.2 (Cellular automaton). The cells can be imagined as positioned at the integer points of the d-dimensional Euclidean lattice $\mathcal{L} = \mathbb{Z}^d$. The *finite set of possible states* of each cell is equal and is denoted by Q.

The state of a cell i at time step $t+1$ depends on the states of cells in a finite neighbourhood $N \subset \mathbb{Z}^d$ at time step t. The elements $n \in N$ are to be interpreted as the relative coordinates of neighbouring cells, whereby $(0, \ldots, 0)$ is the relative coordinate of cell i. A mapping $l \colon N \to Q$ is called a local configuration. It contains exactly the information to update a cell. The mode of operation of a cell is completely determined by its local rule $r \colon Q^N \to Q$.

The global state of a CA (i.e. the ensemble of the state of all cells) at a certain time is called a (global) configuration g. CA are working in discrete time. The global configuration g at time t leads to a new global configuration g' at time $t+1$, whereby all cells enter a new state synchronously according to the local rule. The associated *global rule* is a mapping $R \colon Q^{\mathcal{L}} \to Q^{\mathcal{L}}$.

4.2 Lattice Gas Cellular Automata

The update of the states of the cells for lattice gas cellular automata consists of two parts:

- Collision: During the collision step for each cell a new state of the cell is calculated.

- Streaming or propagation: During the streaming step the state of the cell streams to a specific cell in the neighbourhood.

Depending on the context the abbreviation LGCA stands for lattice gas cellular automaton or lattice gas cellular automata. In the following, the HPP LGCA (named after Hardy, de Pazzis and Pomeau) and the FHP LGCA (named after Frisch, Hasslacher and Pomeau) are presented in detail. Furthermore, in Section 4.2.3 different boundary conditions are described.

4.2.1 HPP Lattice Gas Cellular Automaton

This section is based on Hardy & Pomeau (1972), Hardy et al. (1973), Frisch et al. (1986a) and Wolf-Gladrow (2004). The HPP LGCA was proposed in 1973 and is named after Hardy, de Pazzis and Pomeau, who are the authors of HPP LGCA. It is a two-dimensional LGCA.

Lattice of HPP Lattice Gas Cellular Automaton

The lattice $\mathcal{L}$ is built by squares. At each node of the lattice four cells are located. All cells have a defined state, which can be empty or occupied by a particle (A particle is a general, not further specified object used in the context of LGCA). The maximal number

of particles at a cell is one, i.e. at a node at most four particles can be located. All particles have the same properties, e.g. the same mass (often set to one). Furthermore, the particles cannot be distinguished. The lattice vectors c_i, $i = 1, \dots, 4$, connect a node with its neighbouring nodes. The lattice vectors divided by the time step Δt are the lattice velocities. In general, the time step is set to 1. In Figure 4.5 the lattice and the lattice vectors of the HPP LGCA are shown.
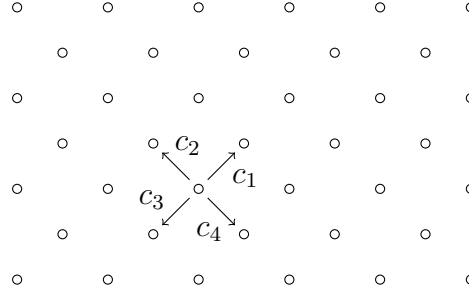
Figure 4.5: Illustration of square lattice and the lattice vectors c_i of the HPP LGCA according to Wolf-Gladrow (2004)

Let l denote the position vector of a node and let $l + c_i$, $i = 1, \dots, 4$, denote the position vectors of the four neighbouring nodes of node l. Each cell of a node has a defined state $s_i(l)$, $i = 1, \dots, 4$, whereby $s_i(l) = 1$ for occupied cells and $s_i(l) = 0$ for empty cells.

Collision of HPP Lattice Gas Cellular Automaton

The collision is a local operator. This means that only the particles located at the same node are involved. For the HPP LGCA there is only one type of collision, which is called the head-on collision. Two cells at opposite locations are occupied and the other ones are empty. After collision the previously occupied cells are empty and the other ones are occupied. In other words, the states $(1, 0, 1, 0)$ are changed to $(0, 1, 0, 1)$ and vice versa. All other settings are not changed during collision. The 2-particle head-on collision is illustrated in Figure 4.6, whereby the filled circles represent occupied cells and the unfilled circles represent empty cells.
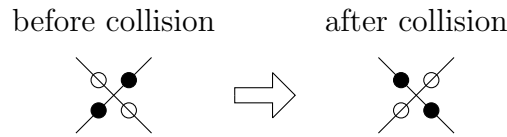
Figure 4.6: Illustration of the 2-particle head-on collision for HPP LGCA according to Wolf-Gladrow (2004)

In the following, the arguments are sometimes omitted for conciseness. The collisions can be formulated for $i = 1, \dots, 4$ (the index j of s_j is defined modulo four and between 1 and 4) by using Boolean relations

$$(s_{i+1} \wedge s_{i+3} \wedge \neg s_i \wedge \neg s_{i+2}) \vee (s_i \wedge s_{i+2} \wedge \neg s_{i+1} \wedge \neg s_{i+3}). \tag{4.2}$$

For defining the collision, the "collision function" $\Delta_i(s)$ is introduced by

$$\Delta_i(s) = s_{i+1}s_{i+3}(1 - s_i)(1 - s_{i+2}) - s_i s_{i+2}(1 - s_{i+1})(1 - s_{i+3}) \tag{4.3}$$

(the index j of s_j is defined modulo four and between 1 and 4). Thus, the collision $\mathcal{C}$ is defined by

$$\mathcal{C} \colon s_i(l) \mapsto s_i(l) + \Delta_i(s(l)). \tag{4.4}$$

Streaming of HPP Lattice Gas Cellular Automaton
During streaming the particles move simultaneously across the lattice. Each particle moves according to its corresponding lattice vector to a neighbouring node. The streaming $\mathcal{S}$ is defined by

$$\mathcal{S} \colon s_i(l) \mapsto s_i(l - c_i),\ i = 1, \ldots, 4. \tag{4.5}$$

Evolution of HPP Lattice Gas Cellular Automaton
Using $\Delta_i(s)$ the updating of the cells can be written as

$$s(t + 1, l + c_i) = s_i(t, l) + \Delta_i(l). \tag{4.6}$$

The evolution is defined by

$$\mathcal{E} := \mathcal{S} \circ \mathcal{C} \tag{4.7}$$

on $s = \{s_i(l),\ i = 1, \ldots, 4,\ l \in \mathcal{L}\}$. $\mathcal{C}$ and $\mathcal{S}$ represent the collision and the streaming, respectively. Based on this definition, the evolution is written as

$$s(t + 1, .) = \mathcal{E}s(t, .), \tag{4.8}$$

whereby the second argument stands for the lattice points.

The dynamics are invariant under all discrete transformations that conserve the square lattice (discrete translations, rotations by $\pi/2$, and mirror-symmetry) and under duality (exchange of 0 and 1).

The collision rules conserve mass and momentum locally. The streaming conserves them globally. To prove this the conservation of mass and momentum for the collision is shown in a first step. The total mass before and after collision has to be the same at each node, i.e.

$$\sum_{i=1}^{4} s_i = \sum_{i=1}^{4} (s_i + \Delta_i(s)),\ \forall s \in \{0, 1\}^4. \tag{4.9}$$

Thus, the conservation of mass for the collision is given by

$$\sum_{i=1}^{4} \Delta_i(s) = 0, \ \forall s \in \{0,1\}^4. \tag{4.10}$$

This is fulfilled because

$$
\begin{aligned}
\sum_{i=1}^{4} \Delta_i(s) &= s_2 s_4 (1 - s_1)(1 - s_3) - s_1 s_3 (1 - s_2)(1 - s_4) \\
&\quad + s_3 s_1 (1 - s_2)(1 - s_4) - s_2 s_4 (1 - s_3)(1 - s_1) \\
&\quad + s_4 s_2 (1 - s_3)(1 - s_1) - s_3 s_1 (1 - s_4)(1 - s_2) \\
&\quad + s_1 s_3 (1 - s_4)(1 - s_2) - s_4 s_2 (1 - s_1)(1 - s_3) \quad = 0.
\end{aligned}
\tag{4.11}
$$

The conservation of momentum $\dot{p} = 0$ is equal to $p_a - p_b = 0$, whereby p_a is the total momentum after collision and p_b the total momentum before collision. The total momentum before and after collision has to be equal at each node, i.e.

$$\sum_{i=1}^{4} c_i s_i = \sum_{i=1}^{4} c_i (s_i + \Delta_i(s)), \ \forall s \in \{0,1\}^4. \tag{4.12}$$

Therefore, the conservation of momentum for the collision is given by

$$\sum_{i=1}^{4} c_i \Delta_i(s) = 0, \ \forall s \in \{0,1\}^4. \tag{4.13}$$

Using $c_3 = -c_1$ and $c_4 = -c_2$ this can be shown by

$$
\begin{aligned}
\sum_{i=1}^{4} c_i \Delta_i(s) &= c_1 (s_2 s_4 (1 - s_1)(1 - s_3) - s_1 s_3 (1 - s_2)(1 - s_4)) \\
&\quad + c_2 (s_3 s_1 (1 - s_2)(1 - s_4) - s_2 s_4 (1 - s_3)(1 - s_1)) \\
&\quad - c_1 (s_4 s_2 (1 - s_3)(1 - s_1) - s_3 s_1 (1 - s_4)(1 - s_2)) \\
&\quad - c_2 (s_1 s_3 (1 - s_4)(1 - s_2) - s_4 s_2 (1 - s_1)(1 - s_3)) \quad = 0.
\end{aligned}
\tag{4.14}
$$

Thus, conservation of mass and momentum for the evolution are given by

$$\sum_{i=1}^{4} s_i(t+1, l + c_i) = \sum_{i=1}^{4} (s_i(t, l) + \Delta_i(s)) \underset{(4.10)}{=} \sum_{i=1}^{4} s_i(t, l) \tag{4.15}$$

and

$$\sum_{i=1}^{4} c_i s_i(t+1, l + c_i) = \sum_{i=1}^{4} c_i (s_i(t, l) + \Delta_i(s)) \underset{(4.13)}{=} \sum_{i=1}^{4} c_i s_i(t, l). \tag{4.16}$$

Due to the conservation of mass, the kinetic energy (each particle has a kinetic energy of $mv^2/2 = 1/2$) is also conserved.

In Figure 4.7 an example for the evolution is depicted.

before collision

after collision

after streaming
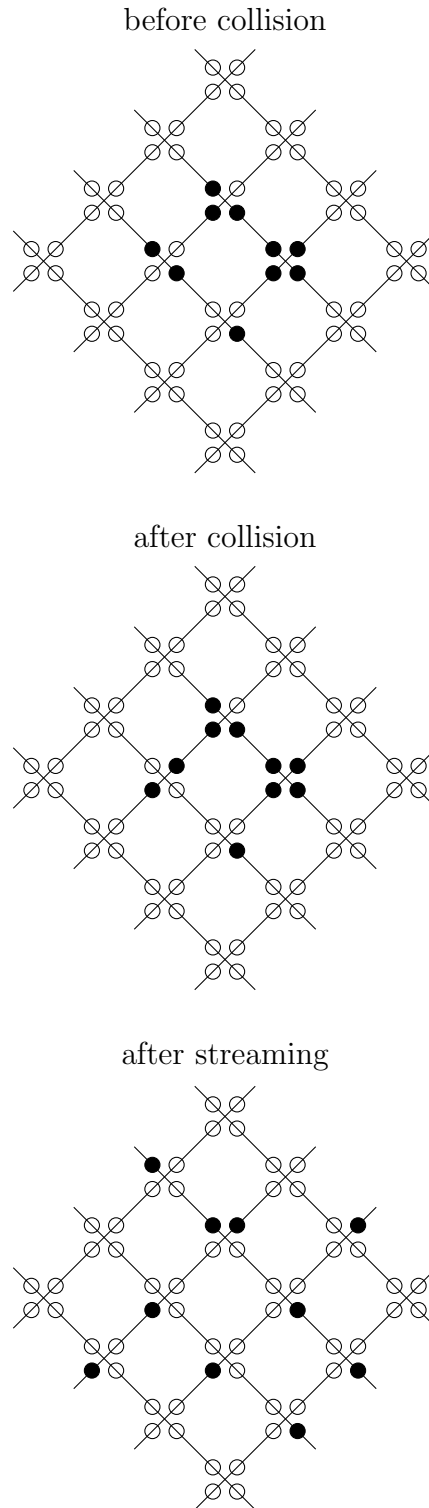
Figure 4.7: Illustration of collision and streaming of the HPP LGCA according to Wolf-Gladrow (2004)

4.2.2 FHP Lattice Gas Cellular Automaton

This section is based on Frisch et al. (1986b), Frisch et al. (1986a), Wolfram (1986), d'Humieres & Lallemand (1987), Rivet & Boon (2001) and Wolf-Gladrow (2004). The FHP LGCA was proposed in 1986 and is named after Frisch, Hasslacher and Pomeau, who are the authors of FHP LGCA. It is a two-dimensional LGCA.

Lattice of FHP Lattice Gas Cellular Automaton
The lattice $\mathcal{L}$ is built by equilateral triangles. At each node of the lattice six cells are located. All cells have a defined state, which can be empty or occupied by a particle (A particle is a general, not further specified object used in the context of LGCA). The maximal number of particles at a cell is one, i.e. at a node at most six particles can be located. All particles have the same properties, e.g. the same mass (often set to one). Furthermore, the particles cannot be distinguished. The lattice vectors c_i, $i = 1, \ldots, 6$, connect a node with its neighbouring nodes. The lattice vectors divided by the time step Δt are the lattice velocities. In general, the time step is set to 1. In Figure 4.8 the lattice and the lattice vectors of the FHP LGCA are shown.
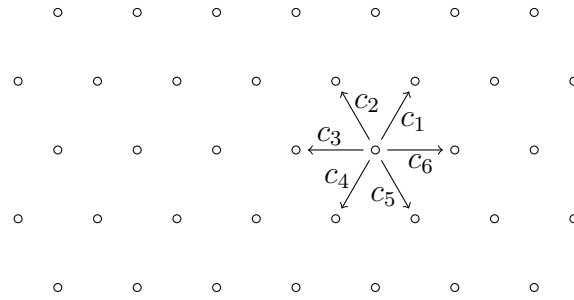
Figure 4.8: Illustration of triangular lattice and the lattice vectors c_i of the FHP LGCA according to Wolf-Gladrow (2004)

The lattice vectors are given by

$$c_i = \left(\cos\left(\frac{\pi}{3}i\right), \sin\left(\frac{\pi}{3}i\right) \right), i = 1, \ldots, 6. \tag{4.17}$$

The lattice shows hexagonal symmetry, i.e. it is invariant under rotations by $n\pi/3 \mod 2\pi$, $n \in \mathbb{N}$, about an axis through a node and orthogonal to the lattice plane.

Let l denote the position vector of a node and let $l + c_i$, $i = 1, \ldots, 6$, denote the position vectors of the six neighbouring nodes of node l. Each cell of a node has a defined state $s_i(l)$, $i = 1, \ldots, 6$, whereby $s_i(l) = 1$ for occupied cells and $s_i(l) = 0$ for empty cells.

Collision of FHP Lattice Gas Cellular Automaton
The collision is a local operator. This means that only the particles located at the same node are involved. In contrast to the HPP LGCA, there are various collision rules for the FHP LGCA and some of them are not deterministic. According to the used collision

rules and the existence of rest particles (used for FHP-II LGCA and FHP-III LGCA; defined below), there are different versions of the FHP LGCA:

Collision of FHP-I Lattice Gas Cellular Automaton:
The 2-particle head-on collision and the symmetric 3-particle collision are included in this FHP LGCA. For obtaining the full set of collision rules rotations of $\pi/3$ have to be applied.

2-particle head-on collision:
Like for the HPP LGCA, there are 2-particle head-on collisions for the FHP LGCA. The node l with $s_1(l) = s_4(l) = 1$ and $s_2(l) = s_3(l) = s_5(l) = s_6(l) = 0$ is considered. For this node there are two different final states, $s_2(l) = s_5(l) = 1$ and $s_1(l) = s_3(l) = s_4(l) = s_6(l) = 0$ (counter-clockwise rotation of particles) on the one hand and $s_3(l) = s_6(l) = 1$ and $s_1(l) = s_2(l) = s_4(l) = s_5(l) = 0$ (clockwise rotation of particles) on the other hand. These transformations conserve mass and momentum. If the same transformation is always used, the model is not invariant under mirror-symmetry. Thus, a non-deterministic rule is used for the 2-particle head-on collisions. In Figure 4.9 an example for a 2-particle head-on collision is shown.
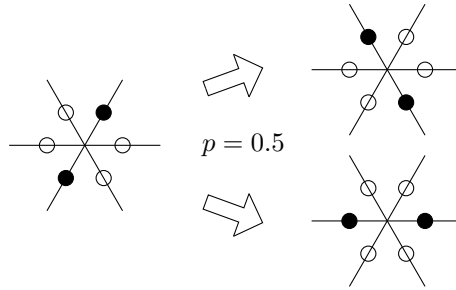
Figure 4.9: Illustration of the 2-particle head-on collision of the FHP-I LGCA according to Wolf-Gladrow (2004)

The 2-particle head-on collisions conserve the difference of the number of particles that stream in opposite directions. To prove this, let $m_i(t)$, $i = 1, \ldots, 6$, denote the total number of particles located at the cells corresponding to c_i, $i = 1, \ldots, 6$, at time step t. Further, $\Delta m_1(t) = m_1(t) - m_4(t)$, $\Delta m_2(t) = m_2(t) - m_5(t)$, and $\Delta m_3(t) = m_3(t) - m_6(t)$ are the differences of particles that stream in opposite directions. Without loss of generality one 2-particle head-on collision $s_1(l) = s_4(l) = 1$ and $s_2(l) = s_3(l) = s_5(l) = s_6(l) = 0$ to $s_2(l) = s_5(l) = 1$ and $s_1(l) = s_3(l) = s_4(l) = s_6(l) = 0$ is considered. Thus, it follows

$$
\begin{aligned}
m_1(t+1) &= m_1(t) - 1 \\
m_2(t+1) &= m_2(t) + 1 \\
m_3(t+1) &= m_3(t) \\
m_4(t+1) &= m_4(t) - 1 \\
m_5(t+1) &= m_5(t) + 1 \\
m_6(t+1) &= m_6(t).
\end{aligned}
\tag{4.18}
$$

Using these relations further calculations give

$$\Delta m_1(t+1) = m_1(t) - 1 - (m_4(t) - 1) = m_1(t) - m_4(t) = \Delta m_1(t)$$
$$\Delta m_2(t+1) = m_2(t) + 1 - (m_5(t) + 1) = m_2(t) - m_5(t) = \Delta m_2(t) \tag{4.19}$$
$$\Delta m_3(t+1) = m_3(t) - m_6(t) = \Delta m_3(t).$$

Thus, it is proven that the 2-particle head-on collisions conserve the difference of particles that stream in opposite directions. This invariant has no counterpart in reality and therefore is called spurious invariant. To prevent the occurrence of this spurious invariant the symmetric 3-particle collision is introduced.

Symmetric 3-particle collision:
The symmetric 3-particle collision is a deterministic rule. Due to this rule the spurious invariant is destroyed. This can be proven by considering one symmetric 3-particle collision at node l with $s_1(l) = s_3(l) = s_5(l) = 1$ and $s_2(l) = s_4(l) = s_6(l) = 0$. After collision the states of the cells are changed to $s_1(l) = s_3(l) = s_5(l) = 0$ and $s_2(l) = s_4(l) = s_6(l) = 1$. Thus,

$$
\begin{aligned}
m_1(t+1) &= m_1(t) - 1 \\
m_2(t+1) &= m_2(t) + 1 \\
m_3(t+1) &= m_3(t) - 1 \\
m_4(t+1) &= m_4(t) + 1 \\
m_5(t+1) &= m_5(t) - 1 \\
m_6(t+1) &= m_6(t) + 1.
\end{aligned}
\tag{4.20}
$$

Using these relations further calculations give

$$\Delta m_1(t+1) = m_1(t) - 1 - (m_4(t) + 1) = m_1(t) - m_4(t) - 2 \neq m_1(t) - m_4(t) = \Delta m_1(t)$$
$$\Delta m_2(t+1) = m_2(t) + 1 - (m_5(t) - 1) = m_2(t) - m_5(t) + 2 \neq m_2(t) - m_5(t) = \Delta m_2(t)$$
$$\Delta m_3(t+1) = m_3(t) - 1 - (m_6(t) + 1) = m_3(t) - m_6(t) - 2 \neq m_3(t) - m_6(t) = \Delta m_3(t).$$
$$\tag{4.21}$$

In Figure 4.10 the symmetric 3-particle collision is shown.
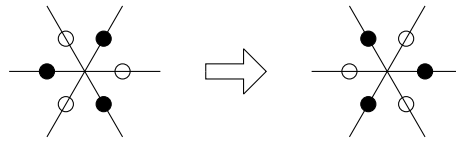
Figure 4.10: Illustration of the symmetric 3-particle collision of the FHP-I LGCA according to Wolf-Gladrow (2004)

"Collision function" of FHP-I Lattice Gas Cellular Automaton:
In the following, the arguments are sometimes omitted for conciseness. Similar to the collision rule of the HPP LGCA, the collisions can be formulated by using Boolean relations. For defining the collision rules, the "collision function" $\Delta_i(s)$ is introduced by

$$\begin{aligned}
\Delta_i(s) = {}& \xi_{t,l} s_{i+1} s_{i+4} (1 - s_i)(1 - s_{i+2})(1 - s_{i+3})(1 - s_{i+5}) \\
& + (1 - \xi_{t,l}) s_{i+2} s_{i+5} (1 - s_i)(1 - s_{i+1})(1 - s_{i+3})(1 - s_{i+4}) \\
& - s_i s_{i+3} (1 - s_{i+1})(1 - s_{i+2})(1 - s_{i+4})(1 - s_{i+5}) \\
& + s_{i+1} s_{i+3} s_{i+5} (1 - s_i)(1 - s_{i+2})(1 - s_{i+4}) \\
& - s_i s_{i+2} s_{i+4} (1 - s_{i+1})(1 - s_{i+3})(1 - s_{i+5})
\end{aligned} \tag{4.22}$$

(the index j of s_j is defined modulo six and between 1 and 6), whereby $\xi_{t,l}$ denotes a time- and site-dependent Boolean variable. $\xi_{t,l}$ is one when the particles are rotated clockwise, and zero when the particles are rotated counter-clockwise. For the two possible values equal probabilities are used, i.e.

$$\mathbb{P}(\xi_{t,l} = 0) = \frac{1}{2} = \mathbb{P}(\xi_{t,l} = 1). \tag{4.23}$$

Furthermore, independence of the $\xi_{t,l}$'s is assumed. Without loss of generality a 2-particle head-on collision with $s_3 = s_6 = 1$ and $s_1 = s_2 = s_4 = s_5 = 0$ is considered.

$$\begin{aligned}
\Delta_1(s) &= 1 - \xi_{t,l} \\
\Delta_2(s) &= \xi_{t,l} \\
\Delta_3(s) &= -1 \\
\Delta_4(s) &= 1 - \xi_{t,l} \\
\Delta_5(s) &= \xi_{t,l} \\
\Delta_6(s) &= -1.
\end{aligned} \tag{4.24}$$

Thus, for $\xi_{t,l} = 1$ the clockwise rotation

$$\begin{aligned}
\Delta_1(s) &= 0 \\
\Delta_2(s) &= 1 \\
\Delta_3(s) &= -1 \\
\Delta_4(s) &= 0 \\
\Delta_5(s) &= 1 \\
\Delta_6(s) &= -1
\end{aligned} \tag{4.25}$$

and for $\xi_{t,l} = 0$ the counter-clockwise rotation

$$\begin{aligned}
\Delta_1(s) &= 1 \\
\Delta_2(s) &= 0 \\
\Delta_3(s) &= -1 \\
\Delta_4(s) &= 1 \\
\Delta_5(s) &= 0 \\
\Delta_6(s) &= -1
\end{aligned} \tag{4.26}$$

results.

The FHP-I LGCA is not invariant under duality. This can be achieved by including the 4-particle head-on collisions (duals of the 2-particle head-on collision).

4-particle head-on collision:
As in the case of the 2-particle head on collision, there are two transformations for the 4-particle head-on collision. Therefore, this is a non-deterministic collision rule. In Figure 4.11 the 4-particle head-on collision is shown.
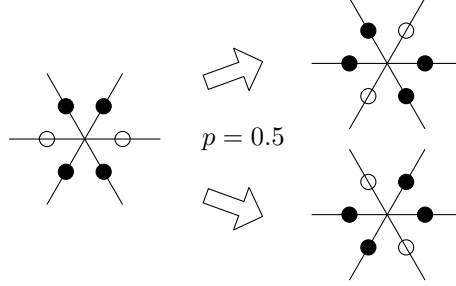
Figure 4.11: Illustration of the 4-particle head-on collision of the FHP-I LGCA according to Wolf-Gladrow (2004)

The collision rules (FHP-I LGCA and 4-particle head-on collision) can be completed by including the 2-particle head-on collisions with spectator. For obtaining the full set of collision rules rotations of $\pi/3$ and mirror imaging on the x-axis have to be applied.

2-particle head-on collision with spectator:
The 2-particle head-on collision with spectator is a deterministic collision rule. In Figure 4.12 the 2-particle head-on collision with spectator is shown.
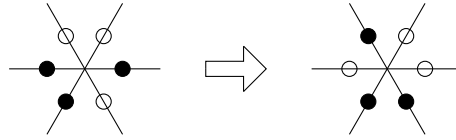
Figure 4.12: Illustration of the 2-particle head-on collision with spectator of the FHP-I LGCA according to Wolf-Gladrow (2004)

Inclusion of Rest Particle for FHP-II and FHP-III Lattice Gas Cellular Automata:
For the FHP-II LGCA and FHP-III LGCA a rest particle is introduced. Therefore, at each node a seventh cell is added. This seventh cell corresponds to the lattice vector $c_0 = (0,0)$ (for c_0 the value of the lattice vector and lattice velocity is always the same). The lattice vectors $c_1, \ldots, c_6$ are used as stated above.

Collision of FHP-II Lattice Gas Cellular Automaton:
FHP-II LGCA uses the collision rules of FHP-I LGCA (2-particle head-on and symmetric 3-particle collisions), the rest particle collisions, the 2-particle head-on collision with spectator rest particle, and the symmetric 3-particle collision with spectator rest particle.

The rest particle is represented by the circle in the middle. For obtaining the full set of collision rules of FHP-II LGCA, rotations of $\pi/3$ and mirror imaging on the x-axis have to be applied.

2-particle head-on collision:
In Figure 4.13 the 2-particle head-on collision is shown.
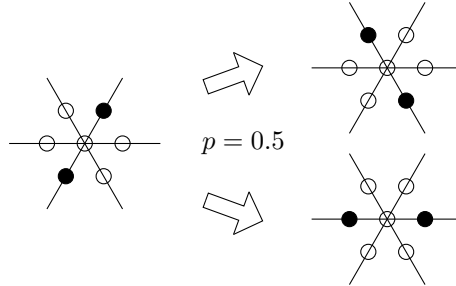
Figure 4.13: Illustration of the 2-particle head-on collision of the FHP-II LGCA according to Frisch et al. (1986a)

Symmetric 3-particle collision:
In Figure 4.14 the symmetric 3-particle collision is shown.
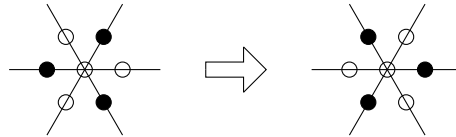
Figure 4.14: Illustration of the symmetric 3-particle collision of the FHP-II LGCA according to Frisch et al. (1986a)

2-particle head-on collision with spectator rest particle:
In Figure 4.15 a 2-particle head-on collision with spectator rest particle is shown.
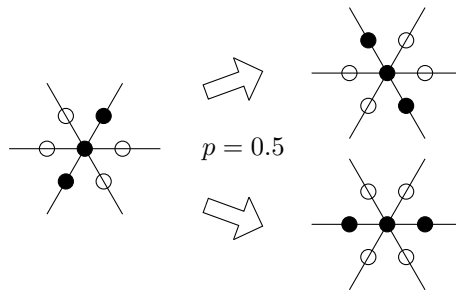
Figure 4.15: Illustration of the 2-particle head-on collision with spectator rest particle of the FHP-II LGCA according to Frisch et al. (1986a)

Symmetric 3-particle collision with spectator rest particle:
In Figure 4.16 the symmetric 3-particle collision with spectator rest particle is shown.
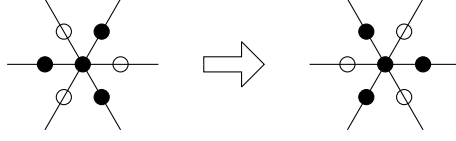
Figure 4.16: Illustration of the symmetric 3-particle collision with spectator rest particle of the FHP-II LGCA according to Frisch et al. (1986a)

Rest particle collisions:
The rest particle is a particle with velocity zero. In Figure 4.17 the rest particle collisions are shown, whereby the rest particle is located in the middle.
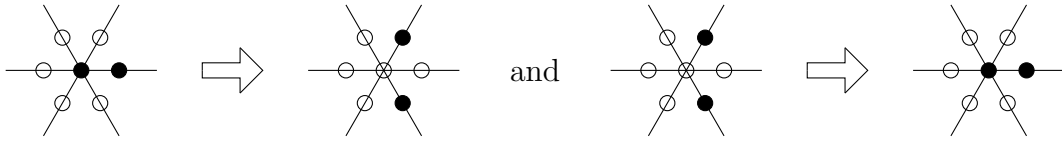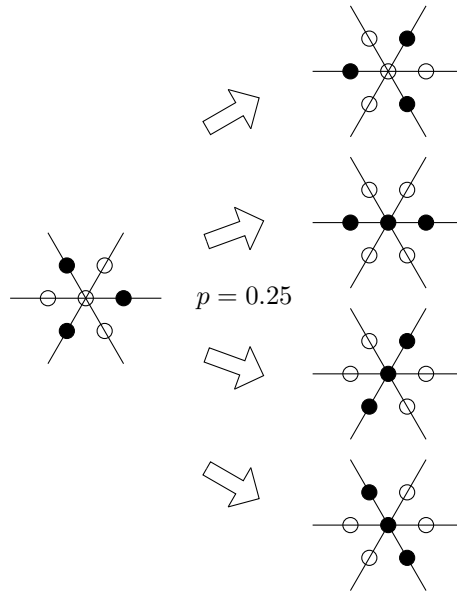

Figure 4.17: Illustration of the rest particle collisions of the FHP-II LGCA according to Frisch et al. (1986a)

"Collision function" of FHP-II Lattice Gas Cellular Automaton:
In the following, the arguments are sometimes omitted for conciseness. Similar to the collision rule of the FHP-I LGCA, the collisions can be formulated by using Boolean relations. For defining the collision rules, the "collision function" $\Delta_i(s)$ is introduced by

$$
\begin{aligned}
\Delta_i(s) = {} & \xi_{t,l} s_{i+1} s_{i+4}(1-s_i)(1-s_{i+2})(1-s_{i+3})(1-s_{i+5}) \\
& + (1-\xi_{t,l}) s_{i+2} s_{i+5}(1-s_i)(1-s_{i+1})(1-s_{i+3})(1-s_{i+4}) \\
& - s_i s_{i+3}(1-s_{i+1})(1-s_{i+2})(1-s_{i+4})(1-s_{i+5}) \\
& + s_{i+1} s_{i+3} s_{i+5}(1-s_i)(1-s_{i+2})(1-s_{i+4}) \\
& - s_i s_{i+2} s_{i+4}(1-s_{i+1})(1-s_{i+3})(1-s_{i+5}) \\
& - s_i(1-s_{i+1})(1-s_{i+2})(1-s_{i+3})(1-s_{i+4})(1-s_{i+5})s_0 \\
& + s_{i+1}(1-s_i)(1-s_{i+2})(1-s_{i+3})(1-s_{i+4})(1-s_{i+5})s_0 \\
& + s_{i+5}(1-s_i)(1-s_{i+1})(1-s_{i+2})(1-s_{i+3})(1-s_{i+4})s_0 \\
& - s_i s_{i+2}(1-s_{i+1})(1-s_{i+3})(1-s_{i+4})(1-s_{i+5})(1-s_0) \\
& - s_i s_{i+4}(1-s_{i+1})(1-s_{i+2})(1-s_{i+3})(1-s_{i+5})(1-s_0) \\
& + s_{i+1} s_{i+5}(1-s_i)(1-s_{i+2})(1-s_{i+3})(1-s_{i+4})(1-s_0)
\end{aligned}
\tag{4.27}
$$

(the index j of s_j is defined modulo six and between 1 and 6), whereby $\xi_{t,l}$ denotes a time- and site-dependent Boolean variable. $\xi_{t,l}$ is one when the particles are rotated clockwise, and zero when the particles are rotated counter-clockwise. For the two possible values

equal probabilities are used, i.e.

$$\mathbb{P}(\xi_{t,l} = 0) = \frac{1}{2} = \mathbb{P}(\xi_{t,l} = 1). \tag{4.28}$$

Furthermore, independence of the $\xi_{t,l}$'s is assumed. There is an additional equation for s_0 (the index j of s_j is defined modulo six and between 1 and 6)

$$
\begin{aligned}
\Delta_0(s) = &- \sum_{i=1}^{6} s_i(1 - s_{i+1})(1 - s_{i+2})(1 - s_{i+3})(1 - s_{i+4})(1 - s_{i+5})s_0 \\
&+ \sum_{i=1}^{6} s_i s_{i+2}(1 - s_{i+1})(1 - s_{i+3})(1 - s_{i+4})(1 - s_{i+5})(1 - s_0).
\end{aligned}
\tag{4.29}
$$

Collision of FHP-III Lattice Gas Cellular Automaton:
According to d'Humieres & Lallemand (1987), the FHP-III LGCA is a collision-saturated version of the FHP-II LGCA. In the following, the reduced set of collision rules for FHP-III LGCA is listed according to Rivet & Boon (2001). For obtaining the full set of collision rules rotations of $\pi/3$, mirror imaging on the x-axis, and duality (exchange of 1 and 0) have to be applied. As in the case of the FHP-II LGCA there is a rest particle (represented by the circle in the middle).

2-particle head-on collision:
In Figure 4.18 the 2-particle head-on collision is shown.
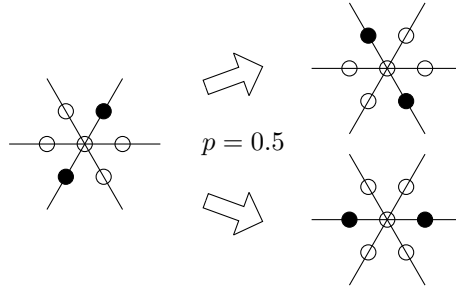
Figure 4.18: Illustration of the 2-particle head-on collision of the FHP-III LGCA according to Rivet & Boon (2001)

Rest particle collisions:
In Figure 4.19 the rest particle collisions are shown.
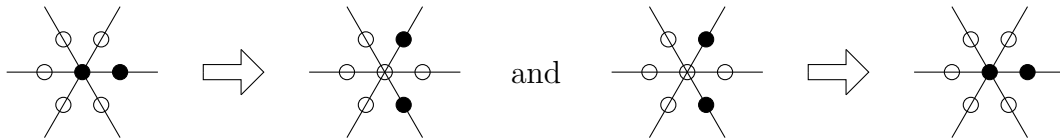
Figure 4.19: Illustration of the rest particle collisions of the FHP-III LGCA according to Rivet & Boon (2001)

Symmetric 3-particle collision:
In Figure 4.20 the symmetric 3-particle collision is shown.

Figure 4.20: Illustration of the symmetric 3-particle collision of the FHP-III LGCA according to Rivet & Boon (2001)

2-particle head-on collision with rest particle:
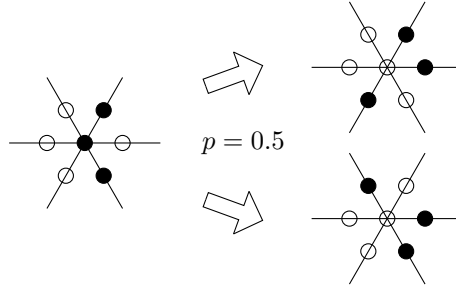In Figure 4.21 the 2-particle head-on collision with rest particle is shown.
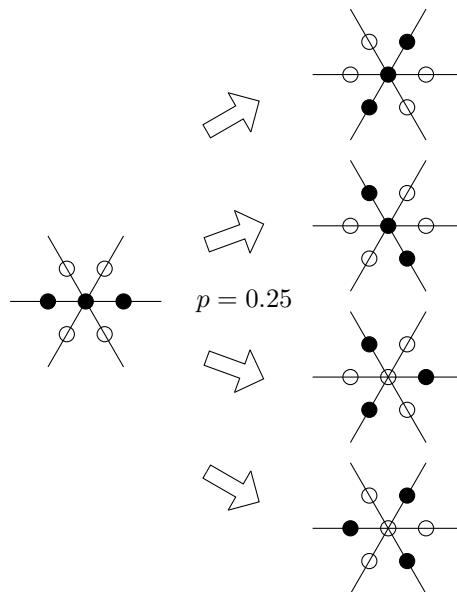
Figure 4.21: Illustration of the 2-particle head-on collision with rest particle of the FHP-III LGCA according to Rivet & Boon (2001)

2-particle collision with rest particle:
In Figure 4.22 the 2-particle collision with rest particle is shown.

Figure 4.22: Illustration of the 2-particle collision with rest particle of the FHP-III LGCA according to Rivet & Boon (2001)

3-particle collision:
In Figure 4.23 the 3-particle collision is shown.
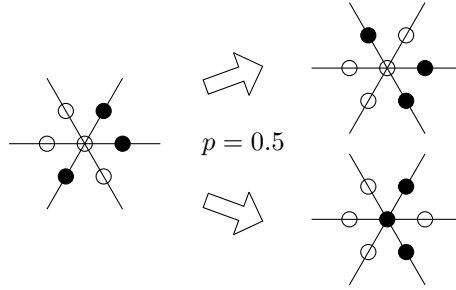
Figure 4.23: Illustration of the 3-particle collision of the FHP-III LGCA according to Rivet & Boon (2001)

"Collision function" of FHP-III Lattice Gas Cellular Automaton:
According to Rivet & Boon (2001), it is also possible to write the equations for Δ_i, $i = 1, \ldots, 6$, and Δ_0 for FHP-III LGCA (for FHP-III LGCA there are many more terms than for FHP-II LGCA), but they are not presented here.

Thus, the collision $\mathcal{C}$ is defined by

$$\mathcal{C}\colon s_i(l) \mapsto s_i(l) + \Delta_i(s(l)) \tag{4.30}$$

with $i = 1, \ldots, 6$ (FHP-I LGCA) and $i = 0, \ldots, 6$ (FHP-II LGCA and FHP-III LGCA).

Streaming of FHP Lattice Gas Cellular Automaton
During streaming the particles move simultaneously across the lattice. Each particle moves according to its corresponding lattice vector to a neighbouring node. The streaming $\mathcal{S}$ is defined by

$$\mathcal{S}\colon s_i(l) \mapsto s_i(l - c_i), \, i = 1, \ldots, 6. \tag{4.31}$$

Evolution of FHP Lattice Gas Cellular Automaton

Using $\Delta_i(s)$ the updating of the cells can be written as

$$s(t+1, l+c_i) = s_i(t,l) + \Delta_i(l) \tag{4.32}$$

with $i = 1, \ldots, 6$ (FHP-I LGCA) and $i = 0, \ldots, 6$ (FHP-II LGCA and FHP-III LGCA). The evolution is defined by

$$\mathcal{E} := \mathcal{S} \circ \mathcal{C} \tag{4.33}$$

on $s = \{s_i(l), \; i = 1, \ldots, 6, \; l \in \mathcal{L}\}$ (FHP-I LGCA) and $s = \{s_i(l), \; i = 0, \ldots, 6, \; l \in \mathcal{L}\}$ (FHP-II LGCA and FHP-III LGCA). $\mathcal{C}$ and $\mathcal{S}$ represent the collision and the streaming, respectively. Based on this definition the evolution is written as

$$s(t+1, .) = \mathcal{E}s(t, .), \tag{4.34}$$

whereby the second argument stands for the lattice points.

The dynamics are invariant under all discrete transformations that conserve the triangular lattice (discrete translations, rotations by $\pi/3$, and mirror symmetries with respect to a lattice line).

The collision rules conserve mass and momentum locally. The streaming conserves them globally. In the following the index set I represents $\{1, \ldots, 6\}$ (FHP-I LGCA) and $\{0, \ldots, 6\}$ (FHP-II LGCA and FHP-III LGCA). Using the corresponding "collision function" the conservation of mass for the collision is given by

$$\sum_{i \in I} \Delta_i(s) = 0, \tag{4.35}$$

and the conservation of momentum for the collision is given by

$$\sum_{i \in I} c_i \Delta_i(s) = 0. \tag{4.36}$$

Thus, conservation of mass and momentum for the evolution are given by

$$\sum_{i \in I} s_i(t+1, l+c_i) = \sum_{i \in I} s_i(t,l) \tag{4.37}$$

and

$$\sum_{i \in I} c_i s_i(t+1, l+c_i) = \sum_{i \in I} c_i s_i(t,l). \tag{4.38}$$

As in the case of the HPP LGCA, the kinetic energy (each particle has a kinetic energy of $mv^2/2 = 1/2$) is also conserved for the FHP-I LGCA (2-particle head-on and symmetric 3-particle collisions) due to mass conservation. When using FHP LGCA with rest

particles (FHP-II LGCA or FHP-III LGCA), there are collisions that do not conserve the kinetic energy. The rest particle collisions shown in Figure 4.17 (FHP-II LGCA) and Figure 4.19 (FHP-III LGCA) do not conserve the kinetic energy due to the involved rest particle with the corresponding lattice velocity $(0,0)$.

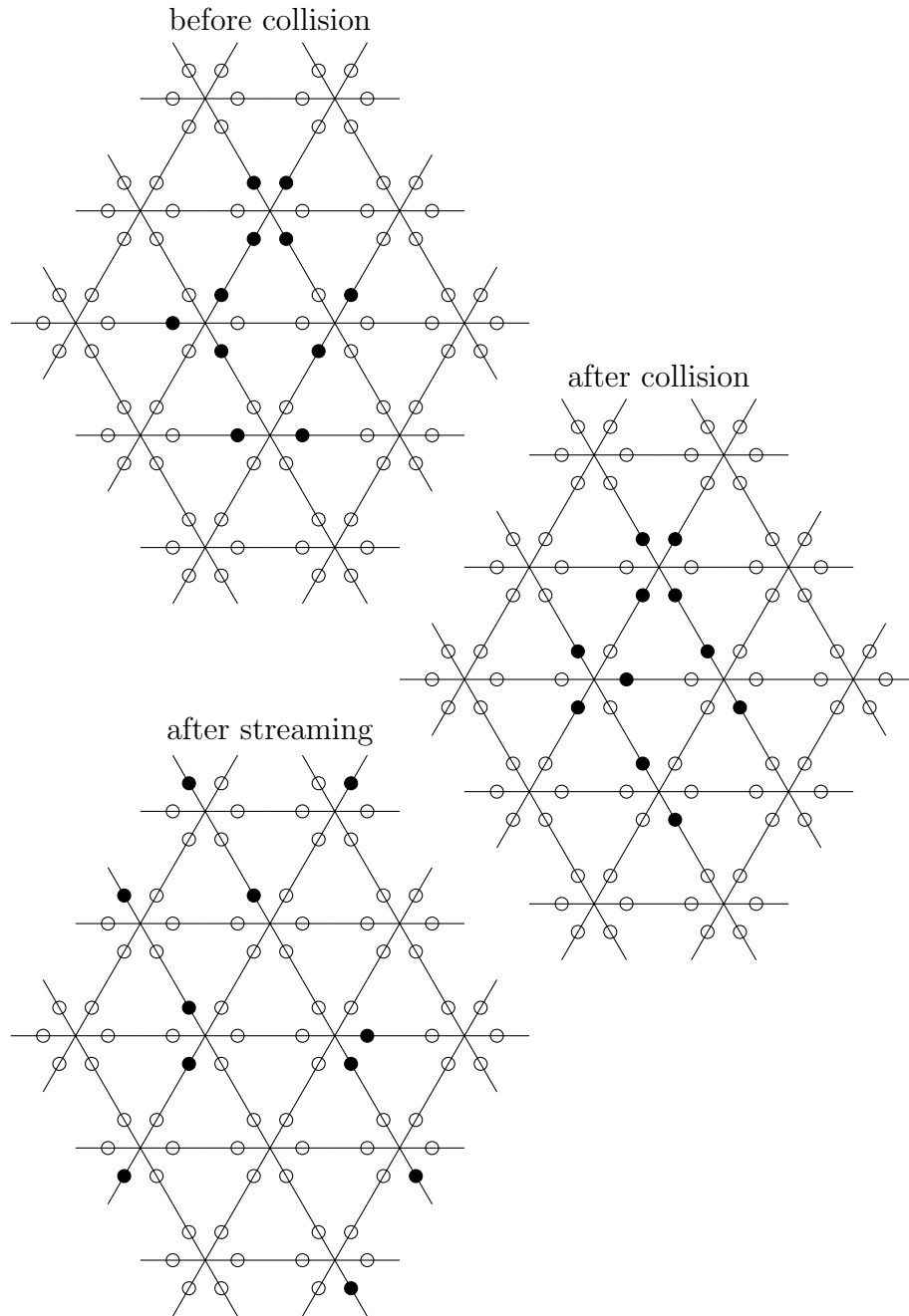In Figure 4.24 an example for the evolution using FHP-I LGCA is depicted.

before collision

after collision

after streaming

Figure 4.24: Illustration of collision and streaming of the FHP-I LGCA according to Wolf-Gladrow (2004)

4.2.3 Boundary Conditions

This section is based on d'Humieres & Lallemand (1987), Rivet & Boon (2001), and Wolf-Gladrow (2004). Boundary conditions are necessary for the edges of the lattice and obstacles within the lattice area. There are various types of boundary conditions. In the following some of them are presented. Without loss of generality the illustrations are shown for nodes with seven cells. Depending on the context the abbreviation BC stands for boundary condition or boundary conditions.

Periodic Boundary Condition:
The particles that leave at one edge enter the opposite edge. Using periodic BC the total mass and momentum are conserved. In Figure 4.25 the periodic BC is illustrated.
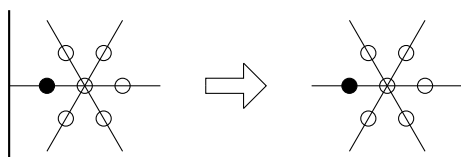
Figure 4.25: Schematic depiction of the periodic BC

Bounce Back Boundary Condition:
The particle is turned around by π. The corresponding lattice vectors are changed according to $c_i \mapsto c_{i+3}$ for $i = 1, \ldots, 6$ (the index j of c_j is defined modulo six and between 1 and 6). Using bounce back BC the total mass is conserved, but the total momentum is not conserved. In Figure 4.26 the bounce back BC is illustrated.
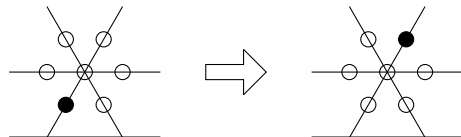
Figure 4.26: Schematic depiction of the bounce back BC according to Rivet & Boon (2001)

Specular Reflection Boundary Condition:
The particle is reflected at the boundary of the wall or obstacle. The corresponding lattice vectors are changed depending on the orientation of the surface of the boundary. Using specular reflection BC the total mass is conserved, but the total momentum is not conserved. In Figure 4.27 the specular reflection BC is illustrated.
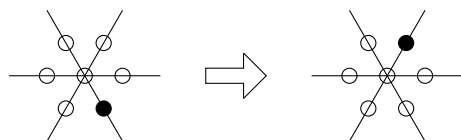
Figure 4.27: Schematic depiction of the specular reflection BC according to Rivet & Boon (2001)

Random Boundary Condition:

The incoming particle is emitted at random on available cells. Using random BC the total mass is conserved, but in general the total momentum is not conserved. In Figure 4.28 the random BC is illustrated.
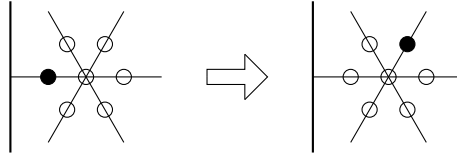

Figure 4.28: Schematic depiction of the random BC

4.3 Random Walk

This section is based on Spitzer (1976) and Lawler & Limic (2010). First, an example is presented.

Example 4.3. The experiment of flipping a coin is considered. Each flip has a probability of 0.5 for heads (H) and tails (T), respectively. A possible result of this experiment is shown in Figure 4.29.
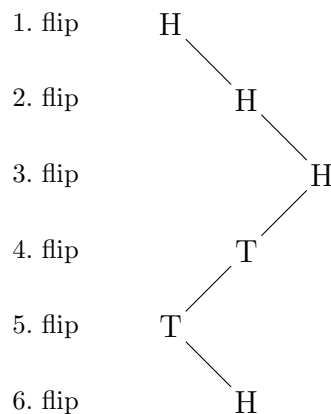
Figure 4.29: Illustration of a result of the experiment coin flipping where H and T are head and tail, respectively

The coin flipping is an example for a random walk, more precisely it is an example for a simple random walk on the lattice $\mathbb{Z}$. The result of this random walk starting at x_0 is calculated in discrete time steps using a non-deterministic rule. The entity moves with probability 0.5 by $+1$ or -1 on the lattice $\mathbb{Z}$. In Figure 4.30 all possible results of this random walk starting at $x_0 = 0$ are illustrated for several time steps t.
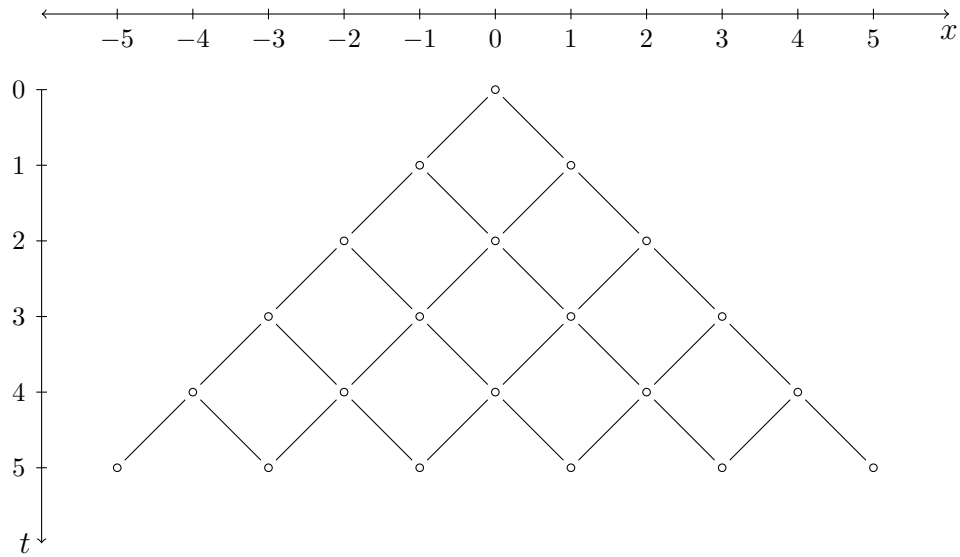
Figure 4.30: Illustration of all possible results of the simple random walk on $\mathbb{Z}$ after five time steps

In Figure 4.31 ten simple random walks starting at $x_0 = 0$, simulated in MATLAB R2018b, are shown.
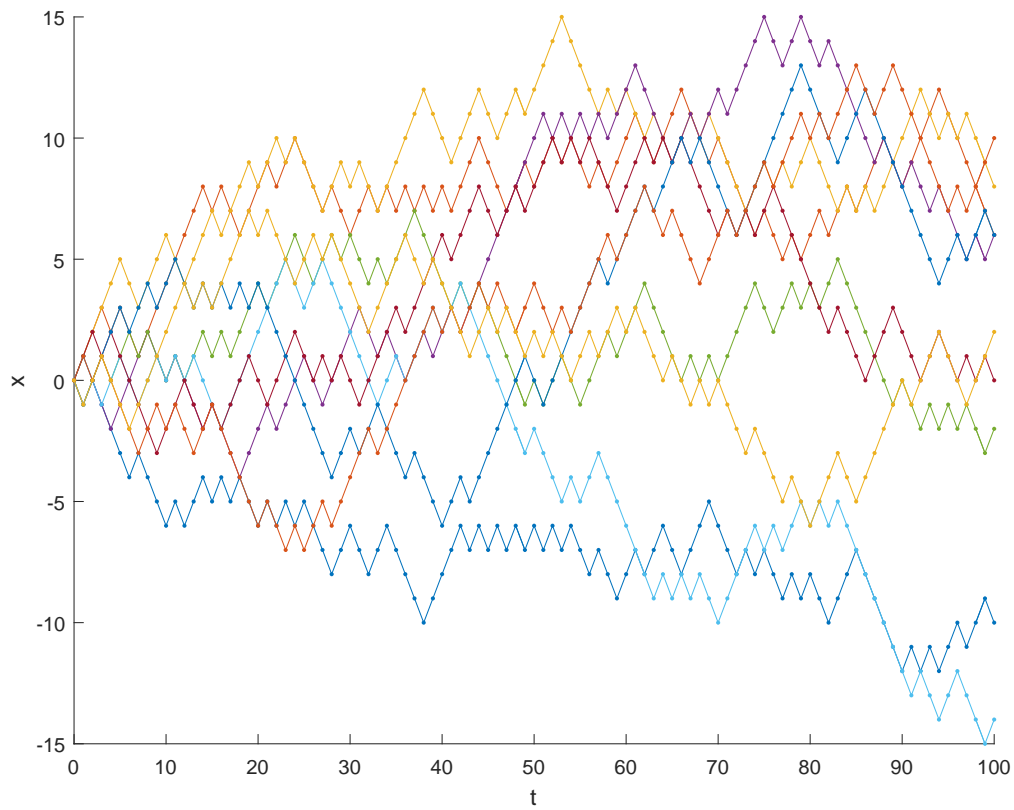

Figure 4.31: Simulation of ten simple random walks on $\mathbb{Z}$ using MATLAB R2018b

Next, the underlying theory is presented. For the formal definition of the random walk, some notation and definitions are necessary.

A lattice is a discrete additive subgroup of $\mathbb{R}^d$ with $d \in \mathbb{N}$ arbitrary but fixed. Discrete means that there is a real neighbourhood of the origin whose intersection with the lattice is just the origin. Often the lattice $\mathbb{Z}^d$ is used. The lattice is denoted by $\mathcal{L}$ and each element of $\mathcal{L}$ is a lattice point. The lattice $\mathcal{L}$ is called the state space of the random walk.

Definition 4.4 (Transition function)**.** For each pair (x, y) in $\mathcal{L} \times \mathcal{L}$ the transition function $P \colon \mathcal{L} \times \mathcal{L} \to \mathbb{R}$ of the random walk has to fulfil

$$0 \leq P(x, y) = P(0, y - x), \qquad \sum_{x \in \mathcal{L}} P(0, x) = 1. \tag{4.39}$$

The property $P(x, y) = P(0, y - x)$ is called spatial homogeneity. Therefore, the transition function can be determined by a function $p \colon \mathcal{L} \to \mathbb{R}$ with $p(x) = P(0, x)$ and the properties

$$0 \leq p(x), \qquad \sum_{x \in \mathcal{L}} p(x) = 1. \tag{4.40}$$

Probability interpretation of the transition function P:
$P(0, x)$ corresponds to the probability of a one-step transition from 0 to x. Therefore, the probability of an n-step transition from 0 to x is denoted by $P_n(0, x)$. It represents the probability that a particle starting at 0 is at x after n transitions described by P. In the following P_n is defined formally.

Definition 4.5 ($P_n(x, y)$)**.** For all $x, y \in \mathcal{L}$ the function $P_n \colon \mathcal{L} \times \mathcal{L} \to \mathbb{R}$ is defined as

$$P_0(x, y) = \begin{cases} 1 & \text{if } x = y, \\ 0 & \text{else,} \end{cases} \tag{4.41}$$

and $P_1(x, y) = P(x, y)$, and

$$P_n(x, y) = \sum_{x_i \in \mathcal{L}, \, i = 1, \dots, n-1} P(x, x_1) P(x_1, x_2) \dots P(x_{n-1}, y), \forall n \geq 2, \tag{4.42}$$

whereby the sum extends over all $n - 1$ tuples $x_1, \dots, x_{n-1}$ of points in $\mathcal{L}$.

Probability interpretation of P_n:
$P_n(x, y)$ represents the probability that a particle starting at x at time 0 will be at y at time n by execution of the random walk represented by P.

According to Spitzer (1976), the transition function P defines the random walk.

Definition 4.6 (Random walk according to Spitzer (1976))**.** A random walk is defined as a function $P \colon \mathcal{L} \times \mathcal{L} \to \mathbb{R}$ that fulfils the properties given in Equation (4.39) for all pairs $x, y \in \mathcal{L}$. A random walk is d-dimensional if the dimension of $\mathcal{L}$ is d.

Using the transition function P and the function P_n the random walk can be considered as sequence of random variables $(S_n)_{n \in \mathbb{N}}$ and $S_0 = x_0$ with

$$\mathbb{P}(S_1 = y | S_0 = x_0) = P(x_0, y) \; \forall \, y \in \mathcal{L}, \tag{4.43}$$

and

$$\mathbb{P}(S_n = y | S_0 = x_0) = P_n(x_0, y) \text{ for } n \geq 2 \text{ and } \forall \, y \in \mathcal{L}. \tag{4.44}$$

Finally, the d-dimensional simple random walk is considered.

Example 4.7. The simple random walk on $\mathbb{Z}^d$ starting at $x_0 \in \mathbb{Z}^d$ is considered. $P(0, x)$ defines the d-dimensional simple random walk if

$$P(0, x) = \begin{cases} \frac{1}{2d} & \text{if } \|x\|_2 = 1, \\ 0 & \text{if } \|x\|_2 \neq 1, \end{cases} \tag{4.45}$$

where $\|.\|_2$ is the Euclidean norm.
On the one hand, the d-dimensional simple random walk can be considered as a sum of a sequence of independent, identically distributed random variables X_i

$$S_n = x_0 + X_1 + \cdots + X_n, n \geq 1, \text{ and } S_0 = x_0 \tag{4.46}$$

where

$$\mathbb{P}(X_j = e_k) = \mathbb{P}(X_j = -e_k) = \frac{1}{2d}, \quad k = 1, \ldots, d, \tag{4.47}$$

and on the other hand, it can be considered as a Markov chain with state space $\mathcal{L}$ and transition probabilities

$$\mathbb{P}(S_{n+1} = y | S_n = x) = \frac{1}{2d}, \quad y - x \in \{\pm e_1, \ldots, \pm e_d\} \tag{4.48}$$

where $(S_n)_{n \in \mathbb{N}}$ is a sequence of random variables and $S_0 = x_0$.

Next, the two-dimensional simple random walk on the triangular lattice is considered.

Example 4.8. The triangular lattice $\mathcal{L}$ as a subset of $\mathbb{R}^2$ is considered. The lattice is generated by 1 and $e^{i\pi/3}$, thus

$$\mathcal{L} = \{k_1 + k_2 e^{i\pi/3} : k_1, k_2 \in \mathbb{Z}\}. \tag{4.49}$$

Each lattice point has six neighbours. During the simple random walk, one of the six neighbours is chosen with equal probability $1/6$. Thus, P defines the two-dimensional simple random walk on the triangular lattice by

$$P(0, x) = \begin{cases} \frac{1}{6} & \text{if } \|x\|_2 = 1, \\ 0 & \text{if } \|x\|_2 \neq 1. \end{cases} \tag{4.50}$$

5

Synthesis of Lattice Gas Cellular Automaton and Random Walk

For modelling the gluing in two dimensions an LGCA and a random walk was used. Therefore, a synthesis of LGCA and random walk was developed. The movement of the wood particles and adhesive droplets were described with different methods:

- The wood particles are assumed to be moving according to the FHP LGCA.

- The adhesive droplets are assumed to be moving according to a random walk.

Therefore first the HPP LGCA and the FHP LGCA of Chapter 4 were defined formally. Next, the synthesis of the HPP LGCA and the random walk was defined. Even though the HPP LGCA was not used for the mathematical model of the gluing process the simple geometry of the lattice of the HPP LGCA allows to define the synthesis of the LGCA and the random walk in a concise way. Finally, the synthesis of the FHP LGCA and the random walk was defined. The synthesis of FHP LGCA and random walk sets the basis for the model for the gluing process in Chapter 6.

The novelty of the formal definition of the HPP LGCA and FHP LGCA was to define local and global operators for collision, neighbouring nodes and streaming. Furthermore it was proven that these operators are well-defined. The definitions of these operators were used for the definition of the novel modelling method "synthesis of LGCA and random walk". Within the new method an additional step is carried out. This step allows to include movement according to a random walk. For developing the modelling method "synthesis of LGCA and random walk", a local and global operator "inclusion of random walk" is introduced. Thus, the novel modelling method is based on a LGCA and a random walk is included within the method. Therefore, this modelling method is called "synthesis of LGCA and random walk".

5.1 Formal Definition of HPP Lattice Gas Cellular Automaton

Based on the description of the HPP LGCA in Section 4.2.1, a formal definition of the HPP LGCA is introduced in the present thesis. The set of states is $Q = \{0, 1\}$, whereby 0 and 1 correspond to empty and occupied by a particle, respectively. The lattice, which is the set of lattice points, is denoted by $\mathcal{L}$.

Collision of HPP Lattice Gas Cellular Automaton

Next, a local collision operator $\mathcal{C}_l$ is introduced.

Definition 5.1 (Local collision operator of HPP LGCA)**.** The local collision operator $\mathcal{C}_l \colon Q^{2\times 2} \to Q^{2\times 2}$ is defined as

$$\mathcal{C}_l x := \begin{cases} Rx & \text{if } x_{11} = x_{22} = 1 \text{ and } x_{12} = x_{21} = 0 \\ Rx & \text{if } x_{12} = x_{21} = 1 \text{ and } x_{11} = x_{22} = 0 \\ I\,x & \text{else,} \end{cases} \tag{5.1}$$

whereby I is the identity operator on $Q^{2\times 2}$ and

$$R = \begin{pmatrix} 0 & 1 \\ 1 & 0 \end{pmatrix}. \tag{5.2}$$

Remark 5.2. The entries of the matrix $x \in Q^{2\times 2}$ represent the four cells located at a node. In Figure 5.1 a node and the corresponding matrix x are shown.
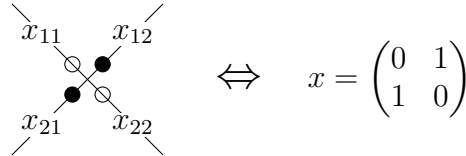
Figure 5.1: Illustration of matrix $x \in Q^{2\times 2}$ and the corresponding cells at a node

Remark 5.3. Instead of $x \in Q^{2\times 2}$ it is also possible to use $x \in Q^{4\times 1}$ or $x \in Q^{1\times 4}$.

In the following, a tensor $X \in Q^{2\times 2\times |\mathcal{L}|}$ is considered: $X_{.,.,i} \in Q^{2\times 2}$ for $i = 1, \dots, |\mathcal{L}|$, whereby the elements of $\mathcal{L}$ are numbered in an arbitrary, fixed order.

Definition 5.4 (Global collision operator of HPP LGCA)**.** The global collision operator $\mathcal{C} \colon Q^{2\times 2\times |\mathcal{L}|} \to Q^{2\times 2\times |\mathcal{L}|}$ is defined elementwise as

$$(\mathcal{C}X)_{.,.,i} := \mathcal{C}_l X_{.,.,i}. \tag{5.3}$$

Streaming of HPP Lattice Gas Cellular Automaton

Next, the local streaming operator is defined.

Definition 5.5 (Local streaming operator of HPP LGCA)**.** The local streaming operator $\mathcal{S}_l \colon Q^{4\times 4} \to Q^{2\times 2}$ is defined as

$$\mathcal{S}_l n := \begin{pmatrix} n_{33} & n_{32} \\ n_{23} & n_{22} \end{pmatrix}. \tag{5.4}$$

Remark 5.6. The entries of the matrix $n \in Q^{4\times 4}$ represent the 16 cells located at the neighbouring nodes. In Figure 5.2 a node, its neighbouring nodes and the corresponding matrix n are shown.

$$\Longleftrightarrow \quad n = \begin{pmatrix} 0 & 1 & 1 & 1 \\ 1 & 0 & 0 & 1 \\ 1 & 1 & 1 & 1 \\ 1 & 1 & 0 & 0 \end{pmatrix}$$
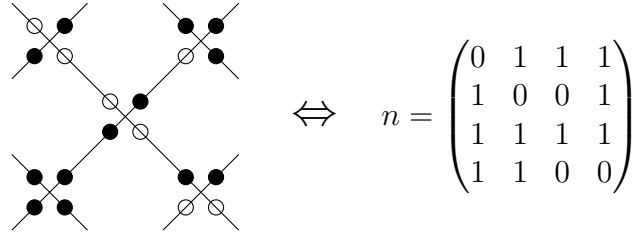
Figure 5.2: Illustration of matrix $n \in Q^{4\times 4}$

For each $X_{\cdot,\cdot,i}$ the states of the cells of the four neighbouring nodes are necessary for calculating the state of the cells of node i for the new time step. The tensor, which contains the states of the cells of the four neighbouring nodes for each lattice point, is denoted by $N \in Q^{4\times 4\times|\mathcal{L}|}$. $N_{\cdot,\cdot,i} \in Q^{4\times 4}$ are the states of the cells of the neighbouring nodes of lattice point i.

Definition 5.7 (Global streaming operator of HPP LGCA)**.** The global streaming operator $\mathcal{S} \colon Q^{4\times 4\times|\mathcal{L}|} \to Q^{2\times 2\times|\mathcal{L}|}$ is defined as

$$(\mathcal{S}N)_{\cdot,\cdot,i} := \mathcal{S}_l N_{\cdot,\cdot,i}. \tag{5.5}$$

Neighbouring Nodes of HPP Lattice Gas Cellular Automaton

For defining the evolution of the HPP LGCA, an operator which assigns to each node the neighbouring nodes is necessary. More precise a global operator, which assigns the states of the cells of the neighbouring nodes to each node in $Q^{2\times 2}$ is defined.

Definition 5.8 (Neighbouring nodes operator of HPP LGCA)**.** The neighbouring nodes operator $\mathcal{N} \colon Q^{2\times 2\times|\mathcal{L}|} \to Q^{4\times 4\times|\mathcal{L}|}$ is defined as

$$(\mathcal{N}X)_{\cdot,\cdot,i} := N_{\cdot,\cdot,i}. \tag{5.6}$$

Evolution of HPP Lattice Gas Cellular Automaton

Finally, the evolution operator of the HPP LGCA is defined.

Definition 5.9 (Evolution operator of HPP LGCA)**.** The evolution operator $\mathcal{E}\colon Q^{2\times 2\times |\mathcal{L}|} \to Q^{2\times 2\times |\mathcal{L}|}$ is defined by

$$\mathcal{E} := \mathcal{S} \circ \mathcal{N} \circ \mathcal{C}, \tag{5.7}$$

whereby $\mathcal{C}$ is the collision operator, $\mathcal{N}$ the neighbouring nodes operator, and $\mathcal{S}$ is the streaming operator.

5.2 Formal Definition of FHP Lattice Gas Cellular Automaton

Based on the description of the FHP LGCA in Section 4.2.2, a formal definition of the FHP LGCA was introduced in the present thesis. The set of states is $Q = \{0, 1\}$, whereby 0 and 1 correspond to empty and occupied by a particle, respectively. The lattice, which is the set of lattice points, is denoted by $\mathcal{L}$.

Remark 5.10. The entries of the matrix $x \in Q^{1\times 6}$ represent the six cells located at a node. In Figure 5.3 a node and the corresponding matrix x are shown.

$$x = \begin{pmatrix} 1 & 0 & 1 & 0 & 1 & 0 \end{pmatrix}$$
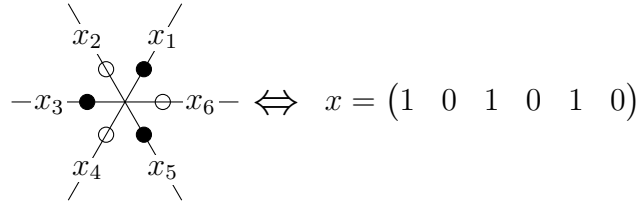
Figure 5.3: Illustration of vector $x \in Q^{1\times 6}$ and the corresponding cells at a node

Collision of FHP Lattice Gas Cellular Automaton

In the following, the collision rules for the different types of FHP LGCA are defined.

Collision of FHP-I Lattice Gas Cellular Automaton:

For defining the two collision types, 2-particle head-on and symmetric 3-particle collision, of the FHP-I LGCA a description for all rotations on the lattice is necessary. Therefore, two permutations π_1 and π_2 are necessary.

$$\pi_1 = \begin{pmatrix} 1 & 2 & 3 & 4 & 5 & 6 \\ 6 & 1 & 2 & 3 & 4 & 5 \end{pmatrix} \text{ and } \pi_2 = \begin{pmatrix} 1 & 2 & 3 & 4 & 5 & 6 \\ 2 & 3 & 4 & 5 & 6 & 1 \end{pmatrix} \tag{5.8}$$

Geometrically the permutations π_1 and π_2 represent the rotation about $\pi/3$ and $-\pi/3$, respectively.

Remark 5.11. The permutations π_1 and π_2 are the inverse permutations of each other.

$$\pi_1 \circ \pi_2 = \mathrm{id} = \pi_2 \circ \pi_1 \tag{5.9}$$

The set Π represents all rotations on the lattice and is given by

$$\Pi = \{\pi_1^n \circ \pi_2^m | n,\, m \in \mathbb{N}_0\} \tag{5.10}$$

with $\pi_i^0 := \mathrm{id}$ for $i = 1,\, 2$.

Remark 5.12. Another description of the set of all rotations on the lattice is

$$\Pi = \{\pi_1^n | n \in \mathbb{Z}\} = \{\pi_2^n | n \in \mathbb{Z}\}. \tag{5.11}$$

In the following, the 2-particle head-on collision and the symmetric 3-particle collision are defined.

2-particle head-on collision:
For defining the 2-particle head-on collision, a standard setting for the states of the cells at a node is necessary. Afterwards, the 2-particle head-on collision operator for this standard setting is defined.

Definition 5.13 (Standard setting for 2-particle head-on collision of FHP-I LGCA)**.** The standard setting for the 2-particle head-on collision is $\sigma_2 = \begin{pmatrix} 0 & 0 & 1 & 0 & 0 & 1 \end{pmatrix}$.

Definition 5.14 (2-particle head-on collision operator for standard setting of FHP-I LGCA)**.** The non-deterministic collision operator for the standard setting $\mathcal{C}_2 \colon \{\sigma_2\} \to Q^{1 \times 6}$ is defined as

$$\mathcal{C}_2 \sigma_2 := \begin{cases} \begin{pmatrix} 1 & 0 & 0 & 1 & 0 & 0 \end{pmatrix} & \text{if } \xi_{t,l} = 0 \\ \begin{pmatrix} 0 & 1 & 0 & 0 & 1 & 0 \end{pmatrix} & \text{if } \xi_{t,l} = 1 \end{cases} \tag{5.12}$$

whereby $\xi_{t,l}$ denotes a time- and site-dependent Boolean variable. $\xi_{t,l}$ is one when the particles are rotated clockwise, and zero when the particles are rotated counter-clockwise. For the two possible values equal probabilities are used, i.e.

$$\mathbb{P}(\xi_{t,l} = 0) = \frac{1}{2} = \mathbb{P}(\xi_{t,l} = 1). \tag{5.13}$$

Furthermore independence of the $\xi_{t,l}$'s is assumed.

Remark 5.15. $\mathcal{C}_2$ can be interpreted as

$$\begin{cases} \pi_1|_{\{\sigma_2\}} & \text{if } \xi_{t,l} = 0 \\ \pi_2|_{\{\sigma_2\}} & \text{if } \xi_{t,l} = 1 \end{cases} \tag{5.14}$$

with a time- and site-dependent Boolean variable $\xi_{t,l}$ as in Definition 5.14.

Symmetric 3-particle collision:
For defining the symmetric 3-particle collision, a standard setting for the states of the cells at a node is necessary. Afterwards, the symmetric 3-particle collision operator for this standard setting is defined.

Definition 5.16 (Standard setting for symmetric 3-particle collision of FHP-I LGCA). The standard setting for the symmetric 3-particle collision is $\sigma_3 = \begin{pmatrix} 0 & 1 & 0 & 1 & 0 & 1 \end{pmatrix}$.

Definition 5.17 (Symmetric 3-particle collision operator for standard setting of FHP-I LGCA). The deterministic collision operator for the standard setting $\mathcal{C}_3 \colon \{\sigma_3\} \to Q^{1\times 6}$ is defined as

$$\mathcal{C}_3\sigma_3 := \begin{pmatrix} 1 & 0 & 1 & 0 & 1 & 0 \end{pmatrix}. \tag{5.15}$$

Remark 5.18. $\mathcal{C}_3$ can be interpreted as permutation ($\pi_1|_{\{\sigma_3\}}$ or $\pi_2|_{\{\sigma_3\}}$).

The local collision operator for the FHP-I LGCA is defined by using the collision operators for the standard settings.

Definition 5.19 (Local collision operator of FHP-I LGCA). The local collision operator $\mathcal{C}_l \colon Q^{1\times 6} \to Q^{1\times 6}$ is defined as

$$\mathcal{C}_l x := \begin{cases} \pi_x^{-1} \circ \mathcal{C}_2 \circ \pi_x x & \text{if } \exists \pi_x \in \Pi \colon \pi_x x = \sigma_2 \\ \pi_x^{-1} \circ \mathcal{C}_3 \circ \pi_x x & \text{if } \exists \pi_x \in \Pi \colon \pi_x x = \sigma_3 \\ \operatorname{id} x & \text{else.} \end{cases} \tag{5.16}$$

In the following, some lemmas for proving that $\mathcal{C}_l$ is well-defined (Theorem 5.24) are presented.

Lemma 5.20. *For different permutations $\pi_x, \tilde{\pi}_x \in \Pi$ it holds $\pi_x^{-1}\pi_1\pi_x = \tilde{\pi}_x^{-1}\pi_1\tilde{\pi}_x$.*

Proof. The permutations have the form $\pi_x = \pi_1^n \circ \pi_2^m$ and $\tilde{\pi}_x = \pi_1^{\tilde{n}} \circ \pi_2^{\tilde{m}}$ with $n, m, \tilde{n}, \tilde{m} \in \mathbb{N}_0$.

$$\begin{aligned} \pi_2^{-m} \circ \pi_1^{-n} \circ \pi_1 \circ \pi_1^n \circ \pi_2^m &= \pi_2^{-m} \circ \pi_1 \circ \pi_2^m = \\ \underset{(5.9)}{=} \pi_2^{-m} \circ \pi_2^{-1} \circ \pi_2^m &= \pi_2^{-1} = \pi_2^{-\tilde{m}} \circ \pi_2^{-1} \circ \pi_2^{\tilde{m}} = \\ \underset{(5.9)}{=} \pi_2^{-\tilde{m}} \circ \pi_1 \circ \pi_2^{\tilde{m}} &= \pi_2^{-\tilde{m}} \circ \pi_1^{-\tilde{n}} \circ \pi_1 \circ \pi_1^{\tilde{n}} \circ \pi_2^{\tilde{m}} \end{aligned} \tag{5.17}$$

$\square$

Lemma 5.21. *For different permutations $\pi_x, \tilde{\pi}_x \in \Pi$ it holds $\pi_x^{-1}\pi_2\pi_x = \tilde{\pi}_x^{-1}\pi_2\tilde{\pi}_x$.*

Proof. The permutations have the form $\pi_x = \pi_1^n \circ \pi_2^m$ and $\tilde{\pi}_x = \pi_1^{\tilde{n}} \circ \pi_2^{\tilde{m}}$ with $n, m, \tilde{n}, \tilde{m} \in \mathbb{N}_0$.

$$\begin{aligned} \pi_2^{-m} \circ \pi_1^{-n} \circ \pi_2 \circ \pi_1^n \circ \pi_2^m &= \\ \underset{(5.9)}{=} \pi_2^{-m} \circ \pi_1^{-n} \circ \pi_1^{-1} \circ \pi_1^n \circ \pi_2^m &= \\ = \pi_2^{-m} \circ \pi_1^{-1} \circ \pi_2^m \underset{(5.9)}{=} \pi_2^{-m} \circ \pi_2 \circ \pi_2^m &= \\ = \pi_2 = \pi_2^{-\tilde{m}} \circ \pi_2 \circ \pi_2^{\tilde{m}} &= \\ \underset{(5.9)}{=} \pi_2^{-\tilde{m}} \circ \pi_1^{-1} \circ \pi_2^{\tilde{m}} &= \\ = \pi_2^{-\tilde{m}} \circ \pi_1^{-\tilde{n}} \circ \pi_1^{-1} \circ \pi_1^{\tilde{n}} \circ \pi_2^{\tilde{m}} &= \\ \underset{(5.9)}{=} \pi_2^{-\tilde{m}} \circ \pi_1^{-\tilde{n}} \circ \pi_2 \circ \pi_1^{\tilde{n}} \circ \pi_2^{\tilde{m}} \end{aligned} \tag{5.18}$$

$\square$

Next, it is shown that $\pi_x^{-1} \circ \mathcal{C}_2 \circ \pi_x x$ is independent of the choice of $\pi_x \in \Pi$.

Lemma 5.22. *For different permutations $\pi_x, \tilde{\pi}_x \in \Pi$ with $\pi_x x = \sigma_2 = \tilde{\pi}_x x$ it holds* $\pi_x^{-1} \mathcal{C}_2 \pi_x x = \tilde{\pi}_x^{-1} \mathcal{C}_2 \tilde{\pi}_x x$.

Proof. Case 1: $\xi_{t,l} = 0$
In this case it holds $\mathcal{C}_2 = \pi_1|_{\{\sigma_2\}}$.

$$\pi_x^{-1} \mathcal{C}_2 \pi_x x \underset{\text{Remark 5.15}}{=} \pi_x^{-1} \circ \pi_1|_{\{\sigma_2\}} \circ \pi_x x \underset{(*)}{=} \pi_x^{-1} \circ \pi_1 \circ \pi_x x$$

$$\underset{\text{Lemma 5.20}}{=} \tilde{\pi}_x^{-1} \circ \pi_1 \circ \tilde{\pi}_x x \underset{(**)}{=} \tilde{\pi}_x^{-1} \circ \pi_1|_{\{\sigma_2\}} \circ \tilde{\pi}_x x \underset{\text{Remark 5.15}}{=} \tilde{\pi}_x^{-1} \mathcal{C}_2 \tilde{\pi}_x x \tag{5.19}$$

$(*)$ Based on the assumption $\pi_x x = \sigma_2$, the requirement that the input argument has to be an element of $\{\sigma_2\}$ (due to $\pi_1|_{\{\sigma_2\}}$) is fulfilled. Therefore, π_1 can be used as an extension of $\pi_1|_{\{\sigma_2\}}$.
$(**)$ Based on the assumption $\tilde{\pi}_x x = \sigma_2$, the input argument is an element of $\{\sigma_2\}$. Therefore, $\pi_1|_{\{\sigma_2\}}$ can be used as restriction of π_1.

Case 2: $\xi_{t,l} = 1$
In this case it holds $\mathcal{C}_2 = \pi_2|_{\{\sigma_2\}}$.

$$\pi_x^{-1} \mathcal{C}_2 \pi_x x \underset{\text{Remark 5.15}}{=} \pi_x^{-1} \circ \pi_2|_{\{\sigma_2\}} \circ \pi_x x \underset{(*)}{=} \pi_x^{-1} \circ \pi_2 \circ \pi_x x =$$

$$\underset{\text{Lemma 5.21}}{=} \tilde{\pi}_x^{-1} \circ \pi_2 \circ \tilde{\pi}_x x \underset{(**)}{=} \tilde{\pi}_x^{-1} \circ \pi_2|_{\{\sigma_2\}} \circ \tilde{\pi}_x x \underset{\text{Remark 5.15}}{=} \tilde{\pi}_x^{-1} \mathcal{C}_2 \tilde{\pi}_x x \tag{5.20}$$

$(*)$ Based on the assumption $\pi_x x = \sigma_2$, the requirement that the input argument has to be an element of $\{\sigma_2\}$ (due to $\pi_2|_{\{\sigma_2\}}$) is fulfilled. Therefore, π_2 can be used as an extension of $\pi_2|_{\{\sigma_2\}}$.
$(**)$ Based on the assumption $\tilde{\pi}_x x = \sigma_2$, the input argument is an element of $\{\sigma_2\}$. Therefore, $\pi_2|_{\{\sigma_2\}}$ can be used as restriction of π_2. $\qquad\square$

Next, it is shown that $\pi_x^{-1} \circ \mathcal{C}_3 \circ \pi_x x$ is independent of the choice of $\pi_x \in \Pi$.

Lemma 5.23. *For different permutations $\pi_x, \tilde{\pi}_x \in \Pi$ with $\pi_x x = \sigma_3 = \tilde{\pi}_x x$ it holds* $\pi_x^{-1} \mathcal{C}_3 \pi_x x = \tilde{\pi}_x^{-1} \mathcal{C}_3 \tilde{\pi}_x x$.

Proof. According to Remark 5.18 $\mathcal{C}_3$ can be interpreted as $\pi_1|_{\{\sigma_3\}}$ or $\pi_2|_{\{\sigma_3\}}$.
Case 1: $\mathcal{C}_3 = \pi_1|_{\{\sigma_3\}}$

$$\pi_x^{-1} \mathcal{C}_3 \pi_x x \underset{\text{Remark 5.18}}{=} \pi_x^{-1} \circ \pi_1|_{\{\sigma_3\}} \circ \pi_x x \underset{(*)}{=} \pi_x^{-1} \circ \pi_1 \circ \pi_x x =$$

$$\underset{\text{Lemma 5.20}}{=} \tilde{\pi}_x^{-1} \pi_1 \tilde{\pi}_x x \underset{(**)}{=} \tilde{\pi}_x^{-1} \pi_1|_{\{\sigma_3\}} \tilde{\pi}_x x \underset{\text{Remark 5.18}}{=} \tilde{\pi}_x^{-1} \mathcal{C}_3 \tilde{\pi}_x x \tag{5.21}$$

$(*)$ Based on the assumption $\pi_x x = \sigma_3$, the requirement that the input argument has to be an element of $\{\sigma_3\}$ (due to $\pi_1|_{\{\sigma_3\}}$) is fulfilled. Therefore, π_1 can be used as an

extension of $\pi_1|_{\{\sigma_3\}}$.

(**) Based on the assumption $\tilde{\pi}_x x = \sigma_3$, the input argument is an element of $\{\sigma_3\}$. Therefore, $\pi_1|_{\{\sigma_3\}}$ can be used as restriction of π_1.

Case 2: $\mathcal{C}_3 = \pi_2|_{\{\sigma_3\}}$

$$\pi_x^{-1}\mathcal{C}_3\pi_x x \underset{\text{Remark 5.18}}{=} \pi_x^{-1} \circ \pi_2|_{\{\sigma_3\}} \circ \pi_x x \underset{(*)}{=} \pi_x^{-1} \circ \pi_2 \circ \pi_x x =$$
$$\underset{\text{Lemma 5.21}}{=} \tilde{\pi}_x^{-1}\pi_2\tilde{\pi}_x x \underset{(**)}{=} \tilde{\pi}_x^{-1}\pi_2|_{\{\sigma_3\}}\tilde{\pi}_x x \underset{\text{Remark 5.18}}{=} \tilde{\pi}_x^{-1}\mathcal{C}_3\tilde{\pi}_x x \tag{5.22}$$

(*) Based on the assumption $\pi_x x = \sigma_3$, the requirement that the input argument has to be an element of $\{\sigma_3\}$ (due to $\pi_2|_{\{\sigma_3\}}$) is fulfilled. Therefore, π_2 can be used as an extension of $\pi_2|_{\{\sigma_3\}}$.

(**) Based on the assumption $\tilde{\pi}_x x = \sigma_3$, the input argument is an element of $\{\sigma_3\}$. Therefore, $\pi_2|_{\{\sigma_3\}}$ can be used as restriction of π_2. $\qquad\square$

Theorem 5.24. *The local collision operator $\mathcal{C}_l$ is well-defined.*

Proof. In order to prove the theorem, three cases are necessary. For each case it is assumed that $x_1 = x_2$.

Case 1:

Case 1 represents $\exists \pi_{x_1} \in \Pi: \pi_{x_1}x_1 = \sigma_2$ and $\exists \pi_{x_2} \in \Pi: \pi_{x_2}x_2 = \sigma_2$. With Lemma 5.22 it follows

$$\mathcal{C}_l x_1 = \pi_{x_1}^{-1}\mathcal{C}_2\pi_{x_1}x_1 = \tilde{\pi}_{x_2}^{-1}\mathcal{C}_2\tilde{\pi}_{x_2}x_2 = \mathcal{C}_l x_2. \tag{5.23}$$

Case 2:

Case 2 represents $\exists \pi_{x_1} \in \Pi: \pi_{x_1}x_1 = \sigma_3$ and $\exists \pi_{x_2} \in \Pi: \pi_{x_2}x_2 = \sigma_3$. With Lemma 5.23 it follows

$$\mathcal{C}_l x_1 = \pi_{x_1}^{-1}\mathcal{C}_3\pi_{x_1}x_1 = \tilde{\pi}_{x_2}^{-1}\mathcal{C}_3\tilde{\pi}_{x_2}x_2 = \mathcal{C}_l x_2. \tag{5.24}$$

Case 3:

Case 3 is for all $x \in Q^{1\times6}$ that are not covered with case 1 or 2. With the assumption $x_1 = x_2$ it follows

$$\mathcal{C}_l x_1 = \text{id}\, x_1 = \text{id}\, x_2 = \mathcal{C}_l x_2. \tag{5.25}$$

The following statements assure that exactly one case is valid for every $x \in Q^{1\times6}$:

For a node with 0, 1, 4, 5 or 6 occupied cells it is not possible that case 1 or 2 can be applied. This is due to the fact that application of $\pi_x \in \Pi$ does not change the number of particles at a node. Therefore, it is also not possible that it holds case 1 and 2.

For any $x \in Q^{1\times6}$ with exactly two occupied cells, for which case 3 has to be applied, there exists no π_x such that for $\pi_x x$ case 1 is applied. That can be proven by contradiction: it is assumed that for x case 3 is applied and $\exists \tilde{\pi}_x \in \Pi$ such that for $\tilde{\pi}_x x$ case 1 is applied. Thus,

$$\exists \pi_x \in \Pi: \underbrace{\pi_x \tilde{\pi}_x}_{\hat{\pi}_x \in \Pi}\, x = \sigma_2. \tag{5.26}$$

It follows that for x case 1 has to be applied. This is a contradiction to the assumption that case 3 is applied or to the assumption that $\exists \tilde{\pi}_x \in \Pi$ such that for $\tilde{\pi}_x x$ case 1 is applied.

For any $x \in Q^{1 \times 6}$ it is not possible that for x holds case 3 and case 2. The proof is similar to the proof above. $\qquad \square$

Remark 5.25. In general, the local collision operator is not injective due to the non-deterministic 2-particle head-on collision.

In the following a matrix $X \in Q^{|\mathcal{L}| \times 6}$ is considered: $X_{i,.} \in Q^{1 \times 6}$ for $i = 1, \ldots, |\mathcal{L}|$, whereby the elements of $\mathcal{L}$ are numbered in an arbitrary, fixed order.

Definition 5.26 (Global collision operator of FHP-I LGCA)**.** The global collision operator $\mathcal{C} \colon Q^{|\mathcal{L}| \times 6} \to Q^{|\mathcal{L}| \times 6}$ is defined elementwise as

$$(\mathcal{C}X)_{i,.} := \mathcal{C}_l X_{i,.}. \tag{5.27}$$

Collision of FHP-II Lattice Gas Cellular Automaton:
The rest particle is included in the model as seventh cell. Thus, $x \in Q^{1 \times 7}$ and the seventh entry represents the rest particle. For defining the collision rules, two permutations π_1 and π_2 are necessary.

$$\pi_1 = \begin{pmatrix} 1 & 2 & 3 & 4 & 5 & 6 & 7 \\ 6 & 1 & 2 & 3 & 4 & 5 & 7 \end{pmatrix} \text{ and } \pi_2 = \begin{pmatrix} 1 & 2 & 3 & 4 & 5 & 6 & 7 \\ 2 & 3 & 4 & 5 & 6 & 1 & 7 \end{pmatrix} \tag{5.28}$$

Geometrically the permutations π_1 and π_2 represent the rotation about $\pi/3$ and $-\pi/3$, respectively. Due to the corresponding lattice vector $(0,0)$ the seventh position is stationary and therefore not rotated.

Remark 5.27. The permutations π_1 and π_2 are the inverse permutations of each other.

$$\pi_1 \circ \pi_2 = \mathrm{id} = \pi_2 \circ \pi_1 \tag{5.29}$$

The set Π represents all rotations on the lattice and is given by

$$\Pi = \{\pi_1^n \circ \pi_2^m | n, m \in \mathbb{N}_0\} \tag{5.30}$$

with $\pi_i^0 = \mathrm{id}$ for $i = 1, 2$.

Remark 5.28. Another description of the set of all rotations on the lattice is

$$\Pi = \{\pi_1^n | n \in \mathbb{Z}\} = \{\pi_2^n | n \in \mathbb{Z}\}. \tag{5.31}$$

In the following, the 2-particle head-on collision with and without spectator rest particle, the symmetric 3-particle collision with and without spectator rest particle, and the rest particle collisions are defined.

2-particle head-on collision with and without spectator rest particle:
For defining the 2-particle head-on collision with and without spectator rest particle, a standard setting for the states of the cells at a node is necessary. For these collisions the state of the rest particle is not decisive. Thus, for both collisions one collision operator (in the following called 2-particle head on collision operator) using two standard settings is used. Afterwards, the 2-particle head-on collision operator for these standard settings is defined.

Definition 5.29 (Standard setting for 2-particle head-on collision of FHP-II LGCA). The standard settings for the 2-particle head-on collision are $\sigma_{2i} = \begin{pmatrix} 0 & 0 & 1 & 0 & 0 & 1 & i \end{pmatrix}$ for $i = 0, 1$.

Definition 5.30 (2-particle head-on collision operator for standard setting of FHP-II LGCA). The non-deterministic collision operator for the standard setting $\mathcal{C}_2 \colon \{\sigma_{20}, \sigma_{21}\} \to Q^{1\times 7}$ is defined as

$$\mathcal{C}_2\sigma_{2i} := \begin{cases} \begin{pmatrix} 1 & 0 & 0 & 1 & 0 & 0 & i \end{pmatrix} & \text{if } \xi_{t,l} = 0 \\ \begin{pmatrix} 0 & 1 & 0 & 0 & 1 & 0 & i \end{pmatrix} & \text{if } \xi_{t,l} = 1 \end{cases} \tag{5.32}$$

whereby $\xi_{t,l}$ denotes a time- and site-dependent Boolean variable. $\xi_{t,l}$ is one when the particles are rotated clockwise, and zero when the particles are rotated counter-clockwise. For the two possible values equal probabilities are used, i.e.

$$\mathbb{P}(\xi_{t,l} = 0) = \frac{1}{2} = \mathbb{P}(\xi_{t,l} = 1). \tag{5.33}$$

Furthermore independence of the $\xi_{t,l}$'s is assumed.

Remark 5.31. $\mathcal{C}_2$ can be interpreted as

$$\begin{cases} \pi_1|_{\{\sigma_{20}, \sigma_{21}\}} & \text{if } \xi_{t,l} = 0 \\ \pi_2|_{\{\sigma_{20}, \sigma_{21}\}} & \text{if } \xi_{t,l} = 1 \end{cases} \tag{5.34}$$

with a time- and site-dependent Boolean variable $\xi_{t,l}$ as in Definition 5.30.

Symmetric 3-particle collision with and without spectator rest particle:
For defining the symmetric 3-particle collision with and without spectator rest particle, a standard setting for the states of the cells at a node is necessary. For these collisions the state of the rest particle is not decisive. Thus, for both collisions one collision operator (in the following called symmetric 3-particle collision operator) using two standard settings is considered. Afterwards, the symmetric 3-particle collision operator for these standard settings is defined.

Definition 5.32 (Standard setting for symmetric 3-particle collision of FHP-II LGCA). The standard settings for the symmetric 3-particle collision are $\sigma_{3i} = \begin{pmatrix} 0 & 1 & 0 & 1 & 0 & 1 & i \end{pmatrix}$ for $i = 0, 1$.

Definition 5.33 (Symmetric 3-particle collision operator for standard setting of FHP-II LGCA). The deterministic collision operator for the standard setting $\mathcal{C}_3 \colon \{\sigma_{30}, \sigma_{31}\} \to Q^{1 \times 7}$ is defined as

$$\mathcal{C}_3 \sigma_{3i} := \begin{pmatrix} 1 & 0 & 1 & 0 & 1 & 0 & i \end{pmatrix}. \tag{5.35}$$

Remark 5.34. $\mathcal{C}_3$ can be interpreted as permutation $(\pi_1|_{\{\sigma_{30}, \sigma_{31}\}}$ or $\pi_2|_{\{\sigma_{30}, \sigma_{31}\}})$.

Rest particle collision type A:
For defining the rest particle collision type A, a standard setting for the states of the cells at a node is necessary. Afterwards, the rest particle collision type A operator for this standard setting is defined.

Definition 5.35 (Standard setting for rest particle collision type A of FHP-II LGCA). The standard setting for the rest particle collision type A is $\sigma_a = \begin{pmatrix} 0 & 0 & 0 & 0 & 0 & 1 & 1 \end{pmatrix}$.

Definition 5.36 (Rest particle collision type A operator for standard setting of FHP-II LGCA). The deterministic collision operator for the standard setting $\mathcal{C}_a \colon \{\sigma_a\} \to Q^{1 \times 7}$ is defined as

$$\mathcal{C}_a \sigma_a := \begin{pmatrix} 1 & 0 & 0 & 0 & 1 & 0 & 0 \end{pmatrix}. \tag{5.36}$$

Rest particle collision type B:
For defining the rest particle collision type B, a standard setting for the states of the cells at a node is necessary. Afterwards, the rest particle collision type B operator for this standard setting is defined.

Definition 5.37 (Standard setting for rest particle collision type B of FHP-II LGCA). The standard setting for the rest particle collision type B is $\sigma_b = \begin{pmatrix} 1 & 0 & 0 & 0 & 1 & 0 & 0 \end{pmatrix}$.

Definition 5.38 (Rest particle collision type B operator for standard setting of FHP-II LGCA). The deterministic collision operator for the standard setting $\mathcal{C}_b \colon \{\sigma_b\} \to Q^{1 \times 7}$ is defined as

$$\mathcal{C}_b \sigma_b := \begin{pmatrix} 0 & 0 & 0 & 0 & 0 & 1 & 1 \end{pmatrix}. \tag{5.37}$$

Remark 5.39. The collision operators $\mathcal{C}_a$ and $\mathcal{C}_b$ can be interpreted as permutation

$$\pi_a|_{\{\sigma_a\}} = \pi_b|_{\{\sigma_b\}} = \begin{pmatrix} 1 & 2 & 3 & 4 & 5 & 6 & 7 \\ 6 & 2 & 3 & 4 & 7 & 1 & 5 \end{pmatrix}. \tag{5.38}$$

The local collision operator for the FHP-II LGCA is defined by using the collision operators for the standard settings.

Definition 5.40 (Local collision operator of FHP-II LGCA)**.** The local collision operator $\mathcal{C}_l \colon Q^{1 \times 7} \to Q^{1 \times 7}$ is defined as

$$\mathcal{C}_l x := \begin{cases} \pi_x^{-1} \circ C_2 \circ \pi_x x & \text{if } \exists \pi_x \in \Pi \colon \pi_x x \in \{\sigma_{20}, \sigma_{21}\} \\ \pi_x^{-1} \circ C_3 \circ \pi_x x & \text{if } \exists \pi_x \in \Pi \colon \pi_x x \in \{\sigma_{30}, \sigma_{31}\} \\ \pi_x^{-1} \circ C_a \circ \pi_x x & \text{if } \exists \pi_x \in \Pi \colon \pi_x x = \sigma_a \\ \pi_x^{-1} \circ C_b \circ \pi_x x & \text{if } \exists \pi_x \in \Pi \colon \pi_x x = \sigma_b \\ \text{id } x & \text{else.} \end{cases} \tag{5.39}$$

In the following, several lemmas for proving that $\mathcal{C}_l$ is well-defined (Theorem 5.47) are presented.

Lemma 5.41. *For different permutations π_x, $\tilde{\pi}_x \in \Pi$ it holds $\pi_x^{-1} \pi_1 \pi_x = \tilde{\pi}_x^{-1} \pi_1 \tilde{\pi}_x$.*

Proof. The proof is analogous to the proof of Lemma 5.20. $\qquad\square$

Lemma 5.42. *For different permutations π_x, $\tilde{\pi}_x \in \Pi$ it holds $\pi_x^{-1} \pi_2 \pi_x = \tilde{\pi}_x^{-1} \pi_2 \tilde{\pi}_x$.*

Proof. The proof is analogous to the proof of Lemma 5.21. $\qquad\square$

Next, it is shown that $\pi_x^{-1} \circ \mathcal{C}_2 \circ \pi_x x$ is independent of the choice of $\pi_x \in \Pi$.

Lemma 5.43. *For different permutations π_x, $\tilde{\pi}_x \in \Pi$ with $\pi_x x = \sigma_{2i} = \tilde{\pi}_x x$, $i = 0, 1$, it holds $\pi_x^{-1} \mathcal{C}_2 \pi_x x = \tilde{\pi}_x^{-1} \mathcal{C}_2 \tilde{\pi}_x x$.*

Proof. The proof for σ_{2i}, $i = 0, 1$, is analogous to the proof of Lemma 5.22. $\qquad\square$

Next, it is shown that $\pi_x^{-1} \circ \mathcal{C}_3 \circ \pi_x x$ is independent of the choice of $\pi_x \in \Pi$.

Lemma 5.44. *For different permutations π_x, $\tilde{\pi}_x \in \Pi$ with $\pi_x x = \sigma_{3i} = \tilde{\pi}_x x$, $i = 0, 1$, it holds $\pi_x^{-1} \mathcal{C}_3 \pi_x x = \tilde{\pi}_x^{-1} \mathcal{C}_3 \tilde{\pi}_x x$.*

Proof. The proof for σ_{3i}, $i = 0, 1$, is analogous to the proof of Lemma 5.23. $\qquad\square$

Next, it is shown that $\pi_x^{-1} \circ \mathcal{C}_a \circ \pi_x x$ and $\pi_x^{-1} \circ \mathcal{C}_b \circ \pi_x x$ are independent of the choice of $\pi_x \in \Pi$.

Lemma 5.45. *For different permutations π_x, $\tilde{\pi}_x \in \Pi$ with $\pi_x x = \sigma_a = \tilde{\pi}_x x$ it holds $\pi_x^{-1} \mathcal{C}_a \pi_x x = \tilde{\pi}_x^{-1} \mathcal{C}_a \tilde{\pi}_x x$.*

Proof. For the set Π the description of Remark 5.28 is used. Thus, $\pi_x = \pi_1^n$ and $\tilde{\pi}_x = \pi_1^{\tilde{n}}$ with $n, \tilde{n} \in \mathbb{Z}$. It holds

$$\pi_1^n x = \pi_x x = \sigma_a = \tilde{\pi}_x x = \pi_1^{\tilde{n}} x. \tag{5.40}$$

and it follows

$$\pi_1^{n-\tilde{n}} x = x. \tag{5.41}$$

The only rotation with this property is the identity permutation, i.e.

$$\pi_1^{n-\tilde{n}} = \mathrm{id}. \tag{5.42}$$

Using this relationship it holds

$$\pi_x = \pi_1^n = \pi_1^n \pi_1^{\tilde{n}-\tilde{n}} = \pi_1^{\tilde{n}+n-\tilde{n}} = \pi_1^{\tilde{n}} \underbrace{\pi_1^{n-\tilde{n}}}_{=\mathrm{id}} = \pi_1^{\tilde{n}} = \tilde{\pi}_x. \tag{5.43}$$

Thus also the inverse permutations are equal, i.e.

$$\pi_x^{-1} = \tilde{\pi}_x^{-1}. \tag{5.44}$$

Finally, it follows

$$\pi_x^{-1} \mathcal{C}_a \pi_x x = \tilde{\pi}_x^{-1} \mathcal{C}_a \tilde{\pi}_x x. \tag{5.45}$$

$\square$

Lemma 5.46. *For different permutations* $\pi_x, \tilde{\pi}_x \in \Pi$ *with* $\pi_x x = \sigma_b = \tilde{\pi}_x x$ *it holds* $\pi_x^{-1} \mathcal{C}_b \pi_x x = \tilde{\pi}_x^{-1} \mathcal{C}_b \tilde{\pi}_x x$.

Proof. The proof is analogous to the proof of Lemma 5.45. $\square$

Theorem 5.47. *The local collision operator* $\mathcal{C}_l$ *is well-defined.*

Proof. The proof is similar to the proof of Theorem 5.24. In order to prove the theorem, five cases are necessary. For each case it is assumed that $x_1 = x_2$.
Case 1:
For σ_{2i}, $i = 0, 1$, the proof is analogous to the proof of case 1 of Theorem 5.24 (using Lemma 5.43).
Case 2:
For σ_{3i}, $i = 0, 1$, the proof is analogous to the proof of case 2 of Theorem 5.24 (using Lemma 5.44).
Case 3:
Case 3 represents $\exists \pi_{x_1} \in \Pi \colon \pi_{x_1} x_1 = \sigma_a$ and $\exists \pi_{x_2} \in \Pi \colon \pi_{x_2} x_2 = \sigma_a$. With Lemma 5.45 it follows

$$\mathcal{C}_l x_1 = \pi_{x_1}^{-1} \mathcal{C}_a \pi_{x_1} x_1 = \tilde{\pi}_{x_2}^{-1} \mathcal{C}_a \tilde{\pi}_{x_2} x_2 = \mathcal{C}_l x_2. \tag{5.46}$$

Case 4:
Case 4 represents $\exists \pi_{x_1} \in \Pi \colon \pi_{x_1} x_1 = \sigma_b$ and $\exists \pi_{x_2} \in \Pi \colon \pi_{x_2} x_2 = \sigma_b$. With Lemma 5.46 it follows

$$\mathcal{C}_l x_1 = \pi_{x_1}^{-1} \mathcal{C}_b \pi_{x_1} x_1 = \tilde{\pi}_{x_2}^{-1} \mathcal{C}_b \tilde{\pi}_{x_2} x_2 = \mathcal{C}_l x_2. \tag{5.47}$$

Case 5:

Case 5 is for all $x \in Q^{1\times 7}$ that are not covered with the cases 1-4. With the assumption $x_1 = x_2$ it follows

$$\mathcal{C}_l x_1 = \operatorname{id} x_1 = \operatorname{id} x_2 = \mathcal{C}_l x_2. \tag{5.48}$$

The following statements assure that exactly one case is valid for every $x \in Q^{1\times 7}$:

For a node with 0, 1, 5, 6 or 7 occupied cells it is not possible that case 1, 2, 3 or 4 can be applied. This is due to the fact that application of $\pi_x \in \Pi$ does not change the number of particles at a node. Furthermore, application of $\pi_x \in \Pi$ does not change the state of the seventh cell. The "distance" of occupied cells cannot be changed by application of $\pi \in \Pi$. Therefore, it is not possible that two cases of the cases 1-4 hold.

Similarly to the proof of Theorem 5.24, it can be shown that it is not possible that case 5 and one of the other cases hold. $\qquad\square$

Remark 5.48. In general, the local collision operator is not injective due to the non-deterministic 2-particle head-on collision.

In the following, a matrix $X \in Q^{|\mathcal{L}|\times 7}$ is considered: $X_{i,.} \in Q^{1\times 7}$ for $i = 1, \ldots, |\mathcal{L}|$, whereby the elements of $\mathcal{L}$ are numbered in an arbitrary, fixed order.

Definition 5.49 (Global collision operator of FHP-II LGCA)**.** The global collision operator $\mathcal{C}\colon Q^{|\mathcal{L}|\times 7} \to Q^{|\mathcal{L}|\times 7}$ is defined elementwise as

$$(\mathcal{C}X)_{i,.} := \mathcal{C}_l X_{i,.}. \tag{5.49}$$

Collision of FHP-III Lattice Gas Cellular Automaton:
The formal definition for the collision rules of FHP-III LGCA is similar to the definition of FHP-II LGCA. For simplicity it is omitted here.

Streaming of FHP Lattice Gas Cellular Automaton
Next, the local streaming operator is defined. In the following, m denotes the number of cells at each node, whereby $m = 6$ (FHP-I LGCA) and $m = 7$ (FHP-II LGCA and FHP-III LGCA).

Definition 5.50 (Local streaming operator of FHP LGCA)**.** The local streaming operator $\mathcal{S}_l\colon Q^{m\times m} \to Q^{1\times m}$ is defined as

$$\mathcal{S}_l n := \begin{pmatrix} n_{11} & n_{22} & \ldots & n_{mm} \end{pmatrix}. \tag{5.50}$$

Remark 5.51. For FHP-I LGCA the entries of the matrix $n \in Q^{6\times 6}$ represent the 36 cells located at the neighbouring nodes. In Figure 5.4 a node, its neighbouring nodes and the corresponding matrix n are shown.
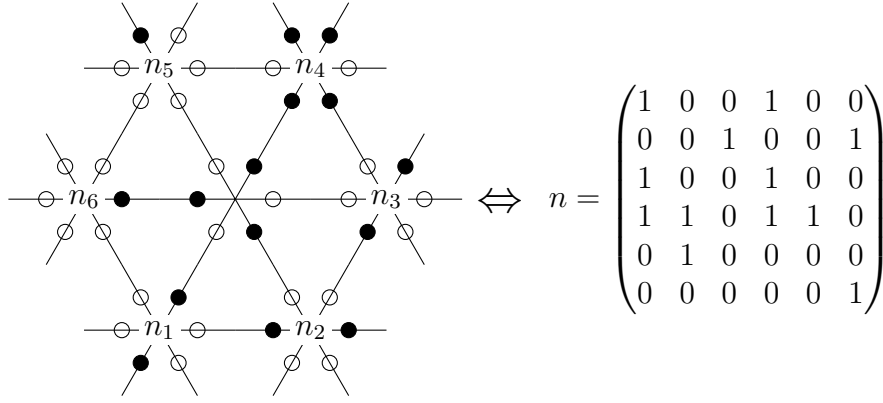
Figure 5.4: Illustration of matrix $n \in Q^{6 \times 6}$ for FHP-I LGCA

For FHP-II LGCA and FHP-III LGCA the seventh row of n represents the cells of the node itself.

Theorem 5.52. *The local streaming operator S_l is well-defined.*

Proof. Consider $S_l x_1 = y_1 \neq y_2 = S_l x_2$. According to the definition of S_l, this means that at least one of the diagonal entries is different and further the matrices are different.

$$y_1 \neq y_2 \Rightarrow \exists i | (x_1)_{ii} \neq (x_2)_{ii} \Rightarrow x_1 \neq x_2 \tag{5.51}$$

Thus, $y_1 \neq y_2 \Rightarrow x_1 \neq x_2$. $\qquad \square$

For each $X_{i,.}$ the states of the cells of the m neighbouring nodes are necessary for calculating the state of the cells of node i for the new time step. The tensor, which contains the states of the cells of the neighbouring nodes for each lattice point, is denoted by $N \in Q^{m \times m \times |\mathcal{L}|}$. $N_{.,.,i} \in Q^{m \times m}$ are the states of the cells of the neighbouring nodes of lattice point i.

Definition 5.53 (Global streaming operator of FHP LGCA)**.** The global streaming operator $\mathcal{S} \colon Q^{m \times m \times |\mathcal{L}|} \to Q^{|\mathcal{L}| \times m}$ is defined as

$$(\mathcal{S}N)_{i,.} := \mathcal{S}_l N_{.,.,i}. \tag{5.52}$$

Neighbouring Nodes of FHP Lattice Gas Cellular Automaton
For defining the evolution of the FHP LGCA, an operator which assigns to each node the neighbouring nodes is necessary. More precise a global operator, which assigns the states of the cells of the neighbouring nodes to each node in $Q^{1 \times m}$ is defined.

Definition 5.54 (Neighbouring nodes operator of FHP LGCA)**.** The neighbouring nodes operator $\mathcal{N} \colon Q^{|\mathcal{L}| \times m} \to Q^{m \times m \times |\mathcal{L}|}$ is defined as

$$(\mathcal{N}X)_{.,.,i} := N_{.,.,i}. \tag{5.53}$$

Evolution of FHP Lattice Gas Cellular Automaton

Finally, the evolution operator of the FHP LGCA is defined.

Definition 5.55 (Evolution operator of FHP LGCA)**.** The evolution operator
$\mathcal{E}\colon Q^{|\mathcal{L}|\times m} \to Q^{|\mathcal{L}|\times m}$ is defined by

$$\mathcal{E} := \mathcal{S} \circ \mathcal{N} \circ \mathcal{C}, \tag{5.54}$$

whereby $\mathcal{C}$ is the collision operator, $\mathcal{N}$ the neighbouring nodes operator and $\mathcal{S}$ is the streaming operator.

5.3 Formal Definition of the Synthesis of Lattice Gas Cellular Automaton and Random Walk

In this Section the formal definition of the synthesis of LGCA and random walk is described. The collision operator of the synthesis of LGCA and random walk is not changed, i.e. depending on the used LGCA the corresponding collision operator is used. The basic idea of the synthesis of LGCA and random walk was that particles can have different movement properties. The different movement types are, on the one hand, movement according to the classical streaming of the LGCA, and on the other hand, movement according to a two-dimensional random walk. Therefore, the streaming operator is not changed, i.e. the streaming operator of the corresponding LGCA is used for the synthesis of LGCA and random walk. To include these different movement types, an inclusion operator was defined. This inclusion operator is the identity if movement is according to LGCA. For including movement according to random walk the locations of the corresponding cells at a node are changed according to a random walk. Afterwards, the streaming is performed.

First, this synthesis is introduced for the HPP LGCA and two-dimensional random walk using a square lattice. Afterwards, the synthesis of FHP LGCA and two-dimensional random walk on the triangular lattice is defined. For simplicity, both models (synthesis of HPP LGCA and random walk, and the synthesis of FHP LGCA and random walk) are in the corresponding sections also referred to as "synthesis model".

5.3.1 Formal Definition of the Synthesis of HPP Lattice Gas Cellular Automaton and Random Walk

Based on the formal definition of the HPP LGCA in Section 5.1, the formal definition of the synthesis of the HPP LGCA and the two-dimensional random walk on the square lattice was defined. For simplicity, the synthesis of HPP LGCA and random walk is in the following also referred to as "synthesis model".

Like for the HPP LGCA, the set of states for the synthesis model is $Q = \{0, 1\}$, whereby 0 and 1 correspond to empty and occupied by a particle, respectively. The lattice is denoted by $\mathcal{L}$.

Collision of the Synthesis of HPP Lattice Gas Cellular Automaton and Random Walk

The local collision operator $\mathcal{C}_l$ and the global collision operator $\mathcal{C}$ of the synthesis model are defined by Definition 5.1 and Definition 5.4, respectively.

Remark 5.56. In contrast to the deterministic collision rule of the HPP LGCA, for the synthesis model this collision rule becomes non-deterministic. This is due to particles moving according to random walk. Thus, rotations by $\pi/2$ and $-\pi/2$ lead to different final states after collision.

Inclusion of Random Walk of the Synthesis of HPP Lattice Gas Cellular Automaton and Random Walk

In the following, a tensor $X \in Q^{2 \times 2 \times |\mathcal{L}|}$ is considered: $X_{.,.,i} \in Q^{2 \times 2}$ for $i = 1, \ldots, |\mathcal{L}|$, whereby the elements of $\mathcal{L}$ are numbered in an arbitrary, fixed order. For defining the evolution of the synthesis model, it is necessary to define the corresponding type of movement: movement according to HPP LGCA or movement according to random walk.

Definition 5.57 (Movement type). The movement type mt of a cell is defined by

$$mt = \begin{cases} 0 & \text{if the state of the cell is 0,} \\ 1 & \text{if movement according to HPP LGCA,} \\ 2 & \text{if movement according to random walk.} \end{cases} \qquad (5.55)$$

The set of movement types is given by $T = \{0, 1, 2\}$.

Next, a classification of movement is introduced. This classification of movement is a matrix containing the corresponding movement types of the four cells located at a node.

Definition 5.58 (Local classification of movement). The local classification of movement is given by $K_l \in T^{2 \times 2}$.

The total number of particles m_{total} is split into two entities, particles moving according to HPP LGCA, m_{LGCA}, and particles moving according to the random walk, m_{RW}. Thus

$$m_{total} = m_{LGCA} + m_{RW}. \qquad (5.56)$$

For all cells with movement type 2 the random walk is included in the model. The formal definition is motivated in the following:

Example 5.59. A node with one cell with state 1 and movement type 2 is considered. The matrix with the states of the cells is denoted by $x \in Q^{2 \times 2}$. In this example not the whole evolution is presented, only the inclusion of random walk (one operator within the evolution) is discussed. The considered random walk is a simple random walk. The simple random walk is included in the model by random choice of the lattice vector. The

lattice vector has a corresponding position of the cell, and thus a corresponding entry in x. A random variable Z with

$$\mathbb{P}(Z = e_k) = \mathbb{P}(Z = -e_k) = \frac{1}{4}, \; k = 1, 2 \tag{5.57}$$

is used for the simple random walk. Further, the entries of x and the vectors $e_k, -e_k$, $k = 1, 2$, are mapped according to

$$
\begin{aligned}
x_{12} &\;\hat{=}\; e_1 \\
x_{11} &\;\hat{=}\; e_2 \\
x_{21} &\;\hat{=}\; -e_1 \\
x_{22} &\;\hat{=}\; -e_2.
\end{aligned}
\tag{5.58}
$$

For

$$x = \begin{pmatrix} 0 & 1 \\ 0 & 0 \end{pmatrix} \text{ with classification of movement } K_l = \begin{pmatrix} 0 & 2 \\ 0 & 0 \end{pmatrix} \tag{5.59}$$

and $Z = -e_2$ the simple random walk is included in the model by changing x to

$$x = \begin{pmatrix} 0 & 0 \\ 0 & 1 \end{pmatrix}. \tag{5.60}$$

In Figure 5.5 this inclusion of simple random walk is shown.
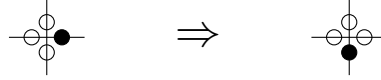
Figure 5.5: Illustration of inclusion of simple random walk for synthesis of HPP LGCA and random walk

In the following, the inclusion of the random walk is described formally. First, the mapping of the cells at each node and the lattice vectors c_1, c_2, c_3, c_4 is defined by

$$
\begin{aligned}
x_{12} &\;\hat{=}\; c_1 \\
x_{11} &\;\hat{=}\; c_2 \\
x_{21} &\;\hat{=}\; c_3 \\
x_{22} &\;\hat{=}\; c_4.
\end{aligned}
\tag{5.61}
$$

Thus, for the random variable Z it holds

$$\mathbb{P}(Z = c_i) = \frac{1}{4}, \quad i = 1, \ldots, 4. \tag{5.62}$$

These probabilities change due to the number of particles with movement type 1 and 2. Furthermore, there are different outputs of the inclusion of random walk. In the following, these outputs are described using local operators $\mathcal{R}_{m_1, m_2} \colon Q^{2 \times 2} \to Q^{2 \times 2}$. The indices m_1 and m_2 are the numbers of particles with movement type 1 and 2, respectively.

Remark 5.60. The selection of particles with movement type 2 for the operators $\mathcal{R}_{m_1,m_2}$ can be done in any arbitrary order. This is because the a priori probability that a particle occupies a certain cell after the random walk is the same independent from the order.

One particle with movement type 2:
– Zero particles with movement type 1:

$$\mathbb{P}(Z = c_i) = \frac{1}{4}, \quad \forall i \in I = \{1, \ldots, 4\} \tag{5.63}$$

The local operator $\mathcal{R}_{0,1}\colon Q^{2\times 2} \to Q^{2\times 2}$ is defined by

$$\mathcal{R}_{0,1}x := \begin{cases} \begin{pmatrix} 0 & 1 \\ 0 & 0 \end{pmatrix} & \text{if } Z = c_1, \\[2ex] \begin{pmatrix} 1 & 0 \\ 0 & 0 \end{pmatrix} & \text{if } Z = c_2, \\[2ex] \begin{pmatrix} 0 & 0 \\ 1 & 0 \end{pmatrix} & \text{if } Z = c_3, \\[2ex] \begin{pmatrix} 0 & 0 \\ 0 & 1 \end{pmatrix} & \text{if } Z = c_4. \end{cases} \tag{5.64}$$

– One particle (corresponding lattice vector c_j) with movement type 1:

$$\mathbb{P}(Z = c_i) = \frac{1}{3}, \quad \forall i \in I = \{1, \ldots, 4\}\backslash\{j\} \tag{5.65}$$

and

$$\mathbb{P}(Z = c_j) = 0 \tag{5.66}$$

The local operator $\mathcal{R}_{1,1}\colon Q^{2\times 2} \to Q^{2\times 2}$ is defined by

$$\mathcal{R}_{1,1}x := \begin{cases} \begin{pmatrix} 1 & 1 \\ 0 & 0 \end{pmatrix} & \text{if } Z = c_1 \text{ and } j = 2, \\[2ex] \begin{pmatrix} 0 & 1 \\ 1 & 0 \end{pmatrix} & \text{if } Z = c_1 \text{ and } j = 3, \\[2ex] \begin{pmatrix} 0 & 1 \\ 0 & 1 \end{pmatrix} & \text{if } Z = c_1 \text{ and } j = 4, \\[2ex] \vdots \ \} & \text{analogous for } Z = c_2, \ Z = c_3 \text{ and } Z = c_4. \end{cases} \tag{5.67}$$

– Two particles (corresponding lattice vectors c_{j_1}, c_{j_2}) with movement type 1:

$$\mathbb{P}(Z = c_i) = \frac{1}{2}, \quad \forall i \in I = \{1, \ldots, 4\}\backslash\{j_1, j_2\} \tag{5.68}$$

and

$$\mathbb{P}(Z = c_{j_1}) = \mathbb{P}(Z = c_{j_2}) = 0 \tag{5.69}$$

The local operator $\mathcal{R}_{2,1} \colon Q^{2\times 2} \to Q^{2\times 2}$ is defined by

$$
\mathcal{R}_{2,1}x := \begin{cases}
\begin{pmatrix} 1 & 1 \\ 1 & 0 \end{pmatrix} & \text{if } Z = c_1 \text{ and } \{j_1, j_2\} = \{2, 3\}, \\[2ex]
\begin{pmatrix} 0 & 1 \\ 1 & 1 \end{pmatrix} & \text{if } Z = c_1 \text{ and } \{j_1, j_2\} = \{3, 4\}, \\[2ex]
\begin{pmatrix} 1 & 1 \\ 0 & 1 \end{pmatrix} & \text{if } Z = c_1 \text{ and } \{j_1, j_2\} = \{2, 4\}, \\[2ex]
\vdots \;\} & \text{analogous for } Z = c_2, \ Z = c_3 \text{ and } Z = c_4.
\end{cases} \tag{5.70}
$$

– Three particles (corresponding lattice vectors $c_{j_1}, c_{j_2}, c_{j_3}$) with movement type 1:

$$
\mathbb{P}(Z = c_i) = 1, \quad \forall i \in I = \{1, \dots, 4\} \backslash \{j_1, j_2, j_3\} \tag{5.71}
$$

and

$$
\mathbb{P}(Z = c_{j_1}) = \mathbb{P}(Z = c_{j_2}) = \mathbb{P}(Z = c_{j_3}) = 0 \tag{5.72}
$$

In this case the process is deterministic. Nothing changes in this case (for distinguishable and indistinguishable particles). The local operator $\mathcal{R}_{3,1} \colon Q^{2\times 2} \to Q^{2\times 2}$ is defined by

$$
\mathcal{R}_{3,1}x := \begin{pmatrix} 1 & 1 \\ 1 & 1 \end{pmatrix}. \tag{5.73}
$$

Two particles with movement type 2:
– Zero particles with movement type 1:
For the first particle the random variable Z_1 is used in the following way.

$$
\mathbb{P}(Z_1 = c_i) = \frac{1}{4}, \quad \forall i \in I = \{1, \dots, 4\} \tag{5.74}
$$

and the chosen lattice vector is denoted by c_l. For the second particle the random variable Z_2 is used:

$$
\mathbb{P}(Z_2 = c_i) = \frac{1}{3}, \quad \forall i \in I = \{1, \dots, 4\} \backslash \{l\} \tag{5.75}
$$

and

$$
\mathbb{P}(Z_2 = c_l) = 0. \tag{5.76}
$$

The local operator $\mathcal{R}_{0,2} \colon Q^{2\times 2} \to Q^{2\times 2}$ is defined by

$$\mathcal{R}_{0,2}x := \begin{cases} \begin{pmatrix} 1 & 1 \\ 0 & 0 \end{pmatrix} & \text{if } Z_i \neq c_3, c_4,\ i = 1,2, \\[2mm] \begin{pmatrix} 0 & 1 \\ 1 & 0 \end{pmatrix} & \text{if } Z_i \neq c_2, c_4,\ i = 1,2, \\[2mm] \begin{pmatrix} 0 & 1 \\ 0 & 1 \end{pmatrix} & \text{if } Z_i \neq c_2, c_3,\ i = 1,2, \\[2mm] \begin{pmatrix} 1 & 0 \\ 1 & 0 \end{pmatrix} & \text{if } Z_i \neq c_1, c_4,\ i = 1,2, \\[2mm] \begin{pmatrix} 1 & 0 \\ 0 & 1 \end{pmatrix} & \text{if } Z_i \neq c_1, c_3,\ i = 1,2, \\[2mm] \begin{pmatrix} 0 & 0 \\ 1 & 1 \end{pmatrix} & \text{if } Z_i \neq c_1, c_2,\ i = 1,2. \end{cases} \tag{5.77}$$

– One particle (corresponding lattice vector c_j) with movement type 1:
For the first particle the random variable Z_1 is used in the following way.

$$\mathbb{P}(Z_1 = c_i) = \frac{1}{3}, \quad \forall i \in I = \{1, \dots, 4\} \backslash \{j\} \tag{5.78}$$

and

$$\mathbb{P}(Z_1 = c_j) = 0 \tag{5.79}$$

and the chosen lattice vector is denoted by c_l. For the second particle the random variable Z_2 is used:

$$\mathbb{P}(Z_2 = c_i) = \frac{1}{2}, \quad \forall i \in I = \{1, \dots, 4\} \backslash \{j, l\} \tag{5.80}$$

and

$$\mathbb{P}(Z_2 = c_l) = \mathbb{P}(Z_2 = c_j) = 0. \tag{5.81}$$

The local operator $\mathcal{R}_{1,2} \colon Q^{2\times 2} \to Q^{2\times 2}$ is defined by

$$\mathcal{R}_{1,2}x := \begin{cases} \begin{pmatrix} 1 & 1 \\ 1 & 0 \end{pmatrix} & \text{if } Z_i \neq c_3, c_4,\ i = 1,2 \text{ and } j = 3, \\[2mm] \begin{pmatrix} 1 & 1 \\ 0 & 1 \end{pmatrix} & \text{if } Z_i \neq c_3, c_4,\ i = 1,2 \text{ and } j = 4, \\[2mm] \vdots\ \} & \text{analogous for } Z_i \neq c_k, c_l, i = 1,2, k \neq l, k, l \in \{1, \dots, 4\}. \end{cases} \tag{5.82}$$

– Two particles (corresponding lattice vectors c_{j_1}, c_{j_2}) with movement type 1:
For the first particle the random variable Z_1 is used in the following way.

$$\mathbb{P}(Z_1 = c_i) = \frac{1}{2}, \quad \forall i \in I = \{1, \dots, 4\} \backslash \{j_1, j_2\} \tag{5.83}$$

and

$$\mathbb{P}(Z_1 = c_{j_1}) = \mathbb{P}(Z_1 = c_{j_2}) = 0 \tag{5.84}$$

and the chosen lattice vector is denoted by c_l. For the second particle the random variable Z_2 is used:

$$\mathbb{P}(Z_2 = c_i) = 1, \quad \forall i \in I = \{1, \ldots, 4\} \backslash \{j_1, j_2, l\} \tag{5.85}$$

and

$$\mathbb{P}(Z_2 = c_{j_1}) = \mathbb{P}(Z_2 = c_{j_2}) = \mathbb{P}(Z_2 = c_l) = 0. \tag{5.86}$$

In this case the movement types of the cells do not change. For indistinguishable particles nothing changes. The local operator $\mathcal{R}_{2,2} \colon Q^{2\times 2} \to Q^{2\times 2}$ is defined by

$$\mathcal{R}_{2,2} x := \begin{pmatrix} 1 & 1 \\ 1 & 1 \end{pmatrix}. \tag{5.87}$$

Three particles with movement type 2:
– Zero particles with movement type 1:
For the first particle the random variable Z_1 is used in the following way.

$$\mathbb{P}(Z_1 = c_i) = \frac{1}{4}, \quad \forall i \in I = \{1, \ldots, 4\} \tag{5.88}$$

and the chosen lattice vector is denoted by c_{l_1}. For the second particle the random variable Z_2 is used

$$\mathbb{P}(Z_2 = c_i) = \frac{1}{3}, \quad \forall i \in I = \{1, \ldots, 4\} \backslash \{l_1\} \tag{5.89}$$

and

$$\mathbb{P}(Z_2 = c_{l_1}) = 0 \tag{5.90}$$

and the chosen lattice vector is denoted by c_{l_2}. For the third particle the random variable Z_3 is used

$$\mathbb{P}(Z_3 = c_i) = \frac{1}{2}, \quad \forall i \in I = \{1, \ldots, 4\} \backslash \{l_1, l_2\} \tag{5.91}$$

and

$$\mathbb{P}(Z_3 = c_{l_1}) = \mathbb{P}(Z_3 = c_{l_2}) = 0. \tag{5.92}$$

The local operator $\mathcal{R}_{0,3} \colon Q^{2\times 2} \to Q^{2\times 2}$ is defined by

$$\mathcal{R}_{0,3} x := \begin{cases} \begin{pmatrix} 1 & 0 \\ 1 & 1 \end{pmatrix} & \text{if } Z_i \neq c_1, i = 1, 2, 3, \\[2mm] \begin{pmatrix} 0 & 1 \\ 1 & 1 \end{pmatrix} & \text{if } Z_i \neq c_2, i = 1, 2, 3, \\[2mm] \begin{pmatrix} 1 & 1 \\ 0 & 1 \end{pmatrix} & \text{if } Z_i \neq c_3, i = 1, 2, 3, \\[2mm] \begin{pmatrix} 1 & 1 \\ 1 & 0 \end{pmatrix} & \text{if } Z_i \neq c_4, i = 1, 2, 3. \end{cases} \tag{5.93}$$

– One particle (corresponding lattice vector c_j) with movement type 1:
For the first particle the random variable Z_1 is used in the following way.

$$\mathbb{P}(Z_1 = c_i) = \frac{1}{3}, \quad \forall i \in I = \{1, \ldots, 4\} \backslash \{j\} \tag{5.94}$$

and

$$\mathbb{P}(Z_1 = c_j) = 0 \tag{5.95}$$

and the chosen lattice vector is denoted by c_{l_1}. For the second particle the random variable Z_2 is used

$$\mathbb{P}(Z_2 = c_i) = \frac{1}{2}, \quad \forall i \in I = \{1, \ldots, 4\} \backslash \{j, l_1\} \tag{5.96}$$

and

$$\mathbb{P}(Z_2 = c_j) = \mathbb{P}(Z_2 = c_{l_1}) = 0 \tag{5.97}$$

and the chosen lattice vector is denoted by c_{l_2}. For the third particle the random variable Z_3 is used

$$\mathbb{P}(Z_3 = c_i) = 1, \quad \forall i \in I = \{1, \ldots, 4\} \backslash \{j, l_1, l_2\} \tag{5.98}$$

and

$$\mathbb{P}(Z_3 = c_j) = \mathbb{P}(Z_3 = c_{l_1}) = \mathbb{P}(Z_3 = c_{l_2}) = 0. \tag{5.99}$$

In this case the movement types of the cells do not change. For indistinguishable particles nothing changes. The local operator $\mathcal{R}_{1,3} \colon Q^{2\times2} \to Q^{2\times2}$ is defined by

$$\mathcal{R}_{1,3}x := \begin{pmatrix} 1 & 1 \\ 1 & 1 \end{pmatrix}. \tag{5.100}$$

Four particles with movement type 2:
– Zero particles with movement type 1:
For the first particle the random variable Z_1 is used in the following way.

$$\mathbb{P}(Z_1 = c_i) = \frac{1}{4}, \quad \forall i \in I = \{1, \ldots, 4\} \tag{5.101}$$

and the chosen lattice vector is denoted by c_{l_1}. For the second particle the random variable Z_2 is used

$$\mathbb{P}(Z_2 = c_i) = \frac{1}{3}, \quad \forall i \in I = \{1, \ldots, 4\} \backslash \{l_1\} \tag{5.102}$$

and

$$\mathbb{P}(Z_2 = c_{l_1}) = 0 \tag{5.103}$$

and the chosen lattice vector is denoted by c_{l_2}. For the third particle the random variable Z_3 is used

$$\mathbb{P}(Z_3 = c_i) = \frac{1}{2}, \quad \forall i \in I = \{1, \ldots, 4\} \backslash \{l_1, l_2\} \tag{5.104}$$

and

$$\mathbb{P}(Z_3 = c_{l_1}) = \mathbb{P}(Z_3 = c_{l_2}) = 0 \tag{5.105}$$

and the chosen lattice vector is denoted by c_{l_3}. For the fourth particle the random variable Z_4 is used

$$\mathbb{P}(Z_4 = c_i) = 1, \quad \forall i \in I = \{1, \dots, 4\} \backslash \{l_1, l_2, l_3\} \tag{5.106}$$

and

$$\mathbb{P}(Z_4 = c_{l_1}) = \mathbb{P}(Z_4 = c_{l_2}) = \mathbb{P}(Z_4 = c_{l_3}) = 0. \tag{5.107}$$

For indistinguishable particles nothing changes. The local operator $\mathcal{R}_{0,4} \colon Q^{2\times2} \to Q^{2\times2}$ is defined by

$$\mathcal{R}_{0,4}x := \begin{pmatrix} 1 & 1 \\ 1 & 1 \end{pmatrix}. \tag{5.108}$$

Definition 5.61 (Local inclusion operator of random walk)**.** The local inclusion operator $\mathcal{R}_l \colon Q^{2\times2} \to Q^{2\times2}$ is defined by

$$\mathcal{R}_l x := \begin{cases} \mathrm{I}\,x & \text{if } K_l(i_1, i_2) \neq 2 \, \forall i_1, i_2 \in \{1, 2\} \\ \mathcal{R}_{m_1, m_2}x & \text{if } \exists K_l(i_1, i_2) = 2, \ i_1, i_2 \in \{1, 2\} \end{cases} \tag{5.109}$$

where m_1 and m_2 are the numbers of particles with movement type 1 and 2, respectively.

Definition 5.62 (Global inclusion operator of random walk)**.** The global inclusion operator $\mathcal{R} \colon Q^{2\times2\times|\mathcal{L}|} \to Q^{2\times2\times|\mathcal{L}|}$ is defined by

$$(\mathcal{R}X)_{.,.,i} := \mathcal{R}_l X_{.,.,i}. \tag{5.110}$$

Streaming and Neighbouring Nodes of the Synthesis of HPP Lattice Gas Cellular Automaton and Random Walk

The local streaming operator $\mathcal{S}_l$, the global streaming operator $\mathcal{S}$ and the neighbouring nodes operator $\mathcal{N}$ of the synthesis model are defined by Definition 5.5, Definition 5.7 and Definition 5.8 respectively.

Evolution of the Synthesis of HPP Lattice Gas Cellular Automaton and Random Walk

Finally, the evolution operator of the synthesis model is defined.

Definition 5.63 (Evolution operator of the synthesis model)**.** The evolution operator $\mathcal{E} \colon Q^{2\times2\times|\mathcal{L}|} \to Q^{2\times2\times|\mathcal{L}|}$ is defined by

$$\mathcal{E} := \mathcal{S} \circ \mathcal{N} \circ \mathcal{R} \circ \mathcal{C}, \tag{5.111}$$

whereby $\mathcal{C}$ is the collision operator, $\mathcal{R}$ is the inclusion operator, $\mathcal{N}$ the neighbouring nodes operator and $\mathcal{S}$ is the streaming operator.

Remark 5.64. In addition to the calculation of the evolution of the states of the cells the movement type of the cells has to be updated too.

In Figure 5.6 an example for the evolution of the synthesis model is shown. The particle with movement type 2 is shown in blue.
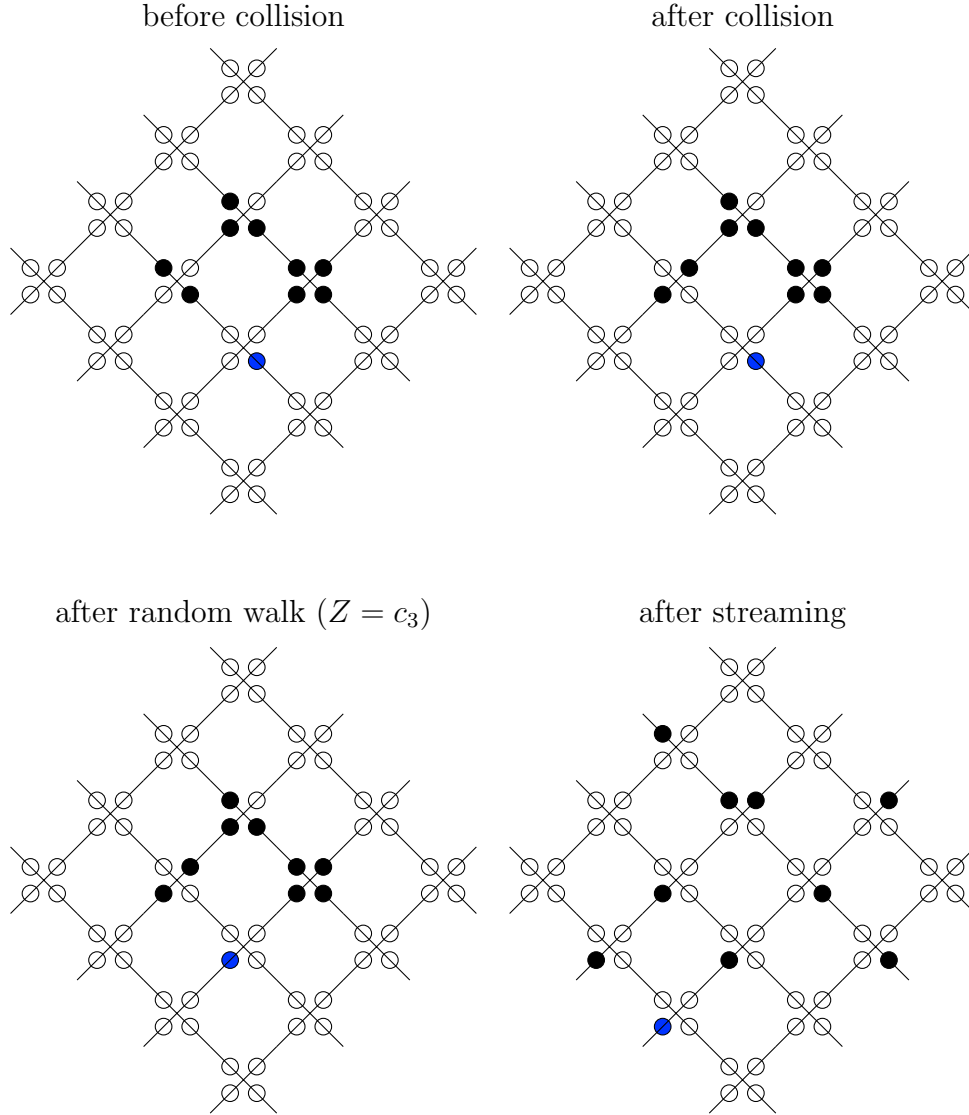
Figure 5.6: Illustration of the evolution of the synthesis of the HPP LGCA and random walk

5.3.2 Formal Definition of the Synthesis of FHP Lattice Gas Cellular Automaton and Random Walk

Based on the definition of the FHP LGCA in Section 5.2, the formal definition of the synthesis of the FHP LGCA and the two-dimensional random walk on the triangular lattice was defined. For simplicity, the synthesis of FHP LGCA and random walk is in

the following also referred to as "synthesis model".

Like for the FHP LGCA, the set of states for the synthesis model is $Q = \{0, 1\}$, whereby 0 and 1 correspond to empty and occupied by a particle, respectively. The lattice is denoted by $\mathcal{L}$.

Collision of the Synthesis of FHP Lattice Gas Cellular Automaton and Random Walk

The local collision operator $\mathcal{C}_l$ and the global collision operator $\mathcal{C}$ of the synthesis model are defined by Definition 5.19 and Definition 5.26 for FHP-I LGCA and by Definition 5.40 and Definition 5.49 for FHP-II LGCA.

Remark 5.65. The deterministic collision rules of the FHP LGCA become non-deterministic for the synthesis model. This is due to particles moving according to random walk. Thus, rotations by $\pi/3$ and $-\pi/3$ lead to different final states after collision.

Inclusion of Random Walk of the Synthesis of FHP Lattice Gas Cellular Automaton and Random Walk

In the following, a matrix $X \in Q^{|\mathcal{L}| \times m}$ with $m = 6$ for FHP-I LGCA and $m = 7$ for FHP-II LGCA is considered: $X_{i,\cdot} \in Q^{1 \times m}$ for $i = 1, \ldots, |\mathcal{L}|$, whereby the elements of $\mathcal{L}$ are numbered in an arbitrary, fixed order. For defining the evolution of the synthesis model, it is necessary to define the corresponding type of movement: movement according to FHP LGCA or movement according to random walk.

Definition 5.66 (movement type)**.** The movement type mt of a cell is defined by

$$mt = \begin{cases} 0 & \text{if the state of the cell is 0,} \\ 1 & \text{if movement according to FHP LGCA,} \\ 2 & \text{if movement according to random walk.} \end{cases} \tag{5.112}$$

The set of movement types is given by $T = \{0, 1, 2\}$.

Next, a classification of movement is introduced. This classification of movement is a vector containing the corresponding movement types of the m cells located at a node.

Definition 5.67 (Local classification of movement)**.** The local classification of movement is given by $K_l \in T^{1 \times m}$ with $m = 6$ for FHP-I LGCA and $m = 7$ for FHP-II LGCA.

The total number of particles m_{total} is split into two entities, particles moving according to the FHP LGCA, m_{LGCA}, and particles moving according to the random walk, m_{RW}. Thus

$$m_{total} = m_{LGCA} + m_{RW}. \tag{5.113}$$

For all cells with movement type 2 the random walk is included in the model. Regardless of using FHP-I LGCA or FHP-II LGCA for the random walk only the lattice vectors

$c_1, \ldots, c_6$ are relevant. First, the mapping of the cells at each node and the lattice vectors $c_1, \ldots, c_6$ is defined by

$$
\begin{aligned}
x_1 &\mathrel{\hat{=}} c_1 \\
x_2 &\mathrel{\hat{=}} c_2 \\
x_3 &\mathrel{\hat{=}} c_3 \\
x_4 &\mathrel{\hat{=}} c_4 \\
x_5 &\mathrel{\hat{=}} c_5 \\
x_6 &\mathrel{\hat{=}} c_6.
\end{aligned}
\tag{5.114}
$$

Thus, for the random variable Z it holds

$$
\mathbb{P}(Z = c_i) = \frac{1}{6}, \quad i = 1, \ldots, 6.
\tag{5.115}
$$

The formal definition is motivated in the following:

Example 5.68. In this example a FHP-I LGCA is considered, i.e. $m = 6$. A node with one cell with state 1 and movement type 2 is considered. The vector with the states of the cells is denoted by $x \in Q^{1 \times 6}$. In this example not the whole evolution is presented, only the inclusion of random walk (one operator within the evolution) is discussed. The considered random walk is a simple random walk. The simple random walk is included in the model by random choice of the lattice vector. The lattice vector has a corresponding position of the cell, and thus, a corresponding entry in x, as described above. A random variable Z is used for the simple random walk. The random variable Z fulfils Equation (5.115). For

$$
x = \begin{pmatrix} 1 & 0 & 0 & 0 & 0 & 0 \end{pmatrix} \text{ with classification of movement } K_l = \begin{pmatrix} 2 & 0 & 0 & 0 & 0 & 0 \end{pmatrix}
\tag{5.116}
$$

and $Z = c_3$ the simple random walk is included in the model by changing x to

$$
x = \begin{pmatrix} 0 & 0 & 1 & 0 & 0 & 0 \end{pmatrix}.
\tag{5.117}
$$

In Figure 5.7 this inclusion of simple random walk is shown.
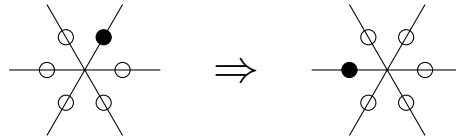
Figure 5.7: Illustration of inclusion of simple random walk for synthesis of FHP LGCA and random walk

In the following, the inclusion of the random walk is described formally. The probabilities given by Equation (5.115) change due to the number of particles with movement type 1

and 2. Furthermore, there are different outputs of the inclusion of random walk. In the following, these outputs are described using local operators $\mathcal{R}_{m_1,m_2} \colon Q^{1\times 6} \to Q^{1\times 6}$. The indices m_1 and m_2 are the numbers of particles with movement type 1 and 2, respectively. Due to the fact that the state of the seventh particle does not change the inclusion of the random walk, it is the same for FHP-I LGCA and FHP-II LGCA. Thus, for FHP-II LGCA only the first six entries are considered for the inclusion of random walk.

Remark 5.69. The selection of particles with movement type 2 for the operators $\mathcal{R}_{m_1,m_2}$ can be done in any arbitrary order. This is because the a priori probability that a particle occupies a certain cell after the random walk is the same independent from the order.

One particle with movement type 2:
– Zero particles with movement type 1:

$$\mathbb{P}(Z = c_i) = \frac{1}{6}, \quad \forall i \in I = \{1, \dots, 6\} \tag{5.118}$$

The local operator $\mathcal{R}_{0,1} \colon Q^{1\times 6} \to Q^{1\times 6}$ is defined by

$$\mathcal{R}_{0,1}x := \begin{cases} \begin{pmatrix} 1 & 0 & 0 & 0 & 0 & 0 \end{pmatrix} & \text{if } Z = c_1, \\ \begin{pmatrix} 0 & 1 & 0 & 0 & 0 & 0 \end{pmatrix} & \text{if } Z = c_2, \\ \begin{pmatrix} 0 & 0 & 1 & 0 & 0 & 0 \end{pmatrix} & \text{if } Z = c_3, \\ \begin{pmatrix} 0 & 0 & 0 & 1 & 0 & 0 \end{pmatrix} & \text{if } Z = c_4, \\ \begin{pmatrix} 0 & 0 & 0 & 0 & 1 & 0 \end{pmatrix} & \text{if } Z = c_5, \\ \begin{pmatrix} 0 & 0 & 0 & 0 & 0 & 1 \end{pmatrix} & \text{if } Z = c_6. \end{cases} \tag{5.119}$$

– One particle (corresponding lattice vectors c_j) with movement type 1:

$$\mathbb{P}(Z = c_i) = \frac{1}{5}, \quad \forall i \in I = \{1, \dots, 6\} \backslash \{j\} \tag{5.120}$$

and

$$\mathbb{P}(Z = c_j) = 0 \tag{5.121}$$

The local operator $\mathcal{R}_{1,1} \colon Q^{1\times 6} \to Q^{1\times 6}$ is defined by

$$\mathcal{R}_{1,1}x := \begin{cases} \begin{pmatrix} 1 & 1 & 0 & 0 & 0 & 0 \end{pmatrix} & \text{if } Z = c_1 \text{ and } j = 2, \\ \begin{pmatrix} 1 & 0 & 1 & 0 & 0 & 0 \end{pmatrix} & \text{if } Z = c_1 \text{ and } j = 3, \\ \begin{pmatrix} 1 & 0 & 0 & 1 & 0 & 0 \end{pmatrix} & \text{if } Z = c_1 \text{ and } j = 4, \\ \begin{pmatrix} 1 & 0 & 0 & 0 & 1 & 0 \end{pmatrix} & \text{if } Z = c_1 \text{ and } j = 5, \\ \begin{pmatrix} 1 & 0 & 0 & 0 & 0 & 1 \end{pmatrix} & \text{if } Z = c_1 \text{ and } j = 6, \\ \vdots \end{cases} \} \text{ analogous for } Z = c_2, Z = c_3, Z = c_4, Z = c_5, Z = c_6. \tag{5.122}$$

– Two particles (corresponding lattice vectors c_{j_1}, c_{j_2}) with movement type 1:

$$\mathbb{P}(Z = c_i) = \frac{1}{4}, \quad \forall i \in I = \{1, \ldots, 6\} \backslash \{j_1, j_2\} \tag{5.123}$$

and

$$\mathbb{P}(Z = c_{j_1}) = \mathbb{P}(Z = c_{j_2}) = 0 \tag{5.124}$$

The local operator $\mathcal{R}_{2,1} \colon Q^{1 \times 6} \to Q^{1 \times 6}$ is defined by

$$\mathcal{R}_{2,1} x := \begin{cases} \begin{pmatrix} 1 & 1 & 1 & 0 & 0 & 0 \end{pmatrix} & \text{if } Z = c_1 \text{ and } \{j_1, j_2\} = \{2, 3\}, \\ \begin{pmatrix} 1 & 1 & 0 & 1 & 0 & 0 \end{pmatrix} & \text{if } Z = c_1 \text{ and } \{j_1, j_2\} = \{2, 4\}, \\ \begin{pmatrix} 1 & 1 & 0 & 0 & 1 & 0 \end{pmatrix} & \text{if } Z = c_1 \text{ and } \{j_1, j_2\} = \{2, 5\}, \\ \begin{pmatrix} 1 & 1 & 0 & 0 & 0 & 1 \end{pmatrix} & \text{if } Z = c_1 \text{ and } \{j_1, j_2\} = \{2, 6\}, \\ \begin{pmatrix} 1 & 0 & 1 & 1 & 0 & 0 \end{pmatrix} & \text{if } Z = c_1 \text{ and } \{j_1, j_2\} = \{3, 4\}, \\ \begin{pmatrix} 1 & 0 & 1 & 0 & 1 & 0 \end{pmatrix} & \text{if } Z = c_1 \text{ and } \{j_1, j_2\} = \{3, 5\}, \\ \begin{pmatrix} 1 & 0 & 1 & 0 & 0 & 1 \end{pmatrix} & \text{if } Z = c_1 \text{ and } \{j_1, j_2\} = \{3, 6\}, \\ \begin{pmatrix} 1 & 0 & 0 & 1 & 1 & 0 \end{pmatrix} & \text{if } Z = c_1 \text{ and } \{j_1, j_2\} = \{4, 5\}, \\ \begin{pmatrix} 1 & 0 & 0 & 1 & 0 & 1 \end{pmatrix} & \text{if } Z = c_1 \text{ and } \{j_1, j_2\} = \{4, 6\}, \\ \begin{pmatrix} 1 & 0 & 0 & 0 & 1 & 1 \end{pmatrix} & \text{if } Z = c_1 \text{ and } \{j_1, j_2\} = \{5, 6\}, \\ \vdots \;\} \text{ analogous for } Z = c_2, Z = c_3, Z = c_4, Z = c_5, Z = c_6. \end{cases} \tag{5.125}$$

– Three particles (corresponding lattice vectors $c_{j_1}, c_{j_2}, c_{j_3}$) with movement type 1:

$$\mathbb{P}(Z = c_i) = \frac{1}{3}, \quad \forall i \in I = \{1, \ldots, 6\} \backslash \{j_1, j_2, j_3\} \tag{5.126}$$

and

$$\mathbb{P}(Z = c_{j_1}) = \mathbb{P}(Z = c_{j_2}) = \mathbb{P}(Z = c_{j_3}) = 0 \tag{5.127}$$

The local operator $\mathcal{R}_{3,1}\colon Q^{1\times 6} \to Q^{1\times 6}$ is defined by

$$
\mathcal{R}_{3,1}x := \begin{cases}
\begin{pmatrix} 1 & 1 & 1 & 1 & 0 & 0 \end{pmatrix} & \text{if } Z = c_1 \text{ and } \{j_1, j_2, j_3\} = \{2,3,4\}, \\
\begin{pmatrix} 1 & 1 & 1 & 0 & 1 & 0 \end{pmatrix} & \text{if } Z = c_1 \text{ and } \{j_1, j_2, j_3\} = \{2,3,5\}, \\
\begin{pmatrix} 1 & 1 & 1 & 0 & 0 & 1 \end{pmatrix} & \text{if } Z = c_1 \text{ and } \{j_1, j_2, j_3\} = \{2,3,6\}, \\
\begin{pmatrix} 1 & 1 & 0 & 1 & 1 & 0 \end{pmatrix} & \text{if } Z = c_1 \text{ and } \{j_1, j_2, j_3\} = \{2,4,5\}, \\
\begin{pmatrix} 1 & 1 & 0 & 1 & 0 & 1 \end{pmatrix} & \text{if } Z = c_1 \text{ and } \{j_1, j_2, j_3\} = \{2,4,6\}, \\
\begin{pmatrix} 1 & 1 & 0 & 0 & 1 & 1 \end{pmatrix} & \text{if } Z = c_1 \text{ and } \{j_1, j_2, j_3\} = \{2,5,6\}, \\
\begin{pmatrix} 1 & 0 & 1 & 1 & 1 & 0 \end{pmatrix} & \text{if } Z = c_1 \text{ and } \{j_1, j_2, j_3\} = \{3,4,5\}, \\
\begin{pmatrix} 1 & 0 & 1 & 1 & 0 & 1 \end{pmatrix} & \text{if } Z = c_1 \text{ and } \{j_1, j_2, j_3\} = \{3,4,6\}, \\
\begin{pmatrix} 1 & 0 & 1 & 0 & 1 & 1 \end{pmatrix} & \text{if } Z = c_1 \text{ and } \{j_1, j_2, j_3\} = \{3,5,6\}, \\
\begin{pmatrix} 1 & 0 & 0 & 1 & 1 & 1 \end{pmatrix} & \text{if } Z = c_1 \text{ and } \{j_1, j_2, j_3\} = \{4,5,6\}, \\
\vdots\ \} & \text{analogous for } Z = c_2, Z = c_3, Z = c_4, Z = c_5, Z = c_6.
\end{cases}
\tag{5.128}
$$

– Four particles (corresponding lattice vectors $c_{j_1}, c_{j_2}, c_{j_3}, c_{j_4}$) with movement type 1:

$$
\mathbb{P}(Z = c_i) = \frac{1}{2}, \quad \forall i \in I = \{1, \ldots, 6\}\setminus\{j_1, j_2, j_3, j_4\}
\tag{5.129}
$$

and

$$
\mathbb{P}(Z = c_{j_1}) = \mathbb{P}(Z = c_{j_2}) = \mathbb{P}(Z = c_{j_3}) = \mathbb{P}(Z = c_{j_4}) = 0
\tag{5.130}
$$

The local operator $\mathcal{R}_{4,1}\colon Q^{1\times 6} \to Q^{1\times 6}$ is defined by

$$
\mathcal{R}_{4,1}x := \begin{cases}
\begin{pmatrix} 1 & 1 & 1 & 1 & 1 & 0 \end{pmatrix} & \text{if } Z = c_1 \text{ and } \{j_1, j_2, j_3, j_4\} = \{2,3,4,5\}, \\
\begin{pmatrix} 1 & 1 & 1 & 1 & 0 & 1 \end{pmatrix} & \text{if } Z = c_1 \text{ and } \{j_1, j_2, j_3, j_4\} = \{2,3,4,6\}, \\
\begin{pmatrix} 1 & 1 & 1 & 0 & 1 & 1 \end{pmatrix} & \text{if } Z = c_1 \text{ and } \{j_1, j_2, j_3, j_4\} = \{2,3,5,6\}, \\
\begin{pmatrix} 1 & 1 & 0 & 1 & 1 & 1 \end{pmatrix} & \text{if } Z = c_1 \text{ and } \{j_1, j_2, j_3, j_4\} = \{2,4,5,6\}, \\
\begin{pmatrix} 1 & 0 & 1 & 1 & 1 & 1 \end{pmatrix} & \text{if } Z = c_1 \text{ and } \{j_1, j_2, j_3, j_4\} = \{3,4,5,6\}, \\
\vdots\ \} & \text{analogous for } Z = c_2, Z = c_3, Z = c_4, Z = c_5, Z = c_6.
\end{cases}
\tag{5.131}
$$

– Five particles (corresponding lattice vectors $c_{j_1}, c_{j_2}, c_{j_3}, c_{j_4}, c_{j_5}$) with movement type 1:

$$
\mathbb{P}(Z = c_i) = 1, \quad \forall i \in I = \{1, \ldots, 6\}\setminus\{j_1, j_2, j_3, j_4, j_5\}
\tag{5.132}
$$

and

$$
\mathbb{P}(Z = c_{j_1}) = \mathbb{P}(Z = c_{j_2}) = \mathbb{P}(Z = c_{j_3}) = \mathbb{P}(Z = c_{j_4}) = \mathbb{P}(Z = c_{j_5}) = 0
\tag{5.133}
$$

In this case the process is deterministic. Nothing changes in this case (for distinguishable and indistinguishable particles). The local operator $\mathcal{R}_{5,1}\colon Q^{1\times 6} \to Q^{1\times 6}$ is defined by

$$\mathcal{R}_{5,1}x := \begin{pmatrix} 1 & 1 & 1 & 1 & 1 & 1 \end{pmatrix}. \tag{5.134}$$

Two particles with movement type 2:
– Zero particles with movement type 1:
For the first particle the random variable Z_1 is used in the following way.

$$\mathbb{P}(Z_1 = c_i) = \frac{1}{6}, \quad \forall i \in I = \{1, \dots, 6\} \tag{5.135}$$

and the chosen lattice vector is denoted by c_{l_1}. For the second particle the random variable Z_2 is used

$$\mathbb{P}(Z_2 = c_i) = \frac{1}{5}, \quad \forall i \in I = \{1, \dots, 6\} \backslash \{l_1\} \tag{5.136}$$

and

$$\mathbb{P}(Z_2 = c_{l_1}) = 0. \tag{5.137}$$

The local operator $\mathcal{R}_{0,2}\colon Q^{1\times 6} \to Q^{1\times 6}$ is defined by

$$\mathcal{R}_{0,2}x := \begin{cases} \begin{pmatrix} 1 & 1 & 0 & 0 & 0 & 0 \end{pmatrix} & \text{if } \{Z_1, Z_2\} = \{c_1, c_2\}, \\ \begin{pmatrix} 1 & 0 & 1 & 0 & 0 & 0 \end{pmatrix} & \text{if } \{Z_1, Z_2\} = \{c_1, c_3\}, \\ \begin{pmatrix} 1 & 0 & 0 & 1 & 0 & 0 \end{pmatrix} & \text{if } \{Z_1, Z_2\} = \{c_1, c_4\}, \\ \begin{pmatrix} 1 & 0 & 0 & 0 & 1 & 0 \end{pmatrix} & \text{if } \{Z_1, Z_2\} = \{c_1, c_5\}, \\ \begin{pmatrix} 1 & 0 & 0 & 0 & 0 & 1 \end{pmatrix} & \text{if } \{Z_1, Z_2\} = \{c_1, c_6\}, \\ \begin{pmatrix} 0 & 1 & 1 & 0 & 0 & 0 \end{pmatrix} & \text{if } \{Z_1, Z_2\} = \{c_2, c_3\}, \\ \begin{pmatrix} 0 & 1 & 0 & 1 & 0 & 0 \end{pmatrix} & \text{if } \{Z_1, Z_2\} = \{c_2, c_4\}, \\ \begin{pmatrix} 0 & 1 & 0 & 0 & 1 & 0 \end{pmatrix} & \text{if } \{Z_1, Z_2\} = \{c_2, c_5\}, \\ \begin{pmatrix} 0 & 1 & 0 & 0 & 0 & 1 \end{pmatrix} & \text{if } \{Z_1, Z_2\} = \{c_2, c_6\}, \\ \begin{pmatrix} 0 & 0 & 1 & 1 & 0 & 0 \end{pmatrix} & \text{if } \{Z_1, Z_2\} = \{c_3, c_4\}, \\ \begin{pmatrix} 0 & 0 & 1 & 0 & 1 & 0 \end{pmatrix} & \text{if } \{Z_1, Z_2\} = \{c_3, c_5\}, \\ \begin{pmatrix} 0 & 0 & 1 & 0 & 0 & 1 \end{pmatrix} & \text{if } \{Z_1, Z_2\} = \{c_3, c_6\}, \\ \begin{pmatrix} 0 & 0 & 0 & 1 & 1 & 0 \end{pmatrix} & \text{if } \{Z_1, Z_2\} = \{c_4, c_5\}, \\ \begin{pmatrix} 0 & 0 & 0 & 1 & 0 & 1 \end{pmatrix} & \text{if } \{Z_1, Z_2\} = \{c_4, c_6\}, \\ \begin{pmatrix} 0 & 0 & 0 & 0 & 1 & 1 \end{pmatrix} & \text{if } \{Z_1, Z_2\} = \{c_5, c_6\}. \end{cases} \tag{5.138}$$

– One particle (corresponding lattice vector c_j) with movement type 1:
For the first particle the random variable Z_1 is used in the following way.

$$\mathbb{P}(Z_1 = c_i) = \frac{1}{5}, \quad \forall i \in I = \{1, \ldots, 6\} \backslash \{j\} \tag{5.139}$$

and

$$\mathbb{P}(Z_1 = c_j) = 0 \tag{5.140}$$

and the chosen lattice vector is denoted by c_{l_1}. For the second particle the random variable Z_2 is used

$$\mathbb{P}(Z_2 = c_i) = \frac{1}{4}, \quad \forall i \in I = \{1, \ldots, 6\} \backslash \{j, l_1\} \tag{5.141}$$

and

$$\mathbb{P}(Z_2 = c_j) = \mathbb{P}(Z_2 = c_{l_1}) = 0. \tag{5.142}$$

The local operator $\mathcal{R}_{1,2} \colon Q^{1 \times 6} \to Q^{1 \times 6}$ is defined by

$$\mathcal{R}_{1,2} x := \begin{cases} \begin{pmatrix} 1 & 1 & 1 & 0 & 0 & 0 \end{pmatrix} & \text{if } \{Z_1, Z_2\} = \{c_1, c_2\} \text{ and } j = 3, \\ \begin{pmatrix} 1 & 1 & 0 & 1 & 0 & 0 \end{pmatrix} & \text{if } \{Z_1, Z_2\} = \{c_1, c_2\} \text{ and } j = 4, \\ \begin{pmatrix} 1 & 1 & 0 & 0 & 1 & 0 \end{pmatrix} & \text{if } \{Z_1, Z_2\} = \{c_1, c_2\} \text{ and } j = 5, \\ \begin{pmatrix} 1 & 1 & 0 & 0 & 0 & 1 \end{pmatrix} & \text{if } \{Z_1, Z_2\} = \{c_1, c_2\} \text{ and } j = 6, \\ \vdots \} & \text{analogous for } Z_i \in \{c_k, c_l\}, i = 1, 2, k \neq l, k, l \in \{1, \ldots, 6\}. \end{cases} \tag{5.143}$$

– Two particles (corresponding lattice vectors c_{j_1}, c_{j_2}) with movement type 1:
For the first particle the random variable Z_1 is used in the following way.

$$\mathbb{P}(Z_1 = c_i) = \frac{1}{4}, \quad \forall i \in I = \{1, \ldots, 6\} \backslash \{j_1, j_2\} \tag{5.144}$$

and

$$\mathbb{P}(Z_1 = c_{j_1}) = \mathbb{P}(Z_1 = c_{j_2}) = 0 \tag{5.145}$$

and the chosen lattice vector is denoted by c_{l_1}. For the second particle the random variable Z_2 is used

$$\mathbb{P}(Z_2 = c_i) = \frac{1}{3}, \quad \forall i \in I = \{1, \ldots, 6\} \backslash \{j_1, j_2, l_1\} \tag{5.146}$$

and

$$\mathbb{P}(Z_2 = c_{j_1}) = \mathbb{P}(Z_2 = c_{j_2}) = \mathbb{P}(Z_2 = c_{l_1}) = 0. \tag{5.147}$$

The local operator $\mathcal{R}_{2,2}\colon Q^{1\times 6} \to Q^{1\times 6}$ is defined by

$$\mathcal{R}_{2,2}x := \begin{cases} \begin{pmatrix} 1 & 1 & 1 & 1 & 0 & 0 \end{pmatrix} & \text{if } \{Z_1, Z_2\} = \{c_1, c_2\} \text{ and } \{j_1, j_2\} = \{3, 4\}, \\ \begin{pmatrix} 1 & 1 & 1 & 0 & 1 & 0 \end{pmatrix} & \text{if } \{Z_1, Z_2\} = \{c_1, c_2\} \text{ and } \{j_1, j_2\} = \{3, 5\}, \\ \begin{pmatrix} 1 & 1 & 1 & 0 & 0 & 1 \end{pmatrix} & \text{if } \{Z_1, Z_2\} = \{c_1, c_2\} \text{ and } \{j_1, j_2\} = \{3, 6\}, \\ \begin{pmatrix} 1 & 1 & 0 & 1 & 1 & 0 \end{pmatrix} & \text{if } \{Z_1, Z_2\} = \{c_1, c_2\} \text{ and } \{j_1, j_2\} = \{4, 5\}, \\ \begin{pmatrix} 1 & 1 & 0 & 1 & 0 & 1 \end{pmatrix} & \text{if } \{Z_1, Z_2\} = \{c_1, c_2\} \text{ and } \{j_1, j_2\} = \{4, 6\}, \\ \begin{pmatrix} 1 & 1 & 0 & 0 & 1 & 1 \end{pmatrix} & \text{if } \{Z_1, Z_2\} = \{c_1, c_2\} \text{ and } \{j_1, j_2\} = \{5, 6\}, \\ \vdots \ \} & \text{analogous for } Z_i \in \{c_k, c_l\}, i = 1, 2, k \neq l, k, l \in \{1, \ldots, 6\}. \end{cases} \quad (5.148)$$

– Three particles (corresponding lattice vectors c_{j_1}, c_{j_2}, c_{j_3}) with movement type 1: For the first particle the random variable Z_1 is used in the following way.

$$\mathbb{P}(Z_1 = c_i) = \frac{1}{3}, \quad \forall i \in I = \{1, \ldots, 6\}\backslash\{j_1, j_2, j_3\} \quad (5.149)$$

and

$$\mathbb{P}(Z_1 = c_{j_1}) = \mathbb{P}(Z_1 = c_{j_2}) = \mathbb{P}(Z_1 = c_{j_3}) = 0 \quad (5.150)$$

and the chosen lattice vector is denoted by c_{l_1}. For the second particle the random variable Z_2 is used

$$\mathbb{P}(Z_2 = c_i) = \frac{1}{2}, \quad \forall i \in I = \{1, \ldots, 6\}\backslash\{j_1, j_2, j_3, l_1\} \quad (5.151)$$

and

$$\mathbb{P}(Z_2 = c_{j_1}) = \mathbb{P}(Z_2 = c_{j_2}) = \mathbb{P}(Z_2 = c_{j_3}) = \mathbb{P}(Z_2 = c_{l_1}) = 0. \quad (5.152)$$

The local operator $\mathcal{R}_{3,2}\colon Q^{1\times 6} \to Q^{1\times 6}$ is defined by

$$\mathcal{R}_{3,2}x := \begin{cases} \begin{pmatrix} 1 & 1 & 1 & 1 & 1 & 0 \end{pmatrix} & \text{if } \{Z_1, Z_2\} = \{c_1, c_2\} \text{ and } \{j_1, j_2, j_3\} = \{3, 4, 5\}, \\ \begin{pmatrix} 1 & 1 & 1 & 1 & 0 & 1 \end{pmatrix} & \text{if } \{Z_1, Z_2\} = \{c_1, c_2\} \text{ and } \{j_1, j_2, j_3\} = \{3, 4, 6\}, \\ \begin{pmatrix} 1 & 1 & 1 & 0 & 1 & 1 \end{pmatrix} & \text{if } \{Z_1, Z_2\} = \{c_1, c_2\} \text{ and } \{j_1, j_2, j_3\} = \{3, 5, 6\}, \\ \begin{pmatrix} 1 & 1 & 0 & 1 & 1 & 1 \end{pmatrix} & \text{if } \{Z_1, Z_2\} = \{c_1, c_2\} \text{ and } \{j_1, j_2, j_3\} = \{4, 5, 6\}, \\ \vdots \ \} & \text{analogous for } Z_i \in \{c_k, c_l\}, i = 1, 2, k \neq l, k, l \in \{1, \ldots, 6\}. \end{cases}$$

$$(5.153)$$

– Four particles (corresponding lattice vectors c_{j_1}, c_{j_2}, c_{j_3}, c_{j_4}) with movement type 1: For the first particle the random variable Z_1 is used in the following way.

$$\mathbb{P}(Z_1 = c_i) = \frac{1}{2}, \quad \forall i \in I = \{1, \ldots, 6\}\backslash\{j_1, j_2, j_3, j_4\} \quad (5.154)$$

and

$$\mathbb{P}(Z_1 = c_{j_1}) = \mathbb{P}(Z_1 = c_{j_2}) = \mathbb{P}(Z_1 = c_{j_3}) = \mathbb{P}(Z_1 = c_{j_4}) = 0 \quad (5.155)$$

and the chosen lattice vector is denoted by c_{l_1}. For the second particle the random variable Z_2 is used

$$\mathbb{P}(Z_2 = c_i) = 1, \quad \forall i \in I = \{1, \ldots, 6\} \backslash \{j_1, j_2, j_3, j_4, l_1\} \tag{5.156}$$

and

$$\mathbb{P}(Z_2 = c_{j_1}) = \mathbb{P}(Z_2 = c_{j_2}) = \mathbb{P}(Z_2 = c_{j_3}) = \mathbb{P}(Z_2 = c_{j_4}) = \mathbb{P}(Z_2 = c_{l_1}) = 0. \tag{5.157}$$

In this case the movement types of the cells do not change. For indistinguishable particles nothing changes. The local operator $\mathcal{R}_{4,2} \colon Q^{1 \times 6} \to Q^{1 \times 6}$ is defined by

$$\mathcal{R}_{4,2} x := \begin{pmatrix} 1 & 1 & 1 & 1 & 1 & 1 \end{pmatrix}. \tag{5.158}$$

Three particles with movement type 2:
– Zero particles with movement type 1:
For the first particle the random variable Z_1 is used in the following way.

$$\mathbb{P}(Z_1 = c_i) = \frac{1}{6}, \quad \forall i \in I = \{1, \ldots, 6\} \tag{5.159}$$

and the chosen lattice vector is denoted by c_{l_1}. For the second particle the random variable Z_2 is used

$$\mathbb{P}(Z_2 = c_i) = \frac{1}{5}, \quad \forall i \in I = \{1, \ldots, 6\} \backslash \{l_1\} \tag{5.160}$$

and

$$\mathbb{P}(Z_2 = c_{l_1}) = 0 \tag{5.161}$$

and the chosen lattice vector is denoted by c_{l_2}. For the third particle the random variable Z_3 is used

$$\mathbb{P}(Z_3 = c_i) = \frac{1}{4}, \quad \forall i \in I = \{1, \ldots, 6\} \backslash \{l_1, l_2\} \tag{5.162}$$

and

$$\mathbb{P}(Z_3 = c_{l_1}) = \mathbb{P}(Z_3 = c_{l_2}) = 0. \tag{5.163}$$

The local operator $\mathcal{R}_{0,3}\colon Q^{1\times 6}\to Q^{1\times 6}$ is defined by

$$
\mathcal{R}_{0,3}:x=\begin{cases}
\begin{pmatrix}0 & 0 & 0 & 1 & 1 & 1\end{pmatrix} & \text{if } Z_i \neq c_1, c_2, c_3, i=1,2,3,\\
\begin{pmatrix}0 & 0 & 1 & 0 & 1 & 1\end{pmatrix} & \text{if } Z_i \neq c_1, c_2, c_4, i=1,2,3,\\
\begin{pmatrix}0 & 0 & 1 & 1 & 0 & 1\end{pmatrix} & \text{if } Z_i \neq c_1, c_2, c_5, i=1,2,3,\\
\begin{pmatrix}0 & 0 & 1 & 1 & 1 & 0\end{pmatrix} & \text{if } Z_i \neq c_1, c_2, c_6, i=1,2,3,\\
\begin{pmatrix}0 & 1 & 0 & 0 & 1 & 1\end{pmatrix} & \text{if } Z_i \neq c_1, c_3, c_4, i=1,2,3,\\
\begin{pmatrix}0 & 1 & 0 & 1 & 0 & 1\end{pmatrix} & \text{if } Z_i \neq c_1, c_3, c_5, i=1,2,3,\\
\begin{pmatrix}0 & 1 & 0 & 1 & 1 & 0\end{pmatrix} & \text{if } Z_i \neq c_1, c_3, c_6, i=1,2,3,\\
\begin{pmatrix}0 & 1 & 1 & 0 & 0 & 1\end{pmatrix} & \text{if } Z_i \neq c_1, c_4, c_5, i=1,2,3,\\
\begin{pmatrix}0 & 1 & 1 & 0 & 1 & 0\end{pmatrix} & \text{if } Z_i \neq c_1, c_4, c_6, i=1,2,3,\\
\begin{pmatrix}0 & 1 & 1 & 1 & 0 & 0\end{pmatrix} & \text{if } Z_i \neq c_1, c_5, c_6, i=1,2,3,\\
\begin{pmatrix}1 & 0 & 0 & 0 & 1 & 1\end{pmatrix} & \text{if } Z_i \neq c_2, c_3, c_4, i=1,2,3,\\
\begin{pmatrix}1 & 0 & 0 & 1 & 0 & 1\end{pmatrix} & \text{if } Z_i \neq c_2, c_3, c_5, i=1,2,3,\\
\begin{pmatrix}1 & 0 & 0 & 1 & 1 & 0\end{pmatrix} & \text{if } Z_i \neq c_2, c_3, c_6, i=1,2,3,\\
\begin{pmatrix}1 & 0 & 1 & 0 & 0 & 1\end{pmatrix} & \text{if } Z_i \neq c_2, c_4, c_5, i=1,2,3,\\
\begin{pmatrix}1 & 0 & 1 & 0 & 1 & 0\end{pmatrix} & \text{if } Z_i \neq c_2, c_4, c_6, i=1,2,3,\\
\begin{pmatrix}1 & 0 & 1 & 1 & 0 & 0\end{pmatrix} & \text{if } Z_i \neq c_2, c_5, c_6, i=1,2,3,\\
\begin{pmatrix}1 & 1 & 0 & 0 & 0 & 1\end{pmatrix} & \text{if } Z_i \neq c_3, c_4, c_5, i=1,2,3,\\
\begin{pmatrix}1 & 1 & 0 & 0 & 1 & 0\end{pmatrix} & \text{if } Z_i \neq c_3, c_4, c_6, i=1,2,3,\\
\begin{pmatrix}1 & 1 & 0 & 1 & 0 & 0\end{pmatrix} & \text{if } Z_i \neq c_3, c_5, c_6, i=1,2,3,\\
\begin{pmatrix}1 & 1 & 1 & 0 & 0 & 0\end{pmatrix} & \text{if } Z_i \neq c_4, c_5, c_6, i=1,2,3.
\end{cases}
\tag{5.164}
$$

– One particle (corresponding lattice vector c_j) with movement type 1:
For the first particle the random variable Z_1 is used in the following way.

$$
\mathbb{P}(Z_1 = c_i) = \frac{1}{5}, \quad \forall i \in I = \{1,\ldots,6\}\backslash\{j\}
\tag{5.165}
$$

and

$$
\mathbb{P}(Z_1 = c_j) = 0
\tag{5.166}
$$

and the chosen lattice vector is denoted by c_{l_1}. For the second particle the random variable Z_2 is used

$$
\mathbb{P}(Z_2 = c_i) = \frac{1}{4}, \quad \forall i \in I = \{1,\ldots,6\}\backslash\{j, l_1\}
\tag{5.167}
$$

and

$$\mathbb{P}(Z_2 = c_j) = \mathbb{P}(Z_2 = c_{l_1}) = 0 \tag{5.168}$$

and the chosen lattice vector is denoted by c_{l_2}. For the third particle the random variable Z_3 is used

$$\mathbb{P}(Z_3 = c_i) = \frac{1}{3}, \quad \forall i \in I = \{1, \dots, 6\} \backslash \{j, l_1, l_2\} \tag{5.169}$$

and

$$\mathbb{P}(Z_3 = c_j) = \mathbb{P}(Z_3 = c_{l_1}) = \mathbb{P}(Z_3 = c_{l_2}) = 0. \tag{5.170}$$

The local operator $\mathcal{R}_{1,3} \colon Q^{1\times 6} \to Q^{1\times 6}$ is defined by

$$\mathcal{R}_{1,3}x := \begin{cases} \begin{pmatrix} 1 & 1 & 1 & 1 & 0 & 0 \end{pmatrix} & \text{if } Z_i \neq c_4, c_5, c_6, i = 1, 2, 3 \text{ and } j = 4, \\ \begin{pmatrix} 1 & 1 & 1 & 0 & 1 & 0 \end{pmatrix} & \text{if } Z_i \neq c_4, c_5, c_6, i = 1, 2, 3 \text{ and } j = 5, \\ \begin{pmatrix} 1 & 1 & 1 & 0 & 0 & 1 \end{pmatrix} & \text{if } Z_i \neq c_4, c_5, c_6, i = 1, 2, 3 \text{ and } j = 6, \\ \vdots \} & \text{analogous for } Z_i \neq c_k, c_l, c_m, i = 1, 2, 3, k \neq l \neq m, k, l, m \in \{1, \dots, 6\}. \end{cases} \tag{5.171}$$

– Two particles (corresponding lattice vectors c_{j_1}, c_{j_2}) with movement type 1:
For the first particle the random variable Z_1 is used in the following way.

$$\mathbb{P}(Z_1 = c_i) = \frac{1}{4}, \quad \forall i \in I = \{1, \dots, 6\} \backslash \{j_1, j_2\} \tag{5.172}$$

and

$$\mathbb{P}(Z_1 = c_{j_1}) = \mathbb{P}(Z_1 = c_{j_2}) = 0 \tag{5.173}$$

and the chosen lattice vector is denoted by c_{l_1}. For the second particle the random variable Z_2 is used

$$\mathbb{P}(Z_2 = c_i) = \frac{1}{3}, \quad \forall i \in I = \{1, \dots, 6\} \backslash \{j_1, j_2, l_1\} \tag{5.174}$$

and

$$\mathbb{P}(Z_2 = c_{j_1}) = \mathbb{P}(Z_2 = c_{j_2}) = \mathbb{P}(Z_2 = c_{l_1}) = 0 \tag{5.175}$$

and the chosen lattice vector is denoted by c_{l_2}. For the third particle the random variable Z_3 is used

$$\mathbb{P}(Z_3 = c_i) = \frac{1}{2}, \quad \forall i \in I = \{1, \dots, 6\} \backslash \{j_1, j_2, l_1, l_2\} \tag{5.176}$$

and

$$\mathbb{P}(Z_3 = c_{j_1}) = \mathbb{P}(Z_3 = c_{j_2}) = \mathbb{P}(Z_3 = c_{l_1}) = \mathbb{P}(Z_3 = c_{l_2}) = 0. \tag{5.177}$$

The local operator $\mathcal{R}_{2,3} \colon Q^{1\times 6} \to Q^{1\times 6}$ is defined by

$$\mathcal{R}_{2,3}x := \begin{cases} \begin{pmatrix} 1 & 1 & 1 & 1 & 1 & 0 \end{pmatrix} & \text{if } Z_i \neq c_4, c_5, c_6, i = 1, 2, 3 \text{ and } \{j_1, j_2\} = \{4, 5\}, \\ \begin{pmatrix} 1 & 1 & 1 & 1 & 0 & 1 \end{pmatrix} & \text{if } Z_i \neq c_4, c_5, c_6, i = 1, 2, 3 \text{ and } \{j_1, j_2\} = \{4, 6\}, \\ \begin{pmatrix} 1 & 1 & 1 & 0 & 1 & 1 \end{pmatrix} & \text{if } Z_i \neq c_4, c_5, c_6, i = 1, 2, 3 \text{ and } \{j_1, j_2\} = \{5, 6\}, \\ \vdots \} & \text{analogous for } Z_i \neq c_k, c_l, c_m, i = 1, 2, 3, k \neq l \neq m, k, l, m \in \{1, \dots, 6\}. \end{cases} \tag{5.178}$$

– Three particles (corresponding lattice vectors c_{j_1}, c_{j_2}, c_{j_3}) with movement type 1:
For the first particle the random variable Z_1 is used in the following way.

$$\mathbb{P}(Z_1 = c_i) = \frac{1}{3}, \quad \forall i \in I = \{1, \ldots, 6\} \backslash \{j_1, j_2, j_3\} \tag{5.179}$$

and

$$\mathbb{P}(Z_1 = c_{j_1}) = \mathbb{P}(Z_1 = c_{j_2}) = \mathbb{P}(Z_1 = c_{j_3}) = 0 \tag{5.180}$$

and the chosen lattice vector is denoted by c_{l_1}. For the second particle the random variable Z_2 is used

$$\mathbb{P}(Z_2 = c_i) = \frac{1}{2}, \quad \forall i \in I = \{1, \ldots, 6\} \backslash \{j_1, j_2, j_3, l_1\} \tag{5.181}$$

and

$$\mathbb{P}(Z_2 = c_{j_1}) = \mathbb{P}(Z_2 = c_{j_2}) = \mathbb{P}(Z_2 = c_{j_3}) = \mathbb{P}(Z_2 = c_{l_1}) = 0 \tag{5.182}$$

and the chosen lattice vector is denoted by c_{l_2}. For the third particle the random variable Z_3 is used

$$\mathbb{P}(Z_3 = c_i) = 1, \quad \forall i \in I = \{1, \ldots, 6\} \backslash \{j_1, j_2, j_3, l_1, l_2\} \tag{5.183}$$

and

$$\mathbb{P}(Z_3 = c_{j_1}) = \mathbb{P}(Z_3 = c_{j_2}) = \mathbb{P}(Z_3 = c_{j_3}) = \mathbb{P}(Z_3 = c_{l_1}) = \mathbb{P}(Z_3 = c_{l_2}) = 0. \tag{5.184}$$

In this case the movement types of the cells do not change. For indistinguishable particles nothing changes. The local operator $\mathcal{R}_{3,3} \colon Q^{1 \times 6} \to Q^{1 \times 6}$ is defined by

$$\mathcal{R}_{3,3} x := \begin{pmatrix} 1 & 1 & 1 & 1 & 1 & 1 \end{pmatrix}. \tag{5.185}$$

Four particles with movement type 2:
– Zero particles with movement type 1:
For the first particle the random variable Z_1 is used in the following way.

$$\mathbb{P}(Z_1 = c_i) = \frac{1}{6}, \quad \forall i \in I = \{1, \ldots, 6\} \tag{5.186}$$

and the chosen lattice vector is denoted by c_{l_1}. For the second particle the random variable Z_2 is used

$$\mathbb{P}(Z_2 = c_i) = \frac{1}{5}, \quad \forall i \in I = \{1, \ldots, 6\} \backslash \{l_1\} \tag{5.187}$$

and

$$\mathbb{P}(Z_2 = c_{l_1}) = 0 \tag{5.188}$$

and the chosen lattice vector is denoted by c_{l_2}. For the third particle the random variable Z_3 is used

$$\mathbb{P}(Z_3 = c_i) = \frac{1}{4}, \quad \forall i \in I = \{1, \ldots, 6\} \backslash \{l_1, l_2\} \tag{5.189}$$

and

$$\mathbb{P}(Z_3 = c_{l_1}) = \mathbb{P}(Z_3 = c_{l_2}) = 0 \tag{5.190}$$

and the chosen lattice vector is denoted by c_{l_3}. For the fourth particle the random variable Z_4 is used

$$\mathbb{P}(Z_4 = c_i) = \frac{1}{3}, \quad \forall i \in I = \{1, \ldots, 6\} \backslash \{l_1, l_2, l_3\} \tag{5.191}$$

and

$$\mathbb{P}(Z_4 = c_{l_1}) = \mathbb{P}(Z_4 = c_{l_2}) = \mathbb{P}(Z_4 = c_{l_3}) = 0. \tag{5.192}$$

The local operator $\mathcal{R}_{0,4} \colon Q^{1 \times 6} \to Q^{1 \times 6}$ is defined by

$$\mathcal{R}_{0,4} x := \begin{cases} \begin{pmatrix} 0 & 0 & 1 & 1 & 1 & 1 \end{pmatrix} & \text{if } Z_i \neq c_1, c_2, i = 1, \ldots, 4, \\ \begin{pmatrix} 0 & 1 & 0 & 1 & 1 & 1 \end{pmatrix} & \text{if } Z_i \neq c_1, c_3, i = 1, \ldots, 4, \\ \begin{pmatrix} 0 & 1 & 1 & 0 & 1 & 1 \end{pmatrix} & \text{if } Z_i \neq c_1, c_4, i = 1, \ldots, 4, \\ \begin{pmatrix} 0 & 1 & 1 & 1 & 0 & 1 \end{pmatrix} & \text{if } Z_i \neq c_1, c_5, i = 1, \ldots, 4, \\ \begin{pmatrix} 0 & 1 & 1 & 1 & 1 & 0 \end{pmatrix} & \text{if } Z_i \neq c_1, c_6, i = 1, \ldots, 4, \\ \begin{pmatrix} 1 & 0 & 0 & 1 & 1 & 1 \end{pmatrix} & \text{if } Z_i \neq c_2, c_3, i = 1, \ldots, 4, \\ \begin{pmatrix} 1 & 0 & 1 & 0 & 1 & 1 \end{pmatrix} & \text{if } Z_i \neq c_2, c_4, i = 1, \ldots, 4, \\ \begin{pmatrix} 1 & 0 & 1 & 1 & 0 & 1 \end{pmatrix} & \text{if } Z_i \neq c_2, c_5, i = 1, \ldots, 4, \\ \begin{pmatrix} 1 & 0 & 1 & 1 & 1 & 0 \end{pmatrix} & \text{if } Z_i \neq c_2, c_6, i = 1, \ldots, 4, \\ \begin{pmatrix} 1 & 1 & 0 & 0 & 1 & 1 \end{pmatrix} & \text{if } Z_i \neq c_3, c_4, i = 1, \ldots, 4, \\ \begin{pmatrix} 1 & 1 & 0 & 1 & 0 & 1 \end{pmatrix} & \text{if } Z_i \neq c_3, c_5, i = 1, \ldots, 4, \\ \begin{pmatrix} 1 & 1 & 0 & 1 & 1 & 0 \end{pmatrix} & \text{if } Z_i \neq c_3, c_6, i = 1, \ldots, 4, \\ \begin{pmatrix} 1 & 1 & 1 & 0 & 0 & 1 \end{pmatrix} & \text{if } Z_i \neq c_4, c_5, i = 1, \ldots, 4, \\ \begin{pmatrix} 1 & 1 & 1 & 0 & 1 & 0 \end{pmatrix} & \text{if } Z_i \neq c_4, c_6, i = 1, \ldots, 4, \\ \begin{pmatrix} 1 & 1 & 1 & 1 & 0 & 0 \end{pmatrix} & \text{if } Z_i \neq c_5, c_6, i = 1, \ldots, 4. \end{cases} \tag{5.193}$$

– One particle (corresponding lattice vector c_j) with movement type 1:
For the first particle the random variable Z_1 is used in the following way.

$$\mathbb{P}(Z_1 = c_i) = \frac{1}{5}, \quad \forall i \in I = \{1, \ldots, 6\} \backslash \{j\} \tag{5.194}$$

and

$$\mathbb{P}(Z_1 = c_j) = 0 \tag{5.195}$$

and the chosen lattice vector is denoted by c_{l_1}. For the second particle the random variable Z_2 is used

$$\mathbb{P}(Z_2 = c_i) = \frac{1}{4}, \quad \forall i \in I = \{1, \ldots, 6\} \backslash \{j, l_1\} \tag{5.196}$$

and

$$\mathbb{P}(Z_2 = c_j) = \mathbb{P}(Z_2 = c_{l_1}) = 0 \tag{5.197}$$

and the chosen lattice vector is denoted by c_{l_2}. For the third particle the random variable Z_3 is used

$$\mathbb{P}(Z_3 = c_i) = \frac{1}{3}, \quad \forall i \in I = \{1, \ldots, 6\} \backslash \{j, l_1, l_2\} \tag{5.198}$$

and

$$\mathbb{P}(Z_3 = c_j) = \mathbb{P}(Z_3 = c_{l_1}) = \mathbb{P}(Z_3 = c_{l_2}) = 0 \tag{5.199}$$

and the chosen lattice vector is denoted by c_{l_3}. For the fourth particle the random variable Z_4 is used

$$\mathbb{P}(Z_4 = c_i) = \frac{1}{2}, \quad \forall i \in I = \{1, \ldots, 6\} \backslash \{j, l_1, l_2, l_3\} \tag{5.200}$$

and

$$\mathbb{P}(Z_4 = c_j) = \mathbb{P}(Z_4 = c_{l_1}) = \mathbb{P}(Z_4 = c_{l_2}) = \mathbb{P}(Z_4 = c_{l_3}) = 0. \tag{5.201}$$

The local operator $\mathcal{R}_{1,4} : Q^{1 \times 6} \to Q^{1 \times 6}$ is defined by

$$\mathcal{R}_{1,4} x := \begin{cases} \begin{pmatrix} 1 & 1 & 1 & 1 & 1 & 0 \end{pmatrix} & \text{if } Z_i \neq c_5, c_6, i = 1, \ldots, 4 \text{ and } j = 5, \\ \begin{pmatrix} 1 & 1 & 1 & 1 & 0 & 1 \end{pmatrix} & \text{if } Z_i \neq c_5, c_6, i = 1, \ldots, 4 \text{ and } j = 6, \\ \vdots \} & \text{analogous for } Z_i \neq c_k, c_l, i = 1, \ldots, 4, k \neq l, k, l \in \{1, \ldots, 6\}. \end{cases} \tag{5.202}$$

– Two particles (corresponding lattice vectors c_{j_1}, c_{j_2}) with movement type 1: For the first particle the random variable Z_1 is used in the following way.

$$\mathbb{P}(Z_1 = c_i) = \frac{1}{4}, \quad \forall i \in I = \{1, \ldots, 6\} \backslash \{j_1, j_2\} \tag{5.203}$$

and

$$\mathbb{P}(Z_1 = c_{j_1}) = \mathbb{P}(Z_1 = c_{j_2}) = 0 \tag{5.204}$$

and the chosen lattice vector is denoted by c_{l_1}. For the second particle the random variable Z_2 is used

$$\mathbb{P}(Z_2 = c_i) = \frac{1}{3}, \quad \forall i \in I = \{1, \ldots, 6\} \backslash \{j_1, j_2, l_1\} \tag{5.205}$$

and

$$\mathbb{P}(Z_2 = c_{j_1}) = \mathbb{P}(Z_2 = c_{j_2}) = \mathbb{P}(Z_2 = c_{l_1}) = 0 \tag{5.206}$$

and the chosen lattice vector is denoted by c_{l_2}. For the third particle the random variable Z_3 is used

$$\mathbb{P}(Z_3 = c_i) = \frac{1}{2}, \quad \forall i \in I = \{1, \ldots, 6\} \backslash \{j_1, j_2, l_1, l_2\} \tag{5.207}$$

and

$$\mathbb{P}(Z_3 = c_{j_1}) = \mathbb{P}(Z_3 = c_{j_2}) = \mathbb{P}(Z_3 = c_{l_1}) = \mathbb{P}(Z_3 = c_{l_2}) = 0 \tag{5.208}$$

and the chosen lattice vector is denoted by c_{l_3}. For the fourth particle the random variable Z_4 is used

$$\mathbb{P}(Z_4 = c_i) = 1, \quad \forall i \in I = \{1, \ldots, 6\} \backslash \{j_1, j_2, l_1, l_2, l_3\} \tag{5.209}$$

and

$$\mathbb{P}(Z_4 = c_{j_1}) = \mathbb{P}(Z_4 = c_{j_2}) = \mathbb{P}(Z_4 = c_{l_1}) = \mathbb{P}(Z_4 = c_{l_2}) = \mathbb{P}(Z_4 = c_{l_3}) = 0. \tag{5.210}$$

In this case the movement types of the cells do not change. For indistinguishable particles nothing changes. The local operator $\mathcal{R}_{2,4} \colon Q^{1 \times 6} \to Q^{1 \times 6}$ is defined by

$$\mathcal{R}_{2,4} x := \begin{pmatrix} 1 & 1 & 1 & 1 & 1 & 1 \end{pmatrix}. \tag{5.211}$$

Five particles with movement type 2:
– Zero particles with movement type 1:
For the first particle the random variable Z_1 is used in the following way.

$$\mathbb{P}(Z_1 = c_i) = \frac{1}{6}, \quad \forall i \in I = \{1, \ldots, 6\} \tag{5.212}$$

and the chosen lattice vector is denoted by c_{l_1}. For the second particle the random variable Z_2 is used

$$\mathbb{P}(Z_2 = c_i) = \frac{1}{5}, \quad \forall i \in I = \{1, \ldots, 6\} \backslash \{l_1\} \tag{5.213}$$

and

$$\mathbb{P}(Z_2 = c_{l_1}) = 0 \tag{5.214}$$

and the chosen lattice vector is denoted by c_{l_2}. For the third particle the random variable Z_3 is used

$$\mathbb{P}(Z_3 = c_i) = \frac{1}{4}, \quad \forall i \in I = \{1, \ldots, 6\} \backslash \{l_1, l_2\} \tag{5.215}$$

and

$$\mathbb{P}(Z_3 = c_{l_1}) = \mathbb{P}(Z_3 = c_{l_2}) = 0 \tag{5.216}$$

and the chosen lattice vector is denoted by c_{l_3}. For the fourth particle the random variable Z_4 is used

$$\mathbb{P}(Z_4 = c_i) = \frac{1}{3}, \quad \forall i \in I = \{1, \ldots, 6\} \backslash \{l_1, l_2, l_3\} \tag{5.217}$$

and

$$\mathbb{P}(Z_4 = c_{l_1}) = \mathbb{P}(Z_4 = c_{l_2}) = \mathbb{P}(Z_4 = c_{l_3}) = 0 \tag{5.218}$$

and the chosen lattice vector is denoted by c_{l_4}. For the fifth particle the random variable Z_5 is used

$$\mathbb{P}(Z_5 = c_i) = \frac{1}{2}, \quad \forall i \in I = \{1, \ldots, 6\} \backslash \{l_1, l_2, l_3, l_4\} \tag{5.219}$$

and

$$\mathbb{P}(Z_5 = c_{l_1}) = \mathbb{P}(Z_5 = c_{l_2}) = \mathbb{P}(Z_5 = c_{l_3}) = \mathbb{P}(Z_5 = c_{l_4}) = 0. \qquad (5.220)$$

The local operator $\mathcal{R}_{0,5} \colon Q^{1\times 6} \to Q^{1\times 6}$ is defined by

$$\mathcal{R}_{0,5}x := \begin{cases} \begin{pmatrix} 0 & 1 & 1 & 1 & 1 & 1 \end{pmatrix} & \text{if } Z_i \neq c_1, i = 1, \dots, 5, \\ \begin{pmatrix} 1 & 0 & 1 & 1 & 1 & 1 \end{pmatrix} & \text{if } Z_i \neq c_2, i = 1, \dots, 5, \\ \begin{pmatrix} 1 & 1 & 0 & 1 & 1 & 1 \end{pmatrix} & \text{if } Z_i \neq c_3, i = 1, \dots, 5, \\ \begin{pmatrix} 1 & 1 & 1 & 0 & 1 & 1 \end{pmatrix} & \text{if } Z_i \neq c_4, i = 1, \dots, 5, \\ \begin{pmatrix} 1 & 1 & 1 & 1 & 0 & 1 \end{pmatrix} & \text{if } Z_i \neq c_5, i = 1, \dots, 5, \\ \begin{pmatrix} 1 & 1 & 1 & 1 & 1 & 0 \end{pmatrix} & \text{if } Z_i \neq c_6, i = 1, \dots, 5. \end{cases} \qquad (5.221)$$

– One particle (corresponding lattice vector c_j) with movement type 1:
For the first particle the random variable Z_1 is used in the following way.

$$\mathbb{P}(Z_1 = c_i) = \frac{1}{5}, \quad \forall i \in I = \{1, \dots, 6\} \backslash \{j\} \qquad (5.222)$$

and

$$\mathbb{P}(Z_1 = c_j) = 0 \qquad (5.223)$$

and the chosen lattice vector is denoted by c_{l_1}. For the second particle the random variable Z_2 is used

$$\mathbb{P}(Z_2 = c_i) = \frac{1}{4}, \quad \forall i \in I = \{1, \dots, 6\} \backslash \{j, l_1\} \qquad (5.224)$$

and

$$\mathbb{P}(Z_2 = c_j) = \mathbb{P}(Z_2 = c_{l_1}) = 0 \qquad (5.225)$$

and the chosen lattice vector is denoted by c_{l_2}. For the third particle the random variable Z_3 is used

$$\mathbb{P}(Z_3 = c_i) = \frac{1}{3}, \quad \forall i \in I = \{1, \dots, 6\} \backslash \{j, l_1, l_2\} \qquad (5.226)$$

and

$$\mathbb{P}(Z_3 = c_j) = \mathbb{P}(Z_3 = c_{l_1}) = \mathbb{P}(Z_3 = c_{l_2}) = 0 \qquad (5.227)$$

and the chosen lattice vector is denoted by c_{l_3}. For the fourth particle the random variable Z_4 is used

$$\mathbb{P}(Z_4 = c_i) = \frac{1}{2}, \quad \forall i \in I = \{1, \dots, 6\} \backslash \{j, l_1, l_2, l_3\} \qquad (5.228)$$

and

$$\mathbb{P}(Z_4 = c_j) = \mathbb{P}(Z_4 = c_{l_1}) = \mathbb{P}(Z_4 = c_{l_2}) = \mathbb{P}(Z_4 = c_{l_3}) = 0 \qquad (5.229)$$

and the chosen lattice vector is denoted by c_{l_4}. For the fifth particle the random variable Z_5 is used

$$\mathbb{P}(Z_5 = c_i) = 1, \quad \forall i \in I = \{1, \ldots, 6\}\setminus\{j, l_1, l_2, l_3, l_4\} \tag{5.230}$$

and

$$\mathbb{P}(Z_5 = c_j) = \mathbb{P}(Z_5 = c_{l_1}) = \mathbb{P}(Z_5 = c_{l_2}) = \mathbb{P}(Z_5 = c_{l_3}) = \mathbb{P}(Z_5 = c_{l_4}) = 0. \tag{5.231}$$

In this case the movement types of the cells do not change. For indistinguishable particles nothing changes. The local operator $\mathcal{R}_{1,5}: Q^{1\times 6} \to Q^{1\times 6}$ is defined by

$$\mathcal{R}_{1,5}x := \begin{pmatrix} 1 & 1 & 1 & 1 & 1 & 1 \end{pmatrix}. \tag{5.232}$$

Six particles with movement type 2:
– Zero particles with movement type 1:
For the first particle the random variable Z_1 is used in the following way.

$$\mathbb{P}(Z_1 = c_i) = \frac{1}{6}, \quad \forall i \in I = \{1, \ldots, 6\} \tag{5.233}$$

and the chosen lattice vector is denoted by c_{l_1}. For the second particle the random variable Z_2 is used

$$\mathbb{P}(Z_2 = c_i) = \frac{1}{5}, \quad \forall i \in I = \{1, \ldots, 6\}\setminus\{l_1\} \tag{5.234}$$

and

$$\mathbb{P}(Z_2 = c_{l_1}) = 0 \tag{5.235}$$

and the chosen lattice vector is denoted by c_{l_2}. For the third particle the random variable Z_3 is used

$$\mathbb{P}(Z_3 = c_i) = \frac{1}{4}, \quad \forall i \in I = \{1, \ldots, 6\}\setminus\{l_1, l_2\} \tag{5.236}$$

and

$$\mathbb{P}(Z_3 = c_{l_1}) = \mathbb{P}(Z_3 = c_{l_2}) = 0. \tag{5.237}$$

and the chosen lattice vector is denoted by c_{l_3}. For the fourth particle the random variable Z_4 is used

$$\mathbb{P}(Z_4 = c_i) = \frac{1}{3}, \quad \forall i \in I = \{1, \ldots, 6\}\setminus\{l_1, l_2, l_3\} \tag{5.238}$$

and

$$\mathbb{P}(Z_4 = c_{l_1}) = \mathbb{P}(Z_4 = c_{l_2}) = \mathbb{P}(Z_4 = c_{l_3}) = 0 \tag{5.239}$$

and the chosen lattice vector is denoted by c_{l_4}. For the fifth particle the random variable Z_5 is used

$$\mathbb{P}(Z_5 = c_i) = \frac{1}{2}, \quad \forall i \in I = \{1, \ldots, 6\}\setminus\{l_1, l_2, l_3, l_4\} \tag{5.240}$$

and

$$\mathbb{P}(Z_5 = c_{l_1}) = \mathbb{P}(Z_5 = c_{l_2}) = \mathbb{P}(Z_5 = c_{l_3}) = \mathbb{P}(Z_5 = c_{l_4}) = 0 \tag{5.241}$$

and the chosen lattice vector is denoted by c_{l_5}. For the sixth particle the random variable Z_6 is used

$$\mathbb{P}(Z_6 = c_i) = 1, \quad \forall i \in I = \{1, \ldots, 6\} \setminus \{l_1, l_2, l_3, l_4, l_5\} \tag{5.242}$$

and

$$\mathbb{P}(Z_6 = c_{l_1}) = \mathbb{P}(Z_6 = c_{l_2}) = \mathbb{P}(Z_6 = c_{l_3}) = \mathbb{P}(Z_6 = c_{l_4}) = \mathbb{P}(Z_6 = c_{l_5}) = 0. \tag{5.243}$$

In this case the movement types of the cells do not change. For indistinguishable particles nothing changes. The local operator $\mathcal{R}_{0,6} \colon Q^{1 \times 6} \to Q^{1 \times 6}$ is defined by

$$\mathcal{R}_{0,6} x := \begin{pmatrix} 1 & 1 & 1 & 1 & 1 & 1 \end{pmatrix}. \tag{5.244}$$

Definition 5.70 (Local inclusion operator of random walk for FHP-I LGCA)**.** The local inclusion operator $\mathcal{R}_l \colon Q^{1 \times 6} \to Q^{1 \times 6}$ is defined by

$$\mathcal{R}_l x := \begin{cases} \mathrm{I}\, x & \text{if } K_l(i) \neq 2\, \forall i \in \{1, \ldots, 6\} \\ \mathcal{R}_{m_1, m_2} x & \text{if } \exists K_l(i) = 2,\, i \in \{1, \ldots, 6\} \end{cases} \tag{5.245}$$

where m_1 and m_2 are the numbers of particles with movement type 1 and 2, respectively.

Definition 5.71 (Local inclusion operator of random walk for FHP-II LGCA)**.** The local inclusion operator $\mathcal{R}_l \colon Q^{1 \times 7} \to Q^{1 \times 7}$ is defined by

$$\mathcal{R}_l x := \begin{cases} \mathrm{I}\, x & \text{if } K_l(i) \neq 2\, \forall i \in \{1, \ldots, 6\} \\ \left(\mathcal{R}_{m_1, m_2} P_{1-6} x,\, \mathrm{I}\, P_7 x \right) & \text{if } \exists K_l(i) = 2\, i \in \{1, \ldots, 6\} \end{cases} \tag{5.246}$$

where m_1 and m_2 are the numbers of particles with movement type 1 and 2, respectively, and

$$P_{1-6} \colon Q^{1 \times 7} \to Q^{1 \times 6},\, x \mapsto (x_1, \ldots, x_6), \tag{5.247}$$

and

$$P_7 \colon Q^{1 \times 7} \to Q,\, x \mapsto x_7. \tag{5.248}$$

Definition 5.72 (Global inclusion operator of random walk)**.** The global inclusion operator $\mathcal{R} \colon Q^{|\mathcal{L}| \times m} \to Q^{|\mathcal{L}| \times m}$ is defined by

$$(\mathcal{R}X)_{i,.} := \mathcal{R}_l X_{i,.}. \tag{5.249}$$

Streaming and Neighbouring Nodes of the Synthesis of FHP Lattice Gas Cellular Automaton and Random Walk

The local streaming operator $\mathcal{S}_l$, the global streaming operator $\mathcal{S}$, and the neighbouring nodes operator $\mathcal{N}$ of the synthesis model are defined by Definition 5.50, Definition 5.53 and Definition 5.54, respectively.

Evolution of the Synthesis of FHP Lattice Gas Cellular Automaton and Random Walk

Finally, the evolution operator of the synthesis model is defined.

Definition 5.73 (Evolution operator of the synthesis model)**.** The evolution operator $\mathcal{E}\colon Q^{|\mathcal{L}|\times m} \to Q^{|\mathcal{L}|\times m}$ is defined by

$$\mathcal{E} := \mathcal{S} \circ \mathcal{N} \circ \mathcal{R} \circ \mathcal{C}, \tag{5.250}$$

whereby $\mathcal{C}$ is the collision operator, $\mathcal{R}$ is the inclusion operator, $\mathcal{N}$ is the neighbouring nodes operator and $\mathcal{S}$ is the streaming operator.

Remark 5.74. In addition to the calculation of the evolution of the states of the cells the movement type of the cells has to be updated too.

In Figure 5.8 an example for the evolution of the synthesis model is shown. The collision rules of FHP-I LGCA are used. The particles with movement type 2 are shown in blue.

before collision

after collision

after random walk

after streaming
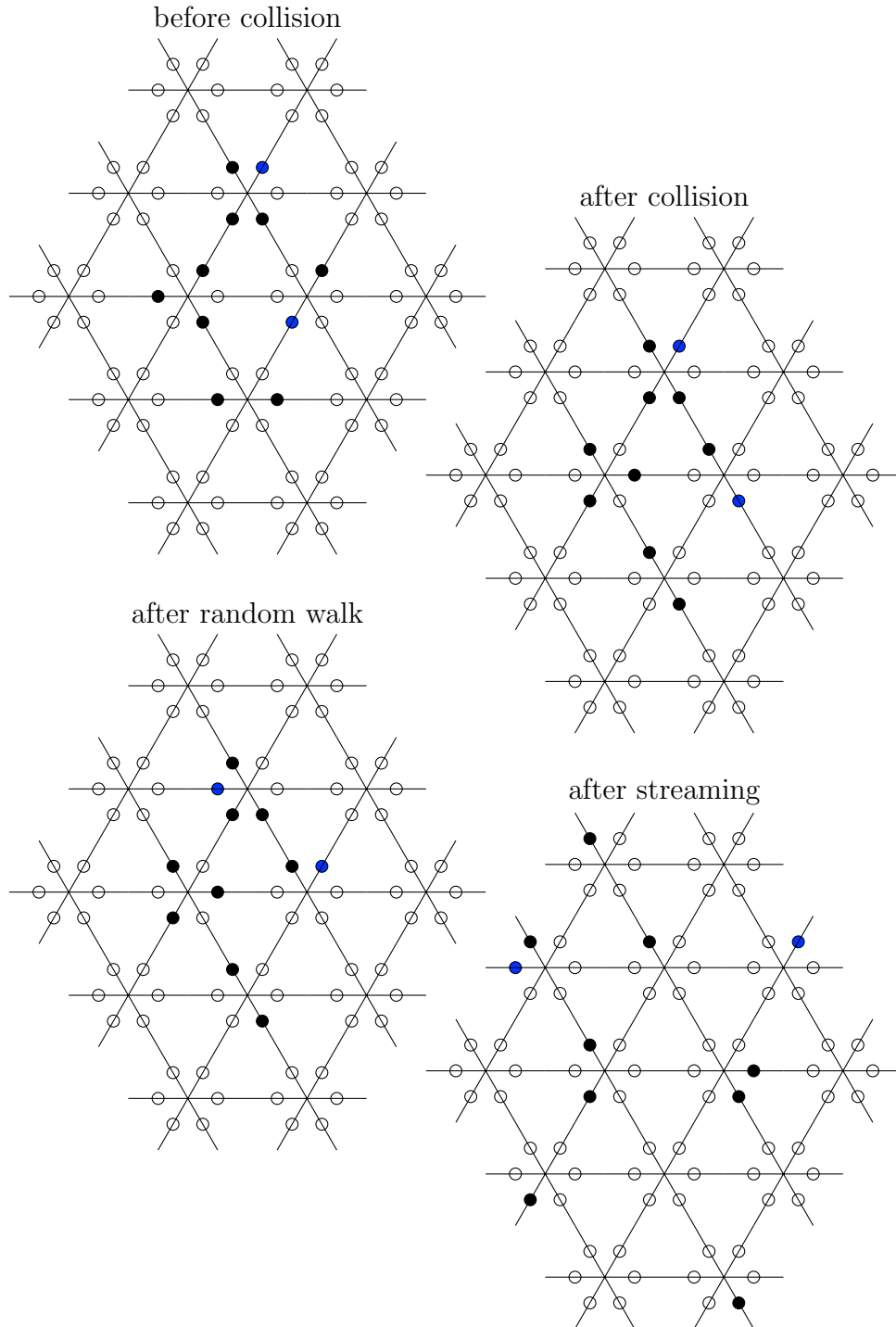
Figure 5.8: Illustration of the evolution of the synthesis of the FHP-I LGCA and random walk

6

Synthesis Model for Gluing

Due to simplification, the first models were developed for the two-dimensional case, i.e. for the cross section of the resinating mixer that is orthogonal to the longitudinal axis. The resulting geometry of the considered part of the mixer is a circle. As modelling method the synthesis model of Section 5.3.2 with different collision rules (these are defined later in this Chapter) was used. For the development of the model the existing objects had to be defined:

- Wood particles:
  Due to simplification, the geometry of the wood particles was chosen to be a rectangle.

- Adhesive droplets:
  The adhesive droplets were assumed to be circles.

- Resinating mixer:
  The resinating mixer constitutes a system boundary. The cross section of the resinating mixer that is orthogonal to the longitudinal axis was considered to be a circle. Due to simplification the shaft was not considered.

- Ploughshares ("mixing arms"):
  The ploughshares are moving objects within the resinating mixer, which force the wood particles to move.

- Knife head:
  The knife head was not considered in the two-dimensional case.

For modelling the movement of the particles it was necessary to define some environmental parameters:

- Time interval:
  Time step for evolution. The time step is calculated using the grid width and the velocities of the wood particles and adhesive droplets, respectively.

- Spatial resolution:
  Distance of the nodes of the lattice (grid width).

- Location of particles:
  Wood particles are located at the bottom of the resinating mixer at the beginning of the simulation. Adhesive droplets have a defined starting position (nozzle at the top of the resinating mixer). The movement of the particles is limited due to their location in the resinating mixer. The location of the wood particles is influenced by the ploughshares.

- Movement of wood particles:
  The wood particles move according to the LGCA of the synthesis model.

- Movement of adhesive droplets:
  The adhesive droplets move according to the random walk of the synthesis model. For the adhesive droplets a defined spraying direction, caused by the nozzle, had to be considered.

6.1 Lattice of Synthesis Model for Gluing

The cross section of the resinating mixer that is orthogonal to the longitudinal axis is assumed to be circle and for this circle a lattice was built. The lattice $\mathcal{L}$ is generated by discretisation of space using nodes, which constitute equilateral triangles. The grid width is given by $h \in \mathbb{R}^+$. Due to the nozzle, a spraying direction is given. This direction is downwards and corresponds to $(0, -1)$. Thus, a lattice with lattice vectors corresponding to the y-axis (vertical axis) is used. Compared with Chapter 4 and Chapter 5 where lattices with lattice vectors corresponding to the x-axis were used, this lattice is rotated by $\pi/2$.

Since the lattice is based on triangles, there are six different directions (edges) at each node (vertex). Additionally, due to the fact that wood particles and adhesive droplets can have zero speed, each node has seven cells. The corresponding lattice vectors are given by

$$
\begin{aligned}
c_i &= h \left(\cos \left(\frac{\pi}{3} i + \frac{\pi}{2} \right), \sin \left(\frac{\pi}{3} i + \frac{\pi}{2} \right) \right), \quad i = 1, \ldots, 6, \\
c_0 &= (0, 0).
\end{aligned}
\tag{6.1}
$$

In Figure 6.1 the lattice vectors c_i, $i = 1, \ldots, 6$, are shown.
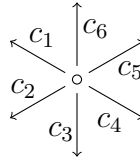
Figure 6.1: Illustration of the lattice vectors c_i, $i = 1, \ldots, 6$

In Figure 6.2 the lattice is illustrated, whereas the light grey dashed line symbolizes the wall of the mixer and the black dots inside represent the nodes (vertices of the equilateral triangles of the lattice). In Figure 6.2 below, a part of the cross section of the resinating mixer is shown in more detail. The black lines build the triangles and the smaller coloured triangles represent the possible directions of movement. Furthermore, the coloured triangles form hexagons whereby the centre of each hexagon is a node of the lattice. These hexagons are the basis for the discretisation of the wood particles. The geometry of the wood particles is assumed to be a rectangle and the rectangular shape is approximated by a set of hexagons.
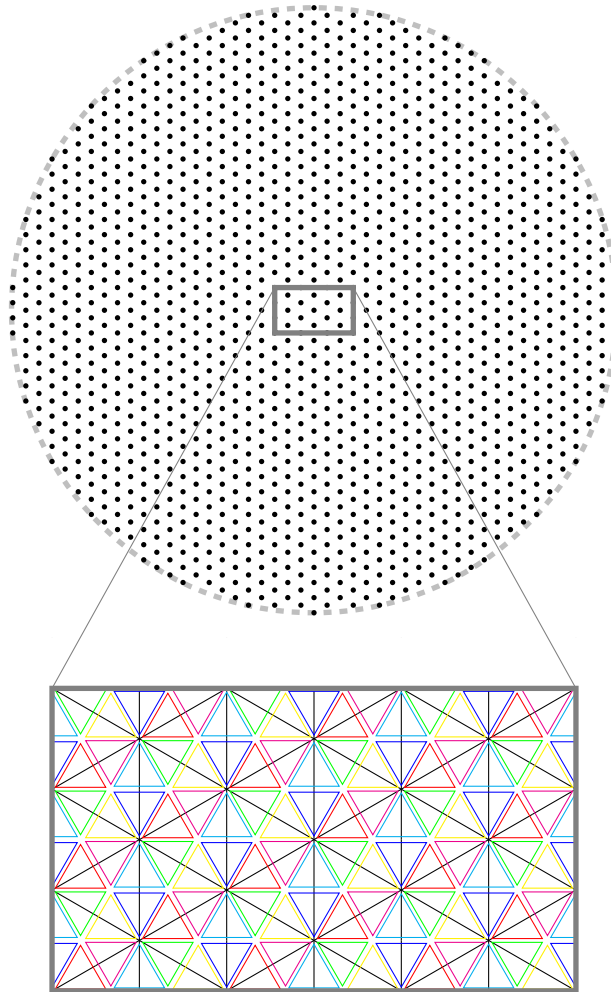
Figure 6.2: Schematic depiction of the lattice used for the cross section of the resinating mixer that is orthogonal to the longitudinal axis

6.2 States and Movement Types of Synthesis Model for Gluing

The set of states for the cells is $Q = \{0, 1\}$:

- Cells with state 0 are not occupied.

- Cells with state 1 are occupied by a wood particle or an adhesive droplet.

The set of movement types is $T = \{0, 1, 2\}$. Each cell has a defined state and movement type:

- Cells with state 0 have movement type 0.

- Cells with state 1 have movement type 1 for wood particles.

- Cells with state 1 have movement type 2 for adhesive droplets.

Thus, using the movement type a distinction between wood particles and adhesive droplets can be performed.

Definition 6.1 (Local classification of movement)**.** The local classification of movement is given by $K_l \in T^{1 \times 7}$.

In the following, an ID-number for the wood particles and adhesive droplets is used.

Definition 6.2 (ID-number)**.** The ID-numbers are given by the set $ID = \{0, 1, \ldots, m\}$, where $m = m_{wp} + m_{ad}$ is the total number of particles (m_{wp} number of wood particles, m_{ad} number of adhesive droplets), whereby ID 0 means that there is neither a wood particle nor an adhesive droplet.

If a wood particle and an adhesive droplet collide, the individual adhesive droplet disappears and the former adhesive droplet is located on the surface of the wood particle. Thus, a part of the wood particle is covered with adhesive. Therefore, a tensor that contains the properties of the wood particles and adhesive droplets is defined.

Definition 6.3 (Properties of wood particles and adhesive droplets)**.** The tensor $A \in \mathbb{R}^{7 \times 6 \times |\mathcal{L}|}$ contains the basic properties of the wood particles and adhesive droplets:

$$
\begin{aligned}
&A(.,1,.) \in Q^{7 \times |\mathcal{L}|} \\
&A(.,2,.) \in T^{7 \times |\mathcal{L}|} \\
&A(.,3,.) \in ID^{7 \times |\mathcal{L}|} \text{ are the ID-numbers of the particles} \\
&A(.,4,.) \in \mathbb{R}_0^{+ \, 7 \times |\mathcal{L}|} \text{ are the masses of wood particles} \\
&A(.,5,.) \in \mathbb{R}_0^{+ \, 7 \times |\mathcal{L}|} \text{ are the masses of adhesive droplets} \\
&A(.,6,.) \in \mathbb{R}_0^{+ \, 7 \times |\mathcal{L}|} \text{ are the radii of adhesive droplets}
\end{aligned}
\tag{6.2}
$$

The first six rows correspond to the lattice velocities c_i, $i = 1, \ldots, 6$. In the seventh row there are the values for the cells corresponding to the lattice vector c_0. Further properties of the wood particles or adhesive droplets can be included within the tensor A by adding columns.

According to the grid width h and the dimensions of the wood particle, wood particles can occupy several nodes of the lattice. At each node that is occupied by the wood particle the state of the cell corresponding to the lattice vector is set to 1. The states of the other cells of these nodes are set to 0. When a collision of wood particles takes place, in general the corresponding lattice vectors of the wood particles change and it has to be ensured that in the other nodes of the wood particle no state other than 0 is overwritten due to the change of the lattice vector.

6.3 Collision of Synthesis Model for Gluing

Due to the different types of particles within the model several collision rules are necessary. These collision rules are merged by composition to one collision operator. In the following, the order of application of collision rules at a node is defined by:

1. Collision of adhesive droplets

2. Collision of wood particles and one adhesive droplet

3. Collision of wood particles

6.3.1 Collision of Adhesive Droplets

This collision is modelled as a perfectly inelastic collision. If several adhesive droplets are at the same node before collision, one adhesive droplet remains after collision. The mass of the droplet after collision is given by $M = \sum_{i=1}^{n} M_i$ where n is the number of adhesive droplets at the node. The radius of the adhesive droplet after collision is calculated by

$$r_M = \left(\frac{3M}{4\pi\rho}\right)^{1/3} \tag{6.3}$$

where ρ is the density of the adhesive. Without loss of generality (as the inclusion operator changes the corresponding lattice vector in any case) the adhesive droplet corresponds to the lattice vector c_3 after collision. The state of the corresponding cell is 1 and the movement type is 2.

Definition 6.4 (Collision of adhesive droplets)**.** The deterministic collision operator for adhesive droplets $\mathcal{C}_{ad}\colon Q^{1\times 7} \to Q^{1\times 7}$ is defined as

$$
\mathcal{C}_{ad}x := \begin{cases} \begin{pmatrix} 0 & 0 & 1 & 0 & 0 & 0 & 0 \end{pmatrix} & \text{if } K_l(i) = 2 \text{ for at least two indices } i \in I = \{1, \ldots, 7\}, \\ \mathrm{I}\, x & \text{else.} \end{cases}
\tag{6.4}
$$

In Figure 6.3, as an example, the collision of two adhesive droplets is depicted schematically.

Figure 6.3: Schematic depiction of collision of two adhesive droplets

6.3.2 Collision of Wood Particles and One Adhesive Droplet

First, the special case of the collision of one wood particle and one adhesive droplet is described. If an adhesive droplet collides with a wood particle, the adhesive droplet adheres to the wood particle. The wood particle has the same corresponding lattice vector before and after the collision. After collision the adhesive droplet no longer exists as adhesive droplet, but its properties are still included in the tensor A. Thus, the mass of the wood particle and the mass of the former adhesive droplet are added if the total mass is considered. The corresponding lattice vector of the wood particle before and after collision is the same.

If more than one wood particle is involved in the collision the mass of the adhesive droplet is split and every wood particle receives the same amount of adhesive which is added in the tensor A. The mass of the adhesive each wood particle receives is calculated by

$$
\frac{M}{m_{wp}},
\tag{6.5}
$$

where M is the mass of the adhesive droplet and m_{wp} is the number of wood particles.

Definition 6.5 (Collision of wood particles and one adhesive droplet)**.** The deterministic collision operator for wood particles and one adhesive droplet $\mathcal{C}_{adwp}\colon Q^{1\times 7} \to Q^{1\times 7}$ is defined elementwise $\forall i \in I = \{1, \ldots, 7\}$ as

$$
(\mathcal{C}_{adwp}x)_i := \begin{cases} \left.\begin{cases} 1 & \text{if } K_l(i) = 1 \\ 0 & \text{if } K_l(i) = 2 \\ 0 & \text{else.} \end{cases}\right\} & \text{if } \exists i_1, i_2 \in I : K_l(i_1) = 1 \text{ and } K_l(i_2) = 2, \\ x_i & \text{else.} \end{cases}
\tag{6.6}
$$

In Figure 6.4 the collision of one wood particle and one adhesive droplet is depicted schematically.
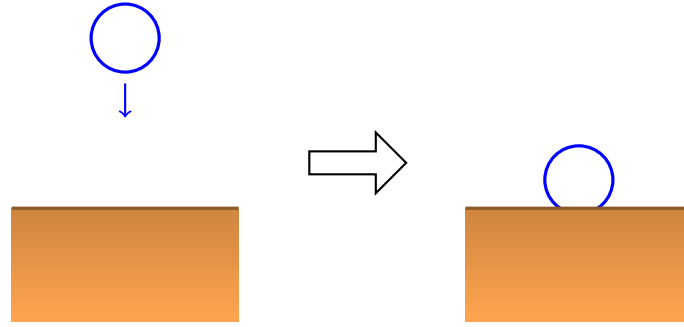
Figure 6.4: Schematic depiction of collision of one wood particle and one adhesive droplet

Due to the behaviour described in Section 3.2 the spreading and penetration are included in the model.

According to the experimental results in Section 7.1 20 % of the adhesive mass penetrates into the wood particle. At every collision between a wood particle and an adhesive droplet 20 % of the mass of the adhesive droplet is reserved for penetration.

The spreading is modelled by increasing the radius of the adhesive droplet by 20 % based on the findings in Section 7.1. In contrast to reality in the model the radius is set immediately at the time of the collision and does not change over time. At the time of collision, there are three cases (in the corresponding figures $\hat{r}_{wp}$ is the radius of the adhesive on the wood particle before collision, $\hat{r}$ is the radius of the adhesive on the wood particle already present before collision and the adhesive was not involved in a collision of wood particles, r the radius of the adhesive on the wood particle after collision without spreading, and r_{wp} is the radius of the adhesive on the wood particle after collision with spreading):

- No adhesive on the wood particle before collision:
  The radius of the adhesive droplet is increased by 20 % and stored in the tensor A (Figure 6.5).

$$r_{wp} = r \cdot 1.2$$
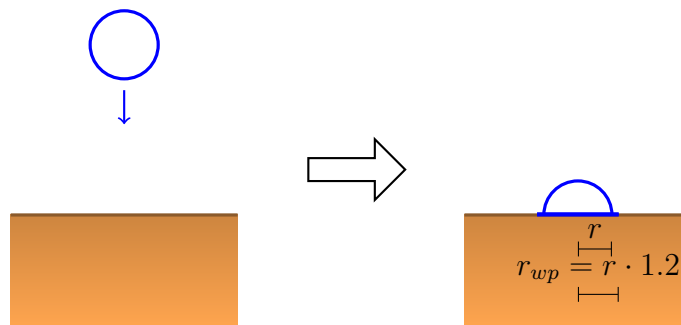
Figure 6.5: Schematic depiction of collision of a wood particle and an adhesive droplet: no adhesive on the wood particle before collision

- Adhesive on the wood particle already present before collision and the adhesive was not involved in a collision of wood particles:
  The mass of the current adhesive droplet and the mass of the adhesive on the wood particle before the collision are summed and the corresponding radius is calculated. The resulting radius is increased by 20 % and compared with the radius of the adhesive on the wood particle before collision (Figure 6.6). The maximum radius is stored in the tensor A.
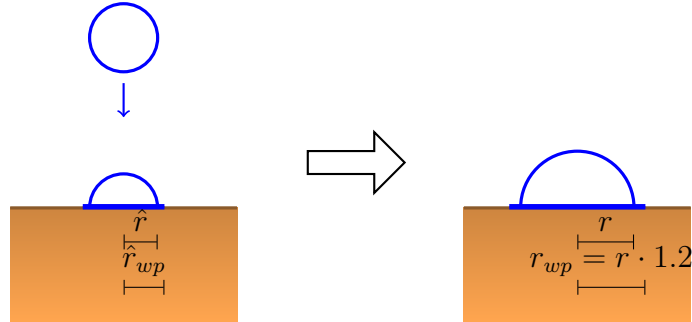
Figure 6.6: Schematic depiction of collision of a wood particle and an adhesive droplet: adhesive on the wood particle already present before collision and the adhesive was not involved in a collision of wood particles

- Adhesive on the wood particle already present before collision and the adhesive was involved in a collision of wood particles (transfer of adhesive):
  The radius of the current adhesive droplet is increased by 20 % and compared with the radius of the adhesive on the wood particle before collision (Figure 6.7 and Figure 6.8). The maximum radius is stored in the tensor A.
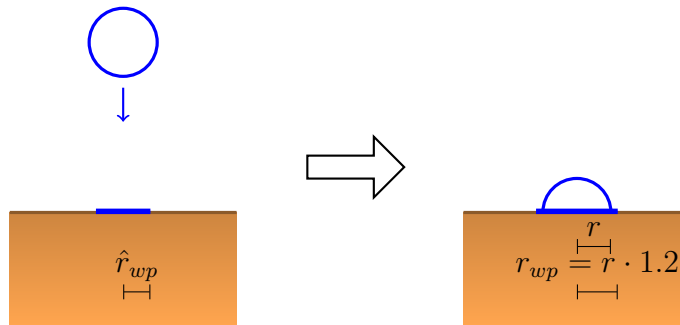
Figure 6.7: Schematic depiction of collision of a wood particle and an adhesive droplet: adhesive on the wood particle already present before collision and the adhesive was involved in a collision of wood particles (radius increases)
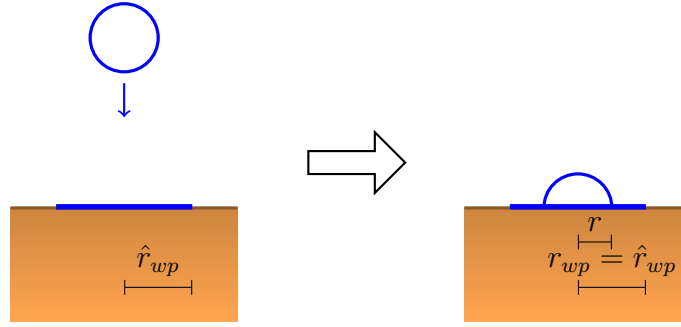
Figure 6.8: Schematic depiction of collision of a wood particle and an adhesive droplet: adhesive on the wood particle already present before collision and the adhesive was involved in a collision of wood particles (radius unchanged)

6.3.3 Collision of Wood Particles

In general, the collision of wood particles is an elastic collision. Due to the fact that the geometry of the wood particles is discretised and that only seven discretised lattice vectors are available, the realistic physical velocities after collision cannot be calculated. The general definition of the collision of wood particles is based on the special case of a collision of two wood particles with the same mass. In the following the collision of two wood particles with the same mass is considered:

The basic idea is to use the rules of an elastic collision of two equal masses. First, two special cases of collision are considered:

- Elastic collision of a resting and a moving mass (depicted in Figure 6.9)
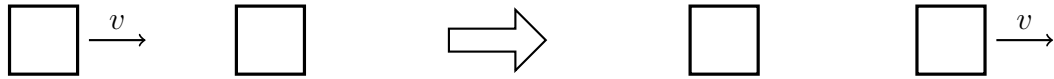
Figure 6.9: Schematic depiction of an elastic collision of a resting and a moving mass

- Elastic head-on collision (depicted in Figure 6.10)
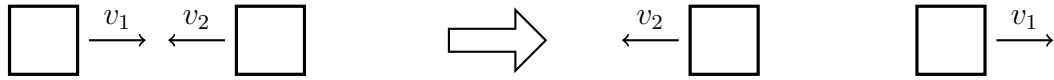
Figure 6.10: Schematic depiction of an elastic head-on collision

In both cases the velocities before and after collision are swapped. This behaviour is used for the general definition of the collision of two wood particles $C_{2,wp}$. For a collision of two wood particles the entries in the tensor A are swapped according to the lattice vectors (indices $i, j \in \{1, \ldots, 7\}$) of the two wood particles determined at the node where the collision takes place:

$$A(i, ., l_i) \mapsto A(j, ., l_i) \, \forall l_i \in L_i \subset \{1, \ldots, |\mathcal{L}|\}$$
$$A(j, ., l_j) \mapsto A(i, ., l_j) \, \forall l_j \in L_j \subset \{1, \ldots, |\mathcal{L}|\}$$

$$(6.7)$$

where L_i, L_j are the indices of the nodes of the corresponding wood particle, respectively. Each collision of two wood particles generates a new collision operator for two wood particles. One of these operators is defined in the following.

Definition 6.6 (Collision of two specific wood particles). The deterministic collision operator for two specific wood particles $\mathcal{C}_{2,wp}: Q^{1\times7} \to Q^{1\times7}$ is defined as

$$
\mathcal{C}_{2,wp}x_\lambda := \begin{cases} \pi_{ij}x_\lambda & \text{if } \lambda \in L_i \cup L_j \\ \mathrm{I}\,x_\lambda & \text{else} \end{cases} \tag{6.8}
$$

where $\lambda \in \{1,\ldots,|\mathcal{L}|\}$ is the index of the node x, π_{ij} is the permutation that swaps the entries i and j and L_i, L_j are the indices of the nodes of the corresponding wood particle, respectively.

Remark 6.7. The collision of two wood particles is not affecting only one node, i.e. it is not operating locally at one node.

If two collisions of two wood particles at different nodes affect the same wood particle, they are called connected (Figure 6.11).
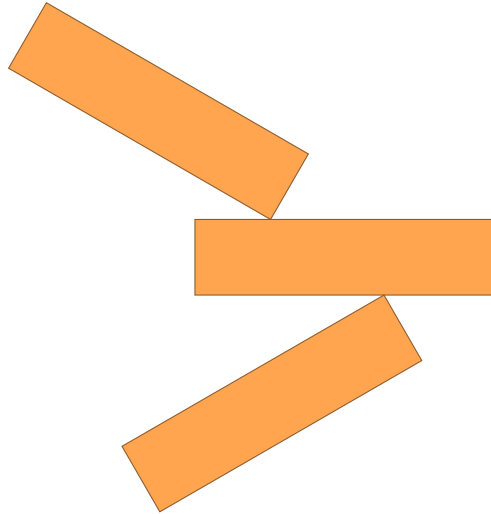
Figure 6.11: Schematic depiction of connected collisions of wood particles

Connected collisions cannot be considered separately. This has two main reasons:

1. The order of application of the collision operators affects the result.

2. It is possible that the second collision operator changes the lattice vectors in such a way that one wood particle has different lattice vectors amongst its nodes.

In order to prevent such a behaviour, a collision operator for connected collisions of two wood particles has to be defined. As a basis for this collision the collision of two wood particles is considered. The idea is to generalise the swapping of the lattice vectors by collecting possible lattice vectors from the involved collisions of two wood particles.

For each wood particle involved in a collision of two wood particles the possible lattice vectors have to be collected.

Definition 6.8 (Collection of lattice vectors). Let $\{C_{2,wp,k}\}$, $k \in \{1, \ldots, N_C\}$, be a set of N_C connected collisions of two wood particles and let $ID_C \subset ID$ be the set of the involved wood particles identified by their ID. The operator $poss\colon ID_C \to 2^{\{c_0,\ldots,c_6\}}$ is defined by

$$c_{\hat{j}} \in poss(id) \Leftrightarrow \exists k\colon id \in A(i, 3, L_{i,k}) \tag{6.9}$$

where $c_{\hat{j}} \in \{c_0, \ldots, c_6\}$ with $\hat{j} = j \mod 7$, $L_{i,k}$ is the set of indices of the nodes of the corresponding wood particle for the lattice vector corresponding to entry i for collision $C_{2,wp,k}$ and j is the other entry in the corresponding collision.

In order to define the corresponding lattice vector after collision for each wood particle, several steps are necessary. If two wood particles are affected by the same collision, they must not have the same corresponding lattice vector after collision. If this holds for all wood particles, the selection of the lattice vectors is valid. The following rules ensure a valid selection of lattice vectors:

1. If for a wood particle $|poss(id)| = 1$, the corresponding lattice vector after collision is set to the only element of $poss(id)$.

2. If for a wood particle $|poss(id)| > 1$, the corresponding lattice vector after collision is chosen randomly from $\{c_1, \ldots, c_6\}$. The selection of the lattice vectors has to ensure the validity of the result.

3. If the first two rules do not lead to a valid selection of lattice vectors, the corresponding lattice vectors after collision are chosen randomly from $\{c_0, \ldots, c_6\}$ for all wood particles involved in the collision. The selection of the lattice vectors has to ensure the validity of the result.

Remark 6.9. The third rule leads to at least one valid result. This is the constellation before collision as it is valid.

Remark 6.10. The selection of the lattice vectors after collision can be interpreted as a graph colouring problem where the wood particles are the vertices, the collisions define the edges and the possible lattice vectors are the possible colours for each vertex. The coloured graph is valid if two adjacent vertices do not have the same colour. This is the same condition as above.

Remark 6.11. The collision of two specific wood particles is a special case of the connected collision of two wood particles where $N_C = 1$. According to the rules above, for this case rule 1 is applied, i.e. the lattice vectors are swapped.

Remark 6.12. For collisions of more than two wood particles colliding in the same node the same rules can be applied. This also holds for connected collisions of more than two wood particles. For three wood particles colliding in the same node rule 2 is applied, i.e. a randomly chosen lattice vector is assigned to each wood particle.

In the following a collision of an arbitrary number of wood particles is denoted by C_{wp}. The rules above define an operator $lv\colon ID_{wp} \to \{c_0, \ldots, c_6\}$ for the currently considered set of connected collisions of wood particles, where ID_{wp} is the set of IDs of all wood particles. This operator assigns a lattice vector (after collision) to every wood particle. If the wood particle is not affected by the collision, the same lattice vector as before the collision is chosen. In the following this operator is defined formally.

Definition 6.13 (Lattice vector operator). Let $\{C_{wp,k}\}$, $k \in \{1, \ldots, N_C\}$, be a set of N_C connected collisions of wood particles and let $ID_C \subset ID_{wp} \subset ID$ be the set of the involved wood particles identified by their ID. The lattice vector operator $lv\colon ID_{wp} \to \{c_0, \ldots, c_6\}$ is defined by

$$
lv(id) := \begin{cases}
c_i \text{ where } c_i \in poss(id) & \text{if } |poss(id)| = 1 \wedge \exists \text{ a valid} \\
& \text{selection based on rule 1 \& 2} \\
c_i \text{ where } c_i \in \{c_1, \ldots, c_6\} \text{ chosen randomly} & \text{if } |poss(id)| > 1 \wedge \exists \text{ a valid} \\
& \text{selection based on rule 1 \& 2} \\
c_i \text{ where } c_i \in \{c_0, \ldots, c_6\} \text{ chosen randomly} & \text{if } \nexists \text{ a valid selection based} \\
& \text{on rule 1 \& 2} \\
c_i \text{ where } \exists \lambda\colon id = A(i, 3, \lambda) & \text{if } id \notin ID_C
\end{cases}
\tag{6.10}
$$

As the operator lv operates on the wood particles and the operators of an LGCA operate on nodes, a collision operator that operates on nodes has to be defined.

Definition 6.14 (Connected collision of wood particles). Let $\{C_{wp,k}\}$, $k \in \{1, \ldots, N_C\}$, be a set of N_C connected collisions of wood particles and let $ID_C \subset ID_{wp} \subset ID$ be the set of the involved wood particles identified by their ID. The collision operator $\mathcal{C}_{conn,wp}\colon Q^{1\times7} \to Q^{1\times7}$ is defined by

$$
\mathcal{C}_{conn,wp} x_\lambda := \begin{cases}
\pi_{wp,\lambda} x_\lambda & \text{if } \exists i \in \{1, \ldots, 7\}\colon K_l(i) = 1 \\
\mathrm{I}\, x_\lambda & \text{else}
\end{cases}
\tag{6.11}
$$

where $\pi_{wp,\lambda}$ is the permutation that permutes the corresponding lattice vectors of every wood particle at node λ based on $lv(id)$.

Using the collision operator for connected collisions of wood particles the collision operator for wood particles can be defined.

Definition 6.15 (Collision of wood particles). The non-deterministic collision operator for wood particles $\mathcal{C}_{wp}\colon Q^{1\times7} \to Q^{1\times7}$ is defined as the composition of the operators of all connected collisions of wood particles $\mathcal{C}_{conn,wp,k}$, $k = 1, \ldots, N$, i.e.

$$
\mathcal{C}_{wp} := \bigcirc_{k=1}^{N} \mathcal{C}_{conn,wp,k}.
\tag{6.12}
$$

Remark 6.16. Each wood particle is affected by a maximum of one collision operator. In particular, for each node at most one collision operator is not the identity operator.

Remark 6.17. The collision operator $\mathcal{C}_{wp}$ is different in every time step of the evolution. The collision of two wood particles (without adhesive on the surface) is depicted in Figure 6.12.
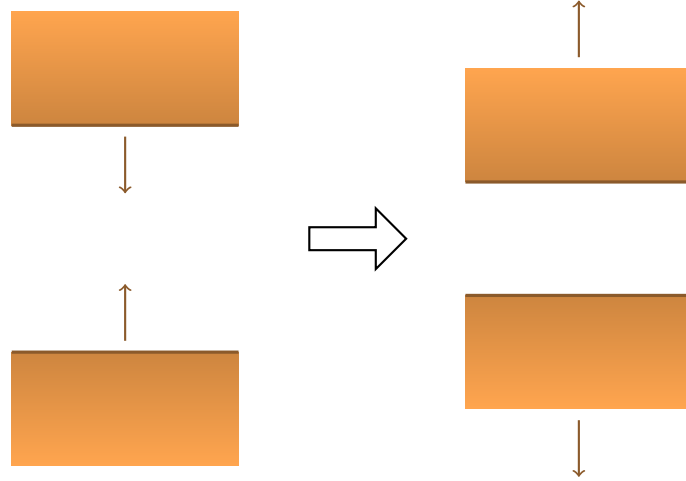
Figure 6.12: Schematic depiction of collision of two wood particles

An additional rule is necessary for including the transfer of adhesive, i.e. a part of the adhesive is transferred from a wood particle to another one during the collision. Based on experimental results, which are described in Section 7.1, it was determined that at first contact 50 % of the total mass of adhesive (including the amount reserved for penetration) is transferred from one wood particle to another. At second contact 30 % of the remaining mass is transferred. For any further collision the transfer of adhesive is negligible. The remaining 35 % of the mass of adhesive is divided in two categories: 20 % for penetration and 15 % on the surface of the wood particle. If more than two wood particles are colliding at the same node, the amount of adhesive that is transferred is split equally between the other wood particles.

6.3.4 Local and Global Collision Operator of Synthesis Model for Gluing

Using the three collision operators $\mathcal{C}_{wp}$, $\mathcal{C}_{adwp}$ and $\mathcal{C}_{ad}$ the local collision operator is defined.

Definition 6.18 (Local collision operator)**.** The local collision operator $\mathcal{C}_l \colon Q^{1\times7} \to Q^{1\times7}$ is defined as

$$\mathcal{C}_l x := \mathcal{C}_{wp} \circ \mathcal{C}_{adwp} \circ \mathcal{C}_{ad} x. \tag{6.13}$$

Definition 6.19 (Global collision operator)**.** The global collision operator $\mathcal{C} \colon Q^{|\mathcal{L}|\times7} \to Q^{|\mathcal{L}|\times7}$ is defined elementwise as

$$(\mathcal{C}X)_{i,\cdot} := \mathcal{C}_l X_{i,\cdot}. \tag{6.14}$$

6.4 Inclusion of Random Walk of Synthesis Model for Gluing

The adhesive droplets are moving according to a random walk. After collision at each node there is at most one adhesive droplet because on the one hand if it was colliding with other adhesive droplets afterwards there is one bigger adhesive droplet and on the other hand if it was colliding with a wood particle it adheres to the wood particle. If no collision took place there is also at most one adhesive droplet. Thus, after collision there is exactly one setting concerning the numbers of particles with movement type 1 and 2 at a node where the inclusion of random walk has to be applied. This setting is zero particles with movement type 1 and one particle with movement type 2. For the inclusion of random walk in the model the operator $\mathcal{R}_{ad}$ is defined in the following. The adhesive droplets are sprayed by the nozzle from above, i.e. they are moving downwards. For the movement of the adhesive droplets only lattice vectors downwards, i.e. according to c_2, c_3, c_4, are possible. Therefore, the probabilities are given by

$$\mathbb{P}(Z = c_i) = \frac{1}{3}, \quad i = 2, 3, 4 \tag{6.15}$$

and

$$\mathbb{P}(Z = c_i) = 0, \quad i = 1, 5, 6. \tag{6.16}$$

The local operator $\mathcal{R}_{ad} \colon Q^{1\times 6} \to Q^{1\times 6}$ is defined by

$$\mathcal{R}_{ad}x := \begin{cases} \begin{pmatrix} 0 & 1 & 0 & 0 & 0 & 0 \end{pmatrix} & \text{if } Z = c_2, \\ \begin{pmatrix} 0 & 0 & 1 & 0 & 0 & 0 \end{pmatrix} & \text{if } Z = c_3, \\ \begin{pmatrix} 0 & 0 & 0 & 1 & 0 & 0 \end{pmatrix} & \text{if } Z = c_4. \end{cases} \tag{6.17}$$

Definition 6.20 (Local inclusion operator of random walk)**.** The local inclusion operator $\mathcal{R}_l \colon Q^{1\times 7} \to Q^{1\times 7}$ is defined by

$$\mathcal{R}_l x := \begin{cases} \mathrm{I}\, x & \text{if } K_l(i) \neq 2 \,\forall i \in \{1, \ldots, 6\} \\ \left(\mathcal{R}_{0,1} P_{1-6}x,\, IP_7 x \right) & \text{if } \exists K_l(i) = 2,\, i \in \{1, \ldots, 6\} \end{cases} \tag{6.18}$$

where

$$P_{1-6} \colon Q^{1\times 7} \to Q^{1\times 6},\, x \mapsto (x_1, \ldots, x_6), \tag{6.19}$$

and

$$P_7 \colon Q^{1\times 7} \to Q,\, x \mapsto x_7. \tag{6.20}$$

Definition 6.21 (Global inclusion operator of random walk)**.** The global inclusion operator $\mathcal{R} \colon Q^{|\mathcal{L}|\times 7} \to Q^{|\mathcal{L}|\times 7}$ is defined by

$$(\mathcal{R}X)_{i,.} := \mathcal{R}_l X_{i,.}. \tag{6.21}$$

6.5 Neighbouring Nodes of Synthesis Model for Gluing

For defining the evolution operator, a neighbouring nodes operator is necessary. This operator is defined in Definition 5.54 and is used here with $m = 7$. This definition is recapitulated here.

Definition 6.22 (Neighbouring nodes operator)**.** The neighbouring nodes operator $\mathcal{N} \colon Q^{|\mathcal{L}| \times 7} \to Q^{7 \times 7 \times |\mathcal{L}|}$ is defined as

$$(\mathcal{N}X)_{.,.,i} := N_{.,.,i}, \tag{6.22}$$

where the tensor, which contains the states of the cells of the neighbouring nodes for each lattice point, is denoted by $N \in Q^{7 \times 7 \times |\mathcal{L}|}$. $N_{.,.,i} \in Q^{7 \times 7}$ are the states of the cells of the neighbouring nodes of lattice point i.

6.6 Streaming of Synthesis Model for Gluing

For defining the streaming operator, the states of the neighbouring nodes are necessary. The local and global streaming operator ($\mathcal{S}_l$ and $\mathcal{S}$) are defined according to Definition 5.50 and Definition 5.53 with $m = 7$, respectively. These definitions are recapitulated in the following.

Definition 6.23 (Local streaming operator)**.** The local streaming operator $\mathcal{S}_l \colon Q^{7 \times 7} \to Q^{1 \times 7}$ is defined by

$$\mathcal{S}_l n := \begin{pmatrix} n_{11} & n_{22} & \ldots & n_{77} \end{pmatrix}. \tag{6.23}$$

Definition 6.24 (Global streaming operator)**.** The global streaming operator $\mathcal{S} \colon Q^{7 \times 7 \times |\mathcal{L}|} \to Q^{|\mathcal{L}| \times 7}$ is defined as

$$(\mathcal{S}N)_{i,.} := \mathcal{S}_l N_{.,.,i}. \tag{6.24}$$

6.7 Boundary Conditions of Synthesis Model for Gluing

The wall of the resinating mixer constitutes the system boundary. A mixing arm is a moving obstacle within the resinating mixer.

6.7.1 Boundary Conditions for Adhesive Droplets

The collision of an adhesive droplet and the wall of the resinating mixer is modelled as an inelastic collision, i.e. the adhesive droplet adheres to the wall. If there is already an adhesive droplet present, a collision of adhesive droplets takes place and the masses are added up. The corresponding lattice vector of the adhesive droplet after collision with the boundary is c_0, i.e. it is stationary after collision. In Figure 6.13 the collision of an adhesive droplet and the wall of the resinating mixer is depicted schematically.
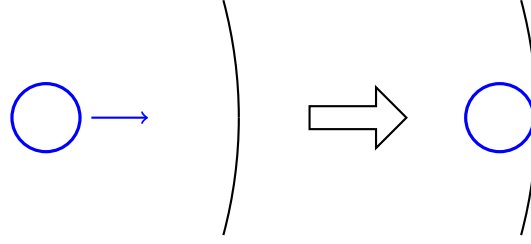
Figure 6.13: Schematic depiction of the boundary condition for a collision of an adhesive droplet and the wall of the resinating mixer

6.7.2 Boundary Conditions for Wood Particles

The collision of a wood particle and the wall of the resinating mixer is a non-deterministic boundary condition. The random boundary condition of Section 4.2.3 is used. Thus, the corresponding lattice vector after collision is determined randomly according to the available cells. If the wood particle is colliding with other wood particles the lattice vectors corresponding to the boundary are not considered as possible lattice vectors for the wood particle.

If there is already an adhesive droplet located at the position of the resinating mixer, the collision operator $\mathcal{C}_{adwp}$ is applied, i.e. no adhesive is left at the boundary.

In Figure 6.14 the collision with the wall is shown schematically.
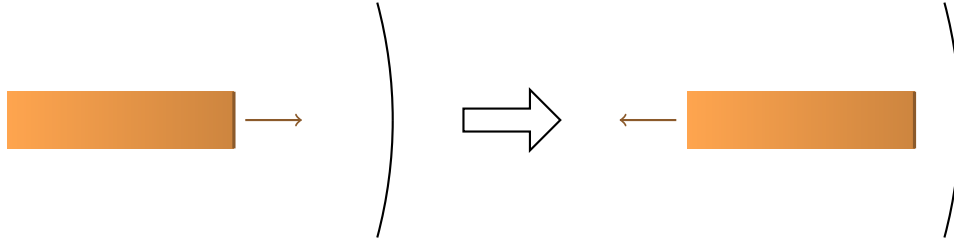
Figure 6.14: Schematic depiction of the boundary condition for a collision of a wood particle with the wall of the resinating mixer

6.7.3 Gravitational Effects

In order to model the effect of gravity an additional boundary condition is applied. Therefore, a wood particle is forced to move downwards if it reaches a specified height. In a certain area below this maximal height the wood particles change direction according to a given probability (falling area). This falling area is defined by a minimal height and the already mentioned maximal height. The probability for falling below the maximal height has to be rather small as it is applied in each time step. The probability for falling at the maximal height is 1.

If the wood particle reaches the bottom of the resinating mixer, defined by an arc between $5\pi/4$ and $7\pi/4$, the lattice vector is changed to c_0, i.e. it is laying at the bottom and

becomes stationary. This is an exception to the boundary condition for wood particles described above.

6.7.4 Effects caused by Mixing Arm

As a simplification the adhesive droplets are not affected by the mixing arm, but it causes movement of the wood particles. The mixing arm is modelled as a moving area and not as a separate entity. If a wood particle is in the area of the mixing arm it is forced to move with a given probability (probability for stimulation of wood particles) and thus changes the corresponding lattice vector. The resulting lattice vector is depending on the position of the mixing arm.

6.8 Evolution of Synthesis Model for Gluing

Finally, the evolution operator is defined.

Definition 6.25 (Evolution operator). The evolution operator $\mathcal{E} \colon Q^{|\mathcal{L}| \times 7} \to Q^{|\mathcal{L}| \times 7}$ is defined by

$$\mathcal{E} := \mathcal{S} \circ \mathcal{N} \circ \mathcal{R} \circ \mathcal{C}, \tag{6.25}$$

whereby $\mathcal{C}$ is the collision operator, $\mathcal{R}$ is the inclusion operator, $\mathcal{N}$ the neighbouring nodes operator and $\mathcal{S}$ is the streaming operator.

Remark 6.26. In addition to the calculation of the evolution of the states of the cells the movement type of the cells and in particular the tensor A have to be updated too.

In Figure 6.15 the evolution of the synthesis model for the gluing process in two dimensions is illustrated (only a part of the lattice is shown). The adhesive droplets and wood particles are shown in blue and brown, respectively. Before collision there are two adhesive droplets and one wood particle. One adhesive droplet is colliding with the wood particle. Therefore, "after collision" there is only one adhesive droplet. For the remaining adhesive droplet the random walk is carried out. Finally, the streaming takes place.

before collision   after collision

after random walk   after streaming
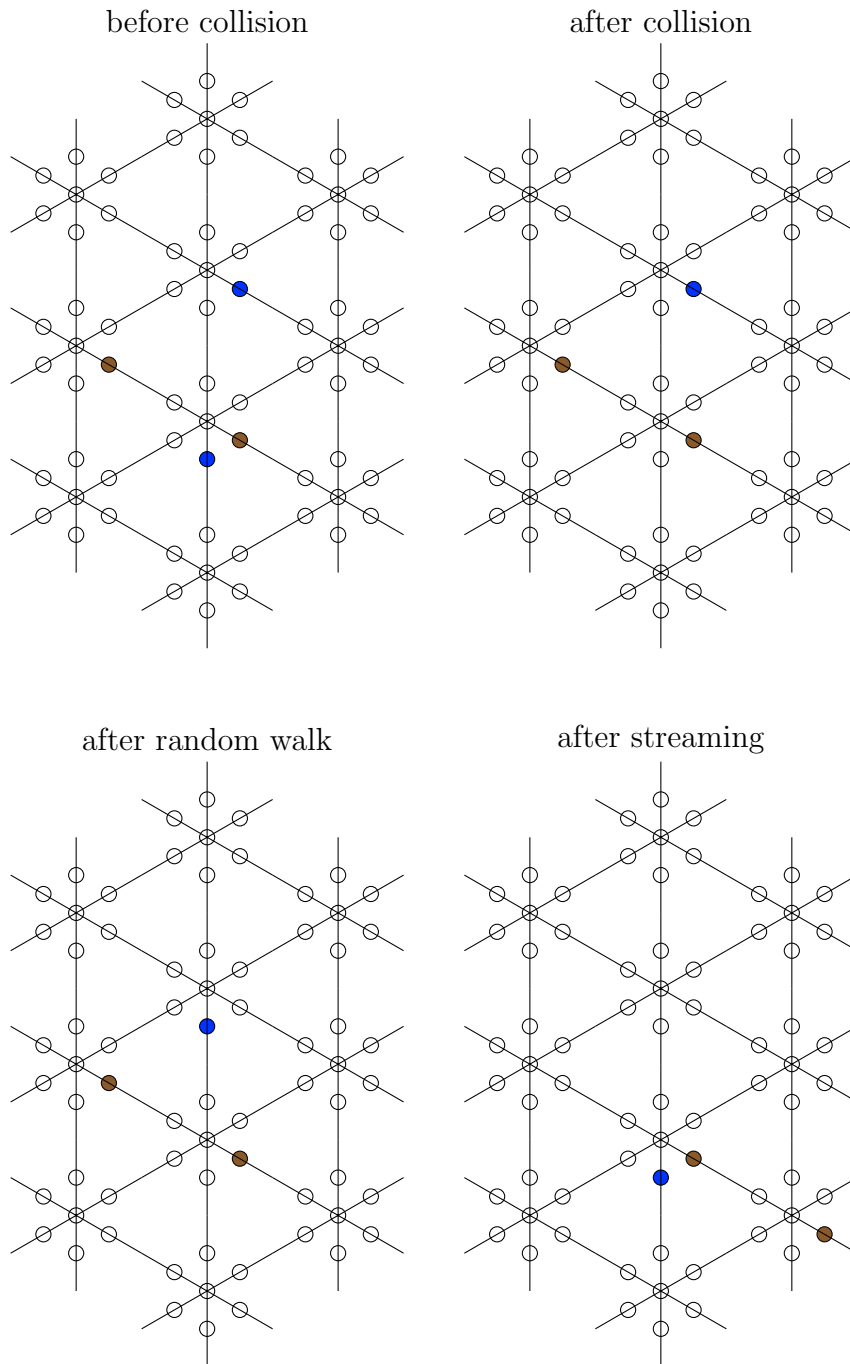
Figure 6.15: Illustration of the evolution of the mathematical model for the gluing process

7

Simulation

The model developed in Chapter 6 was implemented in MATLAB and different scenarios were simulated. The simulations of the different scenarios are necessary for the investigation of the following questions:

- How do the wood particles and adhesive droplets behave during gluing?

- What is the effect of different parameters (e.g. particle size, particle shape) on the adhesive distribution on the surface of the wood particles?

- To what extent does the adhesive distribution on wood particles change during gluing?

- How is the adhesive distributed across the surface of the wood particles after gluing?

The model developed in Chapter 6 was implemented in MATLAB R2018b. A laptop with Intel Core i7 processor (4x 2.20 GHz) and 8 GB DDR3 RAM was used.

7.1 Determination of Parameter Values for Simulation Scenarios

The number of wood particles and the number of adhesive droplets were estimated in Chapter 3. The assumed size and density of a "standard" wood particle and a "standard" adhesive droplet are also given there.

Particles moving in an LGCA have the same speed throughout the simulation. Thus, a suitable speed for wood particles and a suitable speed for adhesive droplets had to be defined.

7.1.1 Parameter Value for Speed of Wood Particles

In the following a framework for the calculation of a parameter value for the speed of the wood particles is described. Therefore, the properties of the mixing arm are considered. The used framework does not take into account the mixing arm itself. For the following calculations the mixing arm is considered by the initial speed v_0 and the rotations per second. For the determination of the parameter value for the speed of the wood particles the differential equation for the free fall using properties of the mixing arm is considered. For the following considerations the wood particle is assumed to be a point mass. The differential equation for the free fall is given by

$$\ddot{x} = -g, \tag{7.1}$$

where $g = 981$ [cm/s^2] is the acceleration of gravity.
The initial speed v_0 [cm/s] is the speed of the mixing arm at radius 10 cm (about the height of the bulk material lying in the mixer). Assuming a speed of rotation of the mixing arm of 1 rotation per second, as it is the case for the considered resinating mixer, v_0 is given by

$$v_0 = 2 \cdot 10 \cdot \pi \approx 62.8. \tag{7.2}$$

The solution of Equation (7.1) is given by

$$x(t) = x_0 + v_0 t - g\frac{t^2}{2}, \tag{7.3}$$

where x_0 is the start position.
Starting at x_0 the wood particle is shot in vertical direction with initial velocity v_0. Without loss of generality it is assumed that $x_0 = 0$. For calculating the maximum height of the wood particle x_{max} [cm] the corresponding time t_{max} [s] has to be calculated using the derivative of Equation (7.3)

$$v(t) = v_0 - g t \tag{7.4}$$

and the fact that the corresponding velocity is zero, thus

$$t_{max} = \frac{v_0}{g} \approx 0.064. \tag{7.5}$$

x_{max} is calculated as

$$x_{max} = v_0 t_{max} - g\frac{t_{max}^2}{2} = \frac{v_0^2}{2g} \approx 2. \tag{7.6}$$

Thus, the average speed v_{wp} [cm/s] is calculated by

$$v_{wp} = \frac{x_{max}}{t_{max}} \approx 31. \tag{7.7}$$

For the simulation scenarios the speed of the moving wood particles is set to v_{wp}.

7.1.2 Parameter Value for Speed of Adhesive Droplets

For the following considerations the adhesive droplet is assumed to be a point mass. In order to approximate the velocity of an adhesive droplet that is sprayed into the resinating mixer, it is assumed that the droplet can fall freely until it hits the wood particles on the bottom of the mixer. Thus, Equation (7.1) can be used. The diameter of the mixer of 40 cm and an assumed height of the bulk material at the bottom of 10 cm, which is also made plausible by the fact that the mixing arm has a height of close to 10 cm, lead to a height of fall of about 30 cm (x_0). The initial downwards velocity is assumed to be 0. The time t_{30} [s] is the time that an adhesive droplet needs to fall 30 cm with $v_0 = 0$. Solving $x(t_{30}) = 0$ using Equation (7.3) it follows

$$30 - \mathrm{g}\frac{t_{30}^2}{2} = 0 \tag{7.8}$$

and further t_{30} is calculated as

$$t_{30} = \sqrt{\frac{60}{\mathrm{g}}} \approx 0.247. \tag{7.9}$$

Thus, the average speed v_{ad} [cm/s] is calculated by

$$v_{ad} = \frac{30}{t_{30}} \approx 120. \tag{7.10}$$

For the simulation scenarios the speed of the moving adhesive droplets is set to v_{ad}.

7.1.3 Parameter Values for Transfer of Adhesive and Penetration

Due to penetration of adhesive into the wood particle, a certain percentage of the mass of the former adhesive droplet is subtracted from the adhesive mass and added to the mass of the wood particle. Thus, a specific amount of the mass of the former adhesive droplet remains at the surface of the wood particle. This remaining mass is available for further collisions.

For determining parameter values for transfer of adhesive and penetration an experiment in the laboratory was carried out.

Material and Method
The experiment was carried out with veneer strips of spruce ($35 \times 100 \times 1.4$ mm) and an adhesive (UF resin). A droplet of adhesive (about 0.06 g) was put on the veneer strip (Figure 7.1 (a)). After a specific waiting time $(20, 30, 40$ s$)$ a first contact with a second uncoated veneer strip was carried out. The two veneer strips were put together and loaded with a weight of about 153 g (Figure 7.1 (b)). The mass of adhesive transferred from the first veneer to the second veneer was determined by weighing the first veneer. After an additional waiting time of 20 s a second contact was carried out. The procedure was the same as described for the first contact. Figure 7.1 (c) shows the second veneer after the experiment.
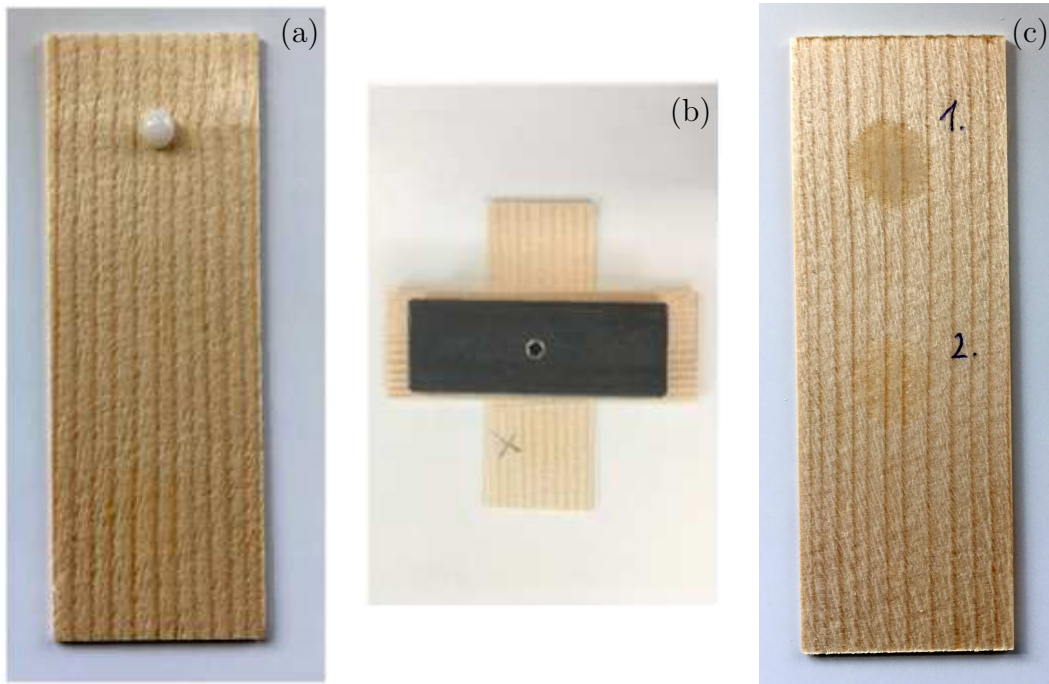
Figure 7.1: Illustration of the experiment for determining the parameter value for transfer of adhesive: (a) application of adhesive droplet at the first veneer strip (b) putting together and loading the two veneer strips (c) adhesive spots of first and second contact at the second veneer strip

After another 20 s the remaining droplet was removed from the first veneer strip and it was weighed. Thus, the penetration was measured at an absolute time of $60, 70, 80$ s, respectively. This result gives the mass of adhesive that penetrated into the veneer strip. For each setting twelve measurements were carried out.

Results

Table 7.1 shows the results of the experiment rounded to whole numbers. For each setting the mean of the twelve values was calculated. The results indicate that the amount of adhesive transferred at the first contact is about 50 %, independent of the time until the first contact. For the second contact about 30 % of the remaining adhesive is transferred. About 20 % of the initial adhesive mass penetrated into the veneer for all settings.

Table 7.1: Experimental results for transfer of adhesive and penetration (rounded to whole numbers)

	transfer at 1$^{\text{st}}$ contact	transfer at 2$^{\text{nd}}$ contact	penetration
1$^{\text{st}}$ contact at 20 s	50 %	31 %	19 %
1$^{\text{st}}$ contact at 30 s	49 %	29 %	23 %
1$^{\text{st}}$ contact at 40 s	53 %	34 %	17 %
mean	51 %	31 %	20 %

The transfer of adhesive including two wood particles at first contact is 50 %, at second contact 30 % and at every following contact no adhesive (0 %) is transferred. For the simulation a more generalised form is necessary because more than two wood particles can be involved in a collision. In this case the corresponding mass of adhesive transferred from one wood particle to the others is divided by the number of the other wood particles. This more generalised form is consistent with the experimental values for two wood particles.

For the simulation scenarios the penetration is set to 20 %.

7.1.4 Parameter Value for Spreading

For determining a parameter value for spreading contact angle measurements were carried out.

Material and Method

The experiment was carried out with veneer strips of birch and an adhesive (UF resin). Metadynea Austria GmbH (Krems, Austria) is kindly acknowledged for providing adhesive and veneer. Using these materials the contact angle and the diameter of the adhesive droplet was measured using the "Drop Shape Analyzer - DSA30" of KRÜSS GmbH.

Results

Table 7.2 shows the results for the contact angle (mean of left and right contact angle) and the diameter of the adhesive droplet. After one second the diameter increased by about 20 %. The results for the contact angle are rounded to one decimal place and the results for the diameter of the adhesive droplet are rounded to two decimal places.

Table 7.2: Experimental results for contact angle and diameter of droplet

time [s]	contact angle [°]	diameter of droplet [mm]
0.02	106.7	2.10
1.02	89.4	2.52
2.02	81.5	2.73
3.02	78.3	2.83
4.02	76.5	2.88
5.02	73.5	2.96
6.02	73.3	2.99
7.02	72.5	3.03
8.02	71.1	3.06
9.00	70.9	3.06
10.00	70.8	3.08
15.00	68.6	3.18
30	64.0	3.33
45	63.3	3.34
60	63.0	3.34

In Figure 7.2 the results for 0.02 s and 60 s are shown.

(a)

(b)
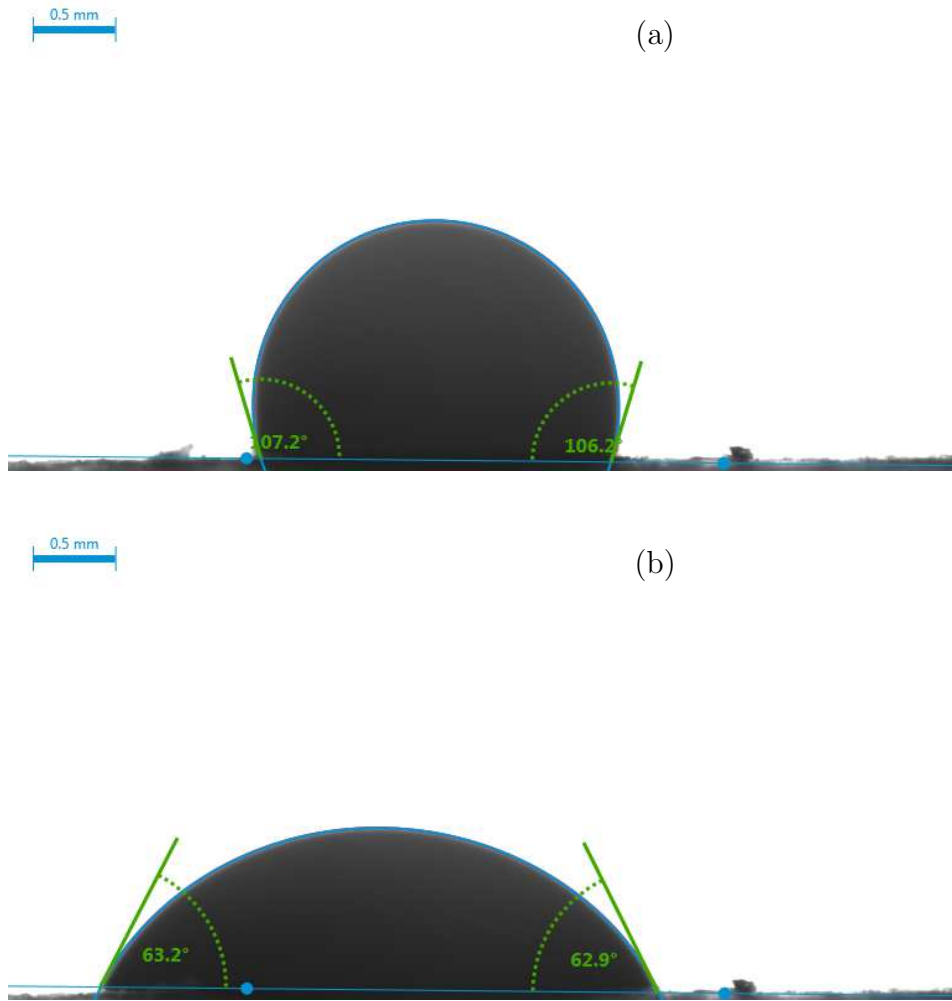
Figure 7.2: Results of contact angle measurement: (a) at 0.02 s (b) at 60 s

For simulation as a value for spreading the relative change of the diameter after one second (a longer time interval is not necessary because typically a collision takes place within one second) is used, i.e.

$$\frac{2.52 - 2.10}{2.10} \cdot 100 = 20\%. \tag{7.11}$$

7.2 Simulation Scenarios

First, general assumptions for all scenarios are presented:

- The cross section of the resinating mixer that is orthogonal to the longitudinal axis was assumed to be a circle (diameter 40 cm, centre of the circle at $(0,0)$). The

shaft was not considered due to simplification.

- Grid width [cm]: 0.1

- The knife head (part of the resinating mixer described in Section 3.3) was not considered for the model as it does not exist in industrial scale.

- For the wood particles certain parameters are the same for all scenarios (except initial position and initial velocity for Scenario 1):

Table 7.3: Properties of wood particles for all scenarios

raw density [g/cm^3]	0.5
initial position	random at bottom
initial velocity	c_0
speed [cm/s]	$v_{wp} = 31$
time step [s]	0.0032
falling area:	
minimum y-coordinate	-10
maximum y-coordinate	1
probability for falling	0.001
probability for falling at maximum y-coordinate	1
total mass of wood [g]	4.2

- For the adhesive droplets certain parameters are the same for all scenarios:

Table 7.4: Properties of adhesive droplets for all scenarios

raw density [g/cm^3]	1.3
initial position (nozzle)	$(0, 20)$ (top node)
initial velocity	random from $\{c_2, c_3, c_4\}$
speed [cm/s]	$v_{ad} = 120$
time step [s]	$8.333 \cdot 10^{-4}$
start time of spraying [s]	15
duration of spraying [s]	90
total mass of adhesive [g]	0.0653

- The parameters for the mixing arm are:

Table 7.5: Properties of mixing arm for all scenarios

arc length [rad]	$\pi/12$
rotations per second [1/s]	1
initial angle [rad]	$\pi/2$
probability for stimulation of wood particles	0.5

- Start time [s]: 0

- End time [s]: 120

- Time step [s]: Minimum of time step of adhesive droplets and time step of wood particles ($8.333 \cdot 10^{-4}$)

- According to the time step, the mixing arm is moving a certain arc length. The corresponding nodes of the lattice which are covered by the mixing arm are determined by the position before movement and the arc length.

- The parameter for spreading is set to 20 %.

- The parameter for penetration is set to 20 %.

- The transfer of adhesive at first contact is 50 %, at second contact 30 % and for every following collision 0 % of the total mass of adhesive is transferred.

Next, the settings for the different scenarios are described.

7.2.1 Scenario 1

Scenario 1 is the most simplified scenario for simulation. In this scenario the mixing arm is not implemented.

- All wood particles have the same properties, see Table 7.6. The dimensions and density of the wood particles were already given in Chapter 3. The thickness is only used for some calculations and not as a parameter due to the fact that two dimensions are considered. The mass is a calculated value using the dimensions and the raw density. In contrast to the general assumptions, the initial position (maximal y-coordinate is 0) and the initial velocity are chosen randomly.

<div align="center">

Table 7.6: Properties of wood particles for Scenario 1

length [cm]	1
width [cm]	0.3
(thickness [cm])	(0.1)
mass per wood particle [g]	0.015
number of wood particles	280
initial position	random
initial velocity	random

</div>

- All adhesive droplets initially have the same properties, see Table 7.7. The dimension and density of the adhesive droplets were already given in Chapter 3. It should be noted that the properties change after collision.

<div align="center">

Table 7.7: Properties of adhesive droplets for Scenario 1

diameter [cm]	0.02
mass [g]	$5.4454 \cdot 10^{-6}$
number of adhesive droplets	$12 \cdot 10^{3}$

</div>

- Without mixing arm

- In contrast to the boundary condition for the wood particles described in Section 6.7, the wood particles are not becoming stationary when they reach the bottom of the resinating mixer. This was changed because there is no mixing arm that is forcing the wood particles to move.

7.2.2 Scenario 2

In Scenario 2 a mixing arm is included.

- Properties of wood particles as in Scenario 1 except initial position and initial velocity are taken from the general assumptions for all scenarios.

- Properties of adhesive droplets as in Scenario 1.

- With mixing arm

7.2.3 Scenario 3

Unless otherwise stated, the parameter values of Scenario 2 are used. In Scenario 3 realistic size distributions for wood particles and adhesive droplets are used.

The properties of the wood particles are changed regarding the geometry. The width of the wood particles is based on a screening curve of spruce wood particles. The distribution of the width of the wood particles is shown in Figure 7.3.
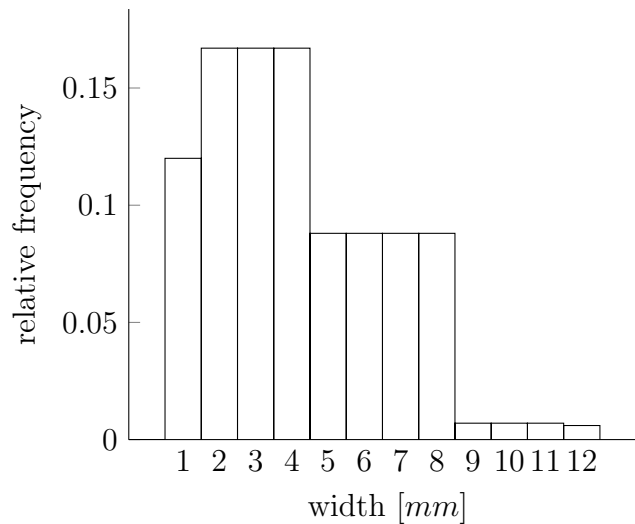
Figure 7.3: Histogram for the distribution of the width of the wood particles

The length/width ratio was determined by measurements with CAMSIZER of Retsch Technology GmbH. For wood particles with width 1 mm the length/width ratio is 3, for

127

wood particles with a width of 2 - 8 mm it is 2.5, and for wood particles with a width of 9 - 12 mm it is 2. The corresponding length of each wood particle was calculated using its width and the experimentally determined length/width ratio. As the total mass of wood particles is the same as in Scenario 2 and the distribution results in more bigger wood particles than in Scenario 2, there are less wood particles in Scenario 3 than in Scenario 2.

The properties of the adhesive droplets are changed regarding the geometry. The diameter of the adhesive droplets is defined to be normally distributed with $\mu = 150$ μm and $\sigma = 30$ μm (Figure 7.4) based on Section 3.3.3. As the total mass of adhesive is the same as in Scenario 2 and the mean diameter of the adhesive droplets is smaller than in Scenario 2, there are more adhesive droplets in Scenario 3 than in Scenario 2.
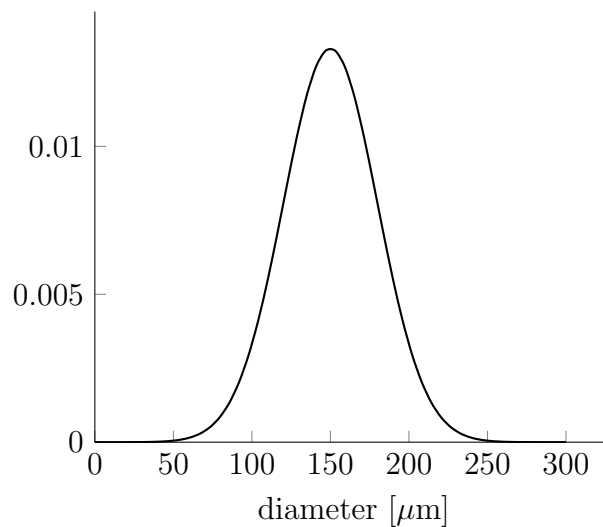
Figure 7.4: Density function for the distribution of the diameter of the adhesive droplets

Additionally, a parameter study was carried out with respect to the total mass of adhesive. Simulation runs with 30 %, 50 %, 70 %, 100 % (Scenario 3), and 130 % of the total mass of adhesive were performed.

7.2.4 Scenario 4

The settings of Scenario 3 are used for Scenario 4. During the collision of wood particles no adhesive is transferred, i.e. the transfer of adhesive is not considered for this Scenario.

7.3 Simulation Results

The quantitative outputs of the simulations are:

- Number of collisions of wood particles in total over time and number of collisions of wood particles with transfer of adhesive over time

- Percentage of wood particles with adhesive (at least one adhesive droplet) over time

- Mean coverage of wood particles over time and coverage of wood particles at specific time steps

- Mean, minimum, and maximum diameter of adhesive areas on the surface of wood particles over time and diameters of adhesive areas on the surface of wood particles at specific time steps

In the following the simulation results for the described scenarios are presented. The wood particles are shown in brown and are represented according to their size. The adhesive droplets are shown in blue. The blue dots only symbolize that at this node an adhesive droplet is located and do not represent the correct size. Nodes of wood particles with adhesive are marked green.

7.3.1 Scenario 1

The initial distribution of the wood particles is shown in Figure 7.5. At the beginning of the simulation the wood particles are randomly distributed within the mixer.

Figure 7.5: Initial position of Scenario 1

About 140 000 collisions of wood particles occur per second whereby about 250 collisions per seconds include a transfer of adhesive. During spraying an average of about 120 collisions of wood particles and adhesive droplets per second take place.

The relative frequency of glued wood particles is 100 % at about 57.8 s. Furthermore, the relative frequency of glued wood nodes after 120 s is about 93.5 %.

The distribution of the coverage of wood particles at the end of the simulation is shown in Figure 7.6. At the end of the simulation the mean coverage is about 20.4 %.
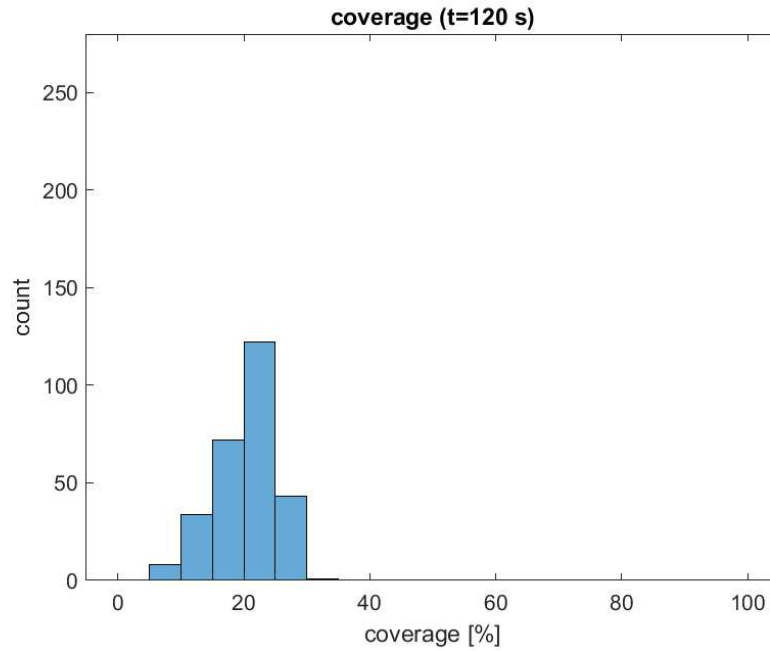
Figure 7.6: Coverage of wood particles at 120 s of Scenario 1

In Figure 7.7 the mean, minimum and maximum diameter of the adhesive areas is shown over time. At the end of the simulation the mean diameter is 227.3 μm, the minimum diameter is 67.0 μm, and the maximum diameter is 578.4 μm.
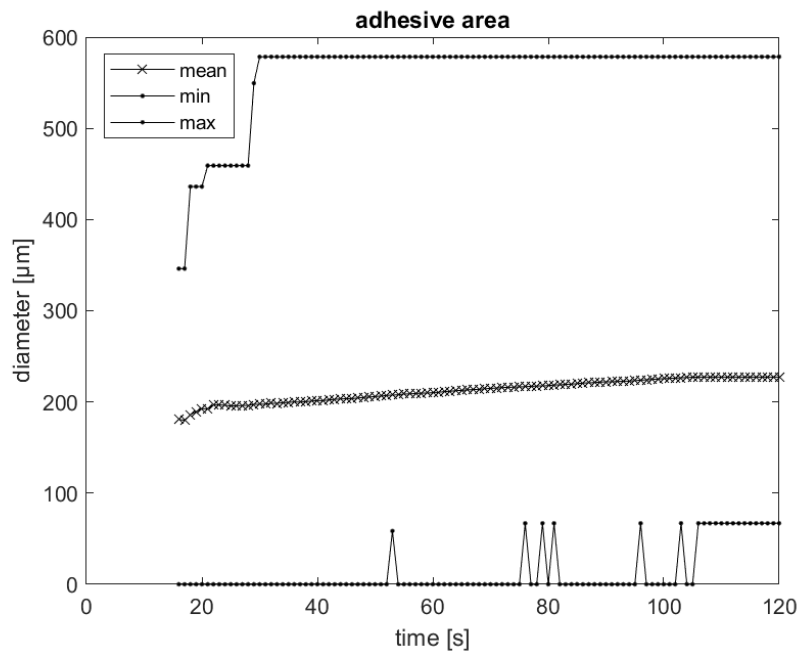
Figure 7.7: Mean, minimum and maximum diameter of adhesive areas on the surface of the wood particles over time of Scenario 1

7.3.2 Scenario 2

The initial distribution of the wood particles is shown in Figure 7.8. At the beginning of the simulation the wood particles are located at the bottom of the mixer and have speed zero.
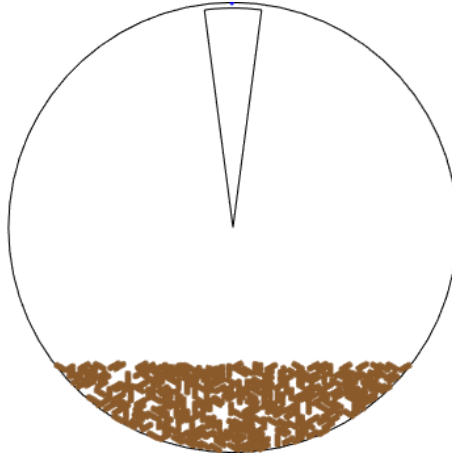
Figure 7.8: Initial position of Scenario 2

In Figure 7.9 the result after 15.5 seconds is shown. Due to the mixing arm, the wood particles are forced to move. The glued wood nodes are shown in green.
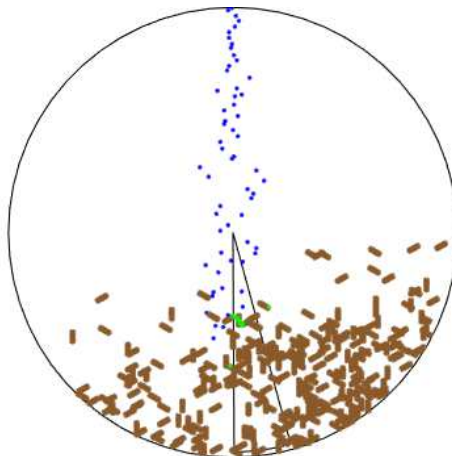
Figure 7.9: Position at 15.5 s of Scenario 2

About 165 000 collisions of wood particles occur per second whereby about 250 collisions per seconds include a transfer of adhesive. During spraying an average of about 120 collisions of wood particles and adhesive droplets per second take place.

The relative frequency of glued wood particles is 100 % at about 61.1 s. Furthermore, the relative frequency of glued wood nodes after 120 s is about 96.6 %.

The distribution of the coverage of wood particles at the end of the simulation is shown

in Figure 7.10. At the end of the simulation the mean coverage is about 21.7 %.
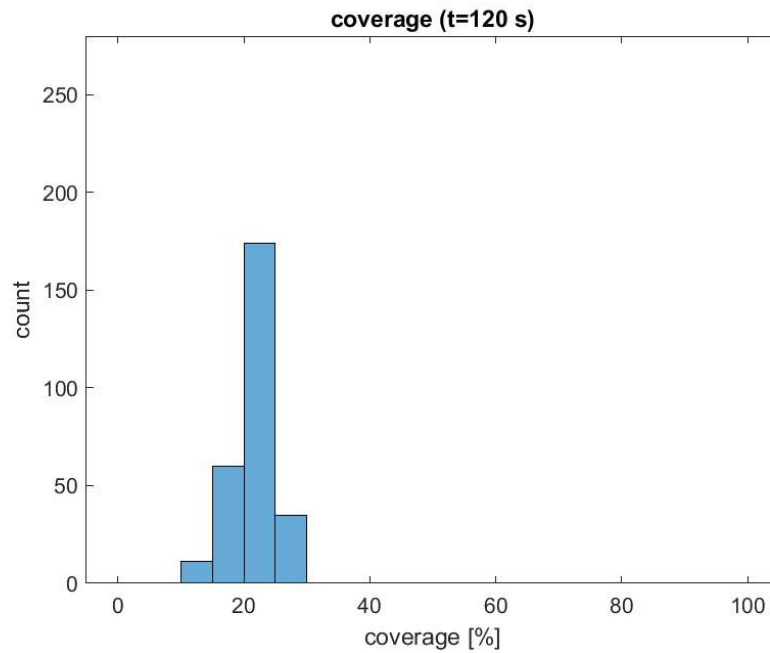
Figure 7.10: Coverage of wood particles at 120 s of Scenario 2

In Figure 7.11 the mean, minimum and maximum diameter of the adhesive areas is shown over time. At the end of the simulation the mean diameter is 232.3 μm, the minimum diameter is 58.5 μm, and the maximum diameter is 480.0 μm.
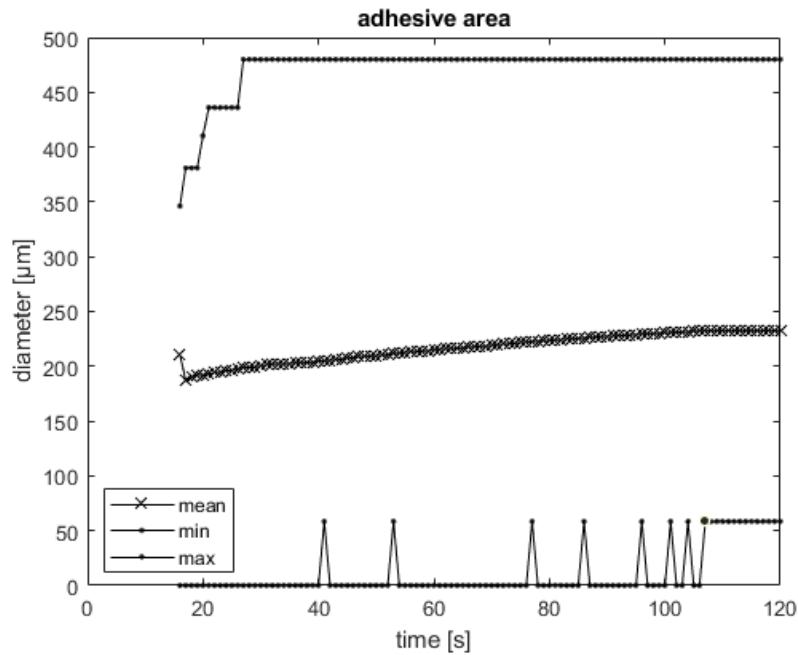
Figure 7.11: Mean, minimum and maximum diameter of adhesive areas on the surface of the wood particles over time of Scenario 2

132

7.3.3 Scenario 3

The initial distribution of the wood particles is shown in Figure 7.12. At the beginning of the simulation the wood particles are located at the bottom of the mixer and have speed zero.
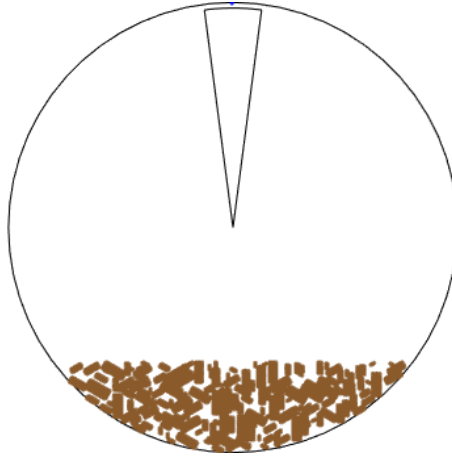
Figure 7.12: Initial position of Scenario 3

In Figure 7.13 the result after 15.5 seconds is shown. Due to the mixing arm, the wood particles are forced to move. The glued wood nodes are shown in green.
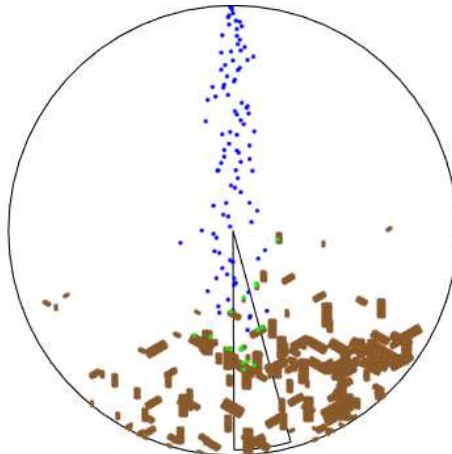
Figure 7.13: Position at 15.5 s of Scenario 3

About 83 500 collisions of wood particles occur per second whereby about 335 collisions per seconds include a transfer of adhesive. During spraying an average of about 195 collisions of wood particles and adhesive droplets per second take place.

The relative frequency of glued wood particles is 100 % at about 51.8 s. Furthermore, the relative frequency of glued wood nodes after 120 s is about 96.4 %.

The distribution of the coverage of wood particles at the end of the simulation is shown

in Figure 7.14. At the end of the simulation the mean coverage is about 25.2 %.
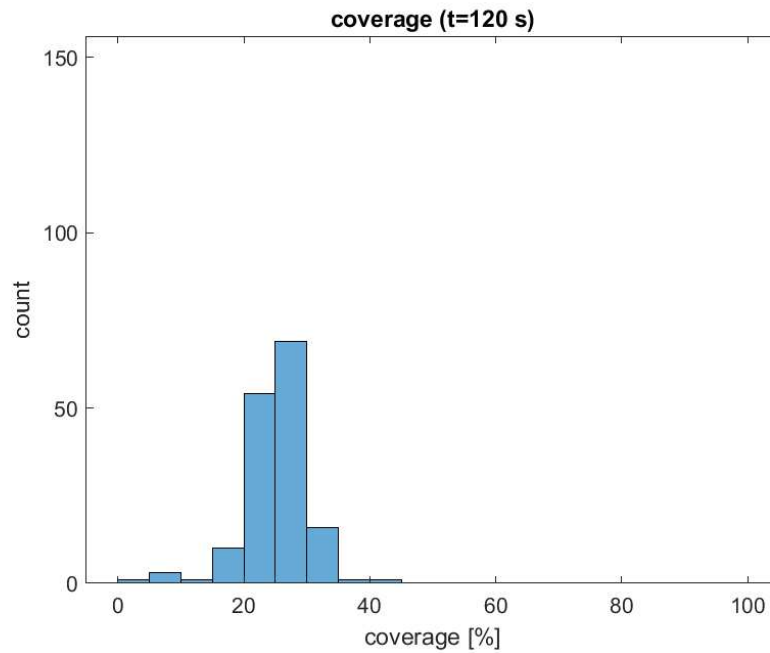
Figure 7.14: Coverage of wood particles at 120 s of Scenario 3

In Figure 7.15 the mean, minimum and maximum diameter of the adhesive areas is shown over time. At the end of the simulation the mean diameter is 242.3 μm, the minimum diameter is 44.1 μm, and the maximum diameter is 651.4 μm.
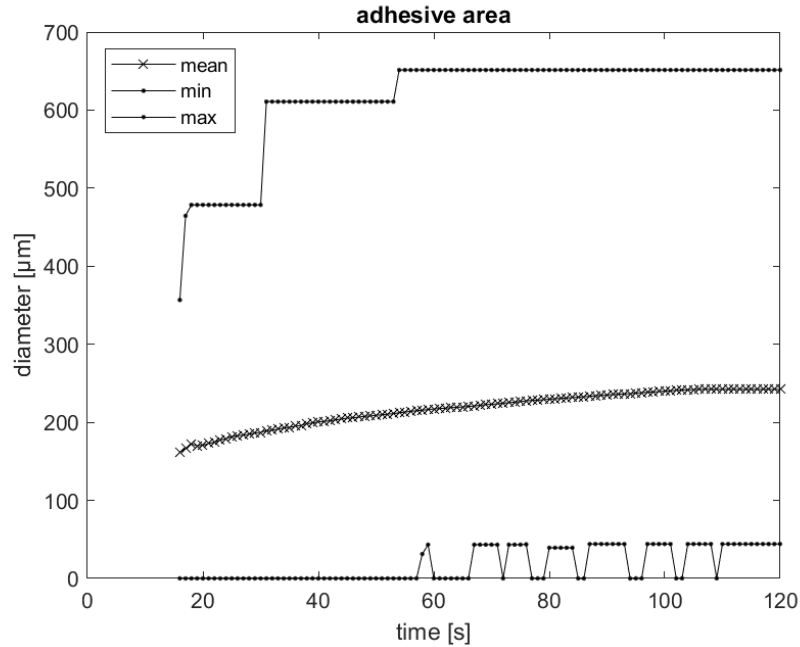
Figure 7.15: Mean, minimum and maximum diameter of adhesive areas on the surface of the wood particles over time of Scenario 3

7.3.4 Scenario 4

For Scenario 4 only results affected by the transfer of adhesive are presented because Scenario 3 and 4 differ only in the transfer of adhesive.

The relative frequency of glued wood particles is 100 % at about 79.0 s. Furthermore, the relative frequency of glued wood nodes after 120 s is about 76.0 %.

The distribution of the coverage of wood particles at the end of the simulation is shown in Figure 7.16. At the end of the simulation the mean coverage is about 30.4 % because the adhesive droplets are steadily becoming bigger as they impinge on top of each other. A reason for the high coverage is that the time-dependent component of the penetration is not considered within the model. Using a time-dependent parameter for penetration the amount of adhesive on the surface of a wood particle would decrease over time and the amount of adhesive penetrated into the wood particle would increase. Therefore, if a new adhesive droplet collides with an already glued wood particle the resulting diameter of the adhesive area on the wood particle would depend on the penetration. Thus, the diameters of the adhesive areas would be smaller than in the presented scenario.
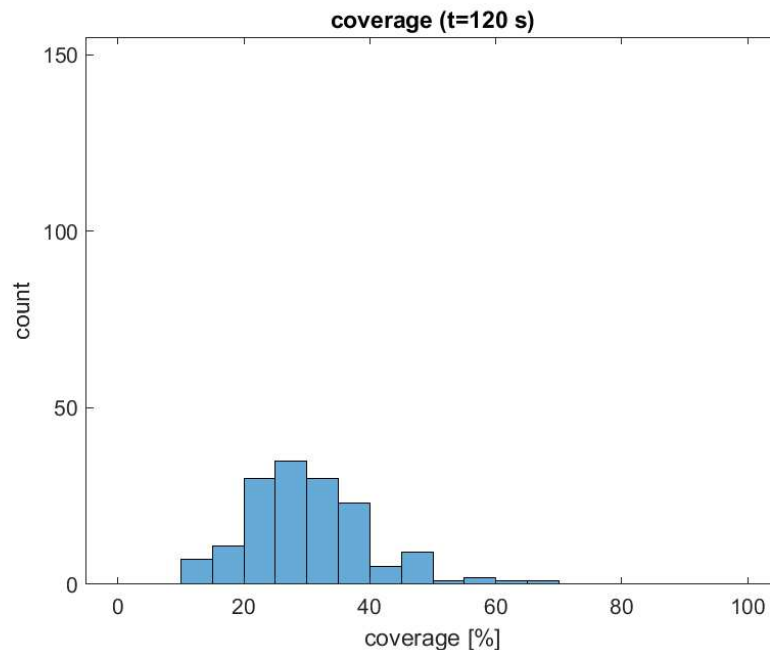
Figure 7.16: Coverage of wood particles at 120 s of Scenario 4

In Figure 7.17 the mean, minimum and maximum diameter of the adhesive areas is shown over time. At the end of the simulation the mean diameter is 342.9 μm, the minimum diameter is 64.5 μm, and the maximum diameter is 734.8 μm. As described before the diameters of the adhesive areas would be smaller using a time-dependent penetration.
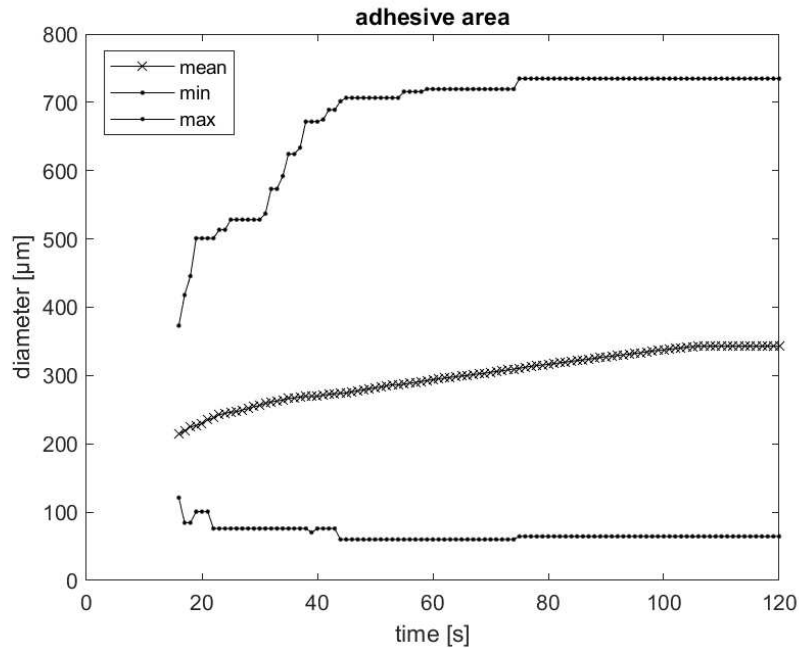
Figure 7.17: Mean, minimum and maximum diameter of adhesive areas on the surface of the wood particles over time of Scenario 4

7.4 Qualitative Validation

The scenarios were selected to investigate the effects of certain parts of the model.

Effect of mixing arm:
Due to the different initial positions of the wood particles in Scenario 1 and Scenario 2, the average number of collisions of wood particles per second is about 15 % lower in Scenario 1. The mean number of collisions of wood particles with transfer of adhesive is the same for the two scenarios. For the other results of Scenario 1 and Scenario 2 the effect of the mixing arm is rather small but the inclusion of the mixing arm is the more realistic scenario.

Effect of realistic size distributions:
Due to the higher number of wood particles in Scenario 2, there are more collisions of wood particles in Scenario 2 than in Scenario 3. On the other hand more collisions of wood particles with transfer of adhesive and collisions of wood particles and adhesive droplets take place in Scenario 3 due to the higher number of adhesive droplets. The mean coverage at the end of the simulation is higher in Scenario 3 probably because of the lower number of wood particles. The realistic size distributions of the wood particles and adhesive droplets cause a more diverse distribution of coverage. The large coverage values may be generated by small wood particles because they have less nodes at the surface while the small coverage values could result from small adhesive droplets. The realistic size of the adhesive droplets leads to a broader range of the diameter of the

adhesive areas.

Effect of transfer of adhesive:
The relative frequency of glued wood nodes at the end of the simulation is 96.4 % for
Scenario 3 and 76.0 % for Scenario 4. Further, the glued wood particles reach 100 %
at 51.8 s for Scenario 3 and at 79.0 s for Scenario 4. This implies that the transfer of
adhesive has a massive effect on the distribution of the adhesive on the surface of the
wood particles. Due to transfer of adhesive, the development in Scenario 3 is much faster
than in Scenario 4.

Effect of total mass of adhesive:
Based on Scenario 3, the total mass of adhesive was varied. The percentages are based
on the value of the total mass of adhesive of Scenario 3. The results in Table 7.8
suggest a linear correlation between the total mass of adhesive and the mean coverage
($R^2 \approx 0.990$).

Table 7.8: Variation of the total mass of adhesive

percentage of total mass of adhesive [%]	mean coverage [%]
30	18.2
50	20.7
70	22.1
100	25.2
130	27.2

Comparison with experimental results:
In Riegler et al. (2012) experiments regarding the detection of adhesive (UF resin) on
the surface of wood particles used for particleboards were carried out. The amount of
applied adhesive was 6 % and 9 % ([g] solid adhesive to [g] absolute dry wood). The
glued wood particles were subsequently stained using a fluorescent dye. Afterwards, the
wood particles were viewed under a microscope and the generated images were used
for calculation of the coverage. For an amount of applied adhesive of 6 % the mean
coverage was about 4.9 % and the standard deviation was about 11.8 %. For an amount
of applied adhesive of 9 % the mean coverage was about 9.6 % and the standard deviation
was about 17.2 %.
The mean coverage of Scenario 3 is about 25.2 % and the corresponding standard devi-
ation is about 5.1 % with an amount of applied adhesive of 8 % used in the underlying
recipe. The simulation leads to a higher mean coverage but the range of the values of
the coverage is nearly within the range of the experimental results.

8

Proof of Concept for 3D

In Chapter 6 the mathematical model for the cross section of the resinating mixer that is orthogonal to the longitudinal axis was developed. The basic idea was to use this model for obtaining a mathematical model for the gluing process in three dimensions. To develop the model in three dimensions, the longitudinal axis is also discretised. At each grid point of the longitudinal axis there is a circle where the two-dimensional model is applied. Depending on the position on the longitudinal axis and the discretisation these two-dimensional models contain:

- a mixing arm or part of a mixing arm

- the nozzle for spraying the adhesive or part of the nozzle

- a border area of the longitudinal axis of the mixer

The wood particles and adhesive droplets can be transported from one layer to another if they are not stationary.

8.1 Mathematical Model in 3D

First, the longitudinal axis (z-axis) of the resinating mixer is discretised. For each grid point of the longitudinal axis a lattice with properties described in Chapter 6 is considered.

For each two-dimensional model the evolution according to Chapter 6 is executed. Afterwards, the shift from one layer to another is performed. In the following, this shift is described:
The wood particles can move from one layer to another one if they are not stationary. In general, there are three possible layers for the shift of the wood particles, i.e. the current layer or one of the neighbouring layers (according to the discretisation of the longitudinal axis). This behaviour is described by using a random variable. At the boundary layers there are two possible layers for the shift due to the system boundary.

The movement of adhesive droplets between layers is similar to the movement between layers of wood particles, i.e. the adhesive droplet stays in the current layer or it moves to one of the neighbouring layers. The adhesive droplets move from one layer to another one according to a random variable. For the adhesive droplets an additional parameter is used. This parameter describes the maximum distance in z-direction from the layer with the nozzle, i.e. this parameter reflects the reach of the spraying in z-direction. Adhesive droplets can move to layers with distance lower or equal to this parameter.

For the proof of concept a three-dimensional model using three layers is used.

8.2 Simulation Results in 3D

The model was implemented in MATLAB R2018b. A laptop with Intel Core i7 processor (4x 2.20 GHz) and 8 GB DDR3 RAM was used. The settings for the simulation are:

- Number of layers: 3

- Parameters of Scenario 3 in Chapter 7

- Location of nozzle: middle layer

- Location of mixing arm: middle layer

- Probability for shift of wood particle per time step: 0.001

- Probability for shift of adhesive droplet per time step: 0.001

The initial distribution of the wood particles in the three layers is shown in Figure 8.1. At the beginning of the simulation the wood particles are located at the bottom and are stationary. Furthermore, the mixing arm and the position of the nozzle in the middle layer can be seen.
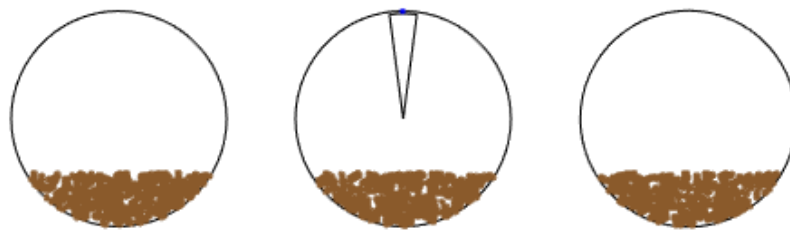
Figure 8.1: Initial position of proof of concept for 3D

Due to the mixing arm, the wood particles are forced to move in the middle layer (Figure 8.2). In the other layers the wood particles are stimulated to move by the shifted wood particles of the middle layer. After 15 seconds the spraying of the adhesive (shown in blue) starts. Glued wood particles are shown in green.
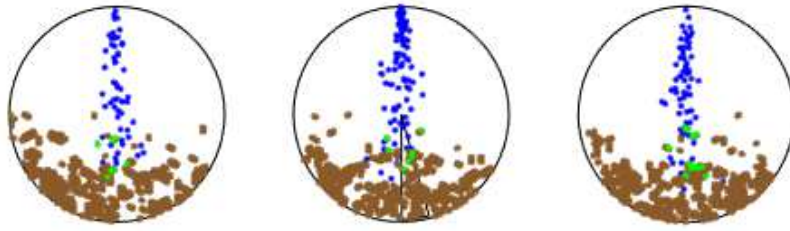
Figure 8.2: Position at 15.5 s of proof of concept for 3D

At the end of the simulation almost all wood nodes are glued (Figure 8.3).
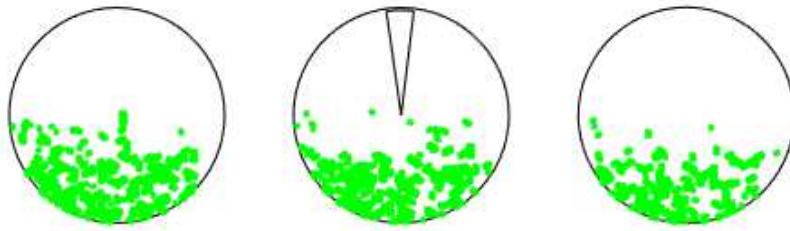
Figure 8.3: Position at 120 s of proof of concept for 3D

Using these settings the following results were obtained. In Figure 8.4 the percentage of wood particles with at least one adhesive droplet over time is shown. After about 50.7 s the relative frequency of glued wood particles is 100 %. Furthermore, the relative frequency of glued wood nodes after 120 s is about 99.6 %. These results are consistent with the results of Scenario 3.
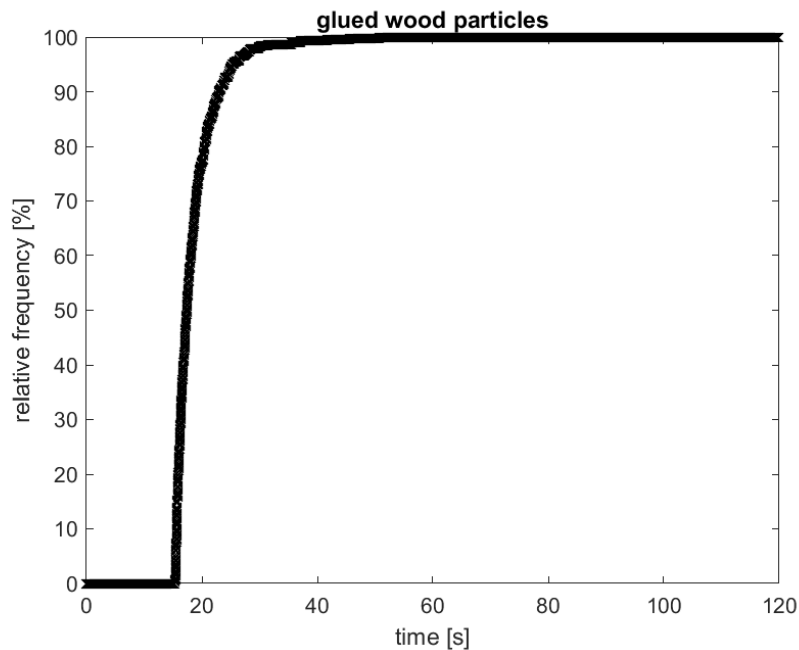
Figure 8.4: Glued wood particles of proof of concept for 3D

The distribution of the coverage of wood particles at the end of the simulation is shown in Figure 8.5. The distribution of the coverage of wood particles is similar compared to the distribution in Scenario 3. The absolute values differ due to the higher number of wood particles in the proof of concept. At the end of the simulation the mean coverage is about 26.2 %.
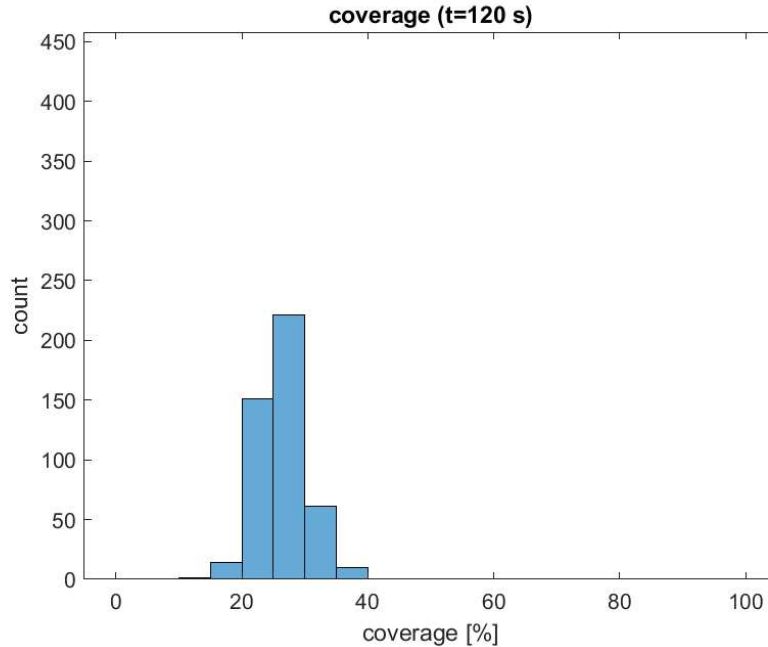
Figure 8.5: Coverage of wood particles of proof of concept for 3D at 120 s

The wood particles in the first and third layer are stationary at the beginning of the simulation. In the middle layer the mixing arm forces the wood particles to move. Due to the shifting of moving wood particles, the wood particles in the first and third layer are stimulated to move by collision. The proof of concept shows that the developed modelling method can be applied to the gluing process in three dimensions.

9

Conclusion and Outlook

Within this thesis a mathematical model for the gluing process was developed. Therefore, first the particleboard production in general and afterwards the gluing process in more detail were described. For simplification the first model was developed in two dimensions. A novel modelling method called "synthesis of lattice gas cellular automaton and random walk" was developed. This new method is based on a LGCA and a random walk. Therefore, first the HPP LGCA and the FHP LGCA were defined formally. Using these formal definitions a random walk on the corresponding lattices of the LGCA was defined and integrated within the setting of the LGCA. This synthesis was developed for the HPP LGCA and the FHP LGCA, respectively. In application of the gluing process, wood particles move according to the streaming of the LGCA and adhesive droplets move according to a random walk included within the LGCA. Based on the two-dimensional model, a proof of concept for three dimensions was developed. The model for two dimensions and the proof of concept for three dimensions were implemented using MATLAB.

Within this thesis several research questions arose. In the following, the answers to these questions are summarized:

- *Which aspects of the process are relevant for modelling?*
  The main objects within the framework of the resinating mixer are the wood particles and the adhesive droplets. The mixing arms affect the movement of the wood particles (without movement of the mixing arms the wood particles are stationary). The movement of the adhesive droplets starts at the nozzle. A central issue is the behaviour of adhesive droplets on the surface of wood particles. On the one hand an adhesive droplet spreads across the surface of a wood particle, while on the other hand a part of it penetrates into the wood particle. Furthermore, adhesive can be transferred from one wood particle to another during collisions between them. A detailed description of gluing and of the emerging processes is presented in Chapter 3. To limit the scope of this thesis no chemical reactions and processes at molecular level were considered.

142

- *Which level of detail is necessary for a model of the process?*
  The choice of the level of detail is a balance between reality itself and the simplification of the actual process. Therefore, it is necessary to determine the fundamental properties of the real process. These properties are described in the answer to the question "Which aspects of the process are relevant for modelling?". As an example the mixing arm is considered. The mixing arm causes the movement of the wood particles. Therefore, it is important for modelling but the movement of the mixing arm itself is not relevant for the evaluation and it is therefore not modelled as a separate entity.

- *Which modelling approaches are suitable for creating a model of the process?*
  A suitable modelling approach needs to have several properties. The relevant aspects of the real process have to be covered by the modelling technique. Furthermore, changes in the level of detail should be covered within the modelling method. Changes of parameters need to be included in the model. An essential task is that the modelling technique has to be able to cover the numbers of wood particles and adhesive droplets. Finally, the model should be able to be transferred from two dimensions to three dimensions. The modelling method developed in Chapter 5 is used for modelling the gluing process. This method is based on LGCA and random walk. These underlying methods are not the only ones that can be used for modelling the gluing process, however were considered to be the most suitable ones. For a detailed presentation of possible modelling methods and their suitability for modelling the gluing process refer to the introduction of Chapter 4.

- *How can different levels of detail be included in the model?*
  For changing the level of detail, the basic structure of the model is not changed, i.e. changing the level of detail does not affect the general properties of the model. For example, a finer discretisation can be included by generating a finer lattice, a further property can be included by adding a column, etc. The selected level of detail has to take into account that the simulation results are realistic while constraints like a limited computation time have to be met. For a more detailed discussion of the question "Can changes of the level of detail be included in the model?" for the possible modelling methods refer to the introduction of Chapter 4.

- *How can the model be parametrised?*
  On the one hand parameters are based on experimental results, on the other hand parameters are estimated, in case experiments cannot be carried out. In order to study the effect of certain parameters, the simulations are carried out for different scenarios regarding the values of the parameters. A detailed overview of the scenarios and corresponding values for the parameters is given in Chapter 7.

- *Which measures regarding data acquisition, data quality, and validation are necessary for applying the model?*
  For validation of the model it is decisive that the raw material is characterised in

detail, i.e. the properties of wood particles and adhesive droplets have to be measured. Additionally, the interactions (penetration, spreading, transfer of adhesive) of wood particles and adhesive droplets need to be empirically determined. Due to lack of available measuring methods, several values of parameters need to be estimated. However, for a proper validation of the model, these values have to be determined as accurate as possible. The mentioned facts are problems regarding data acquisition and data quality. To validate the model all these problems have to be solved, which is beyond the scope of this thesis. After fulfilling these prerequisites, the model can be applied to realistic scenarios and used for predictions.

In general, the developed modelling method is suitable for problems with arbitrary particles moving on a lattice with different moving properties, i.e. moving according to the streaming of the LGCA and according to a random walk. The underlying formal definition is based on the corresponding LGCA and the random walk is included within this framework. The formal definition of this novel method was described in detail in Chapter 5. The definition can be extended according to the considered application.

Simulations of different scenarios were carried out for the investigation of the effects of different parts of the model. The results of the different scenarios were compared and discussed. On the one hand the effects of some changes within the model are reflected within the results (e.g. effect of total mass of adhesive). On the other hand certain changes do not show a high impact on the simulation results (e.g. size distributions). Reasons for this are among other things the underlying assumptions and characteristics of the modelling method.

The developed modelling method for two dimensions can be used for creating a model for three dimensions. This was shown in the proof of concept in Chapter 8. Thus, it can be applied to the gluing process in three dimensions.

Future work should focus on the validation of the presented model for the gluing process. Furthermore, the wood particles could stick together temporarily because of the adhesive. The consideration of this behaviour within the model could lead to more realistic results. The presented three-dimensional model was created by using the two-dimensional model. A further topic for future research should be the development of a three-dimensional model using a three-dimensional lattice and defining the underlying three-dimensional model. Furthermore, a model for the gluing process in industrial scale should be developed and, after validation, used for process control. The runtime of the simulation could be improved significantly by the use of parallelisation. Especially for the simulation of the three-dimensional model the evolution of the different layers could be parallelised.

List of Figures

List of Tables

Nomenclature

BC   boundary condition

CA   cellular automaton/cellular automata depending on the context

CFD   computational fluid dynamics

FHP LGCA   lattice gas cellular automaton named after Frisch, Hasslacher and Pomeau

FHP-I LGCA   version of FHP LGCA defined by the collision rules

FHP-II LGCA   version of FHP LGCA defined by the collision rules

FHP-III LGCA   version of FHP LGCA defined by the collision rules

HPP LGCA   lattice gas cellular automaton named after Hardy, de Pazzis and Pomeau

LGCA lattice gas cellular automaton/lattice gas cellular automata depending on the context

MATLAB   MATrix LABoratory

MDF   medium density fibreboard

MF   melamine formaldehyde

MUF   melamine-urea formaldehyde

PF   phenolformaldehyde

UF   urea formaldehyde

Index

Bibliography

Breitenecker, F., Ecker, H., & Bausch-Gall, I. (1993). Simulieren mit ACSL. *Wiesbaden: Vieweg.*

Cellier, F. E. & Greifeneder, J. (1991). *Continuous System Modeling.* Springer Science & Business Media.

Cellier, F. E. & Kofman, E. (2006). *Continuous System Simulation.* Springer Science & Business Media.

Cundall, P. A. & Strack, O. D. (1979). A discrete numerical model for granular assemblies. *Geotechnique*, 29(1), 47–65.

Dai, C., Yu, C., Groves, K., & Lohrasebi, H. (2007). Theoretical modeling of bonding characteristics and performance of wood composites. part ii. resin distribution. *Wood and Fiber Science*, 39(1), 56–70.

Deppe, H. & Ernst, K. (2000). *Taschenbuch der Spanplattentechnik.* DRW, Leinfelden-Echterdingen, 4th edition.

d'Humieres, D. & Lallemand, P. (1987). Numerical Simulations of Hydrodynamics with Lattice Gas Automata in Two Dimensions. *Complex Systems*, 1, 599–632.

Diem, H., Matthias, G., & Wagner, R. A. (2010). *Amino Resins.* American Cancer Society.

Dix, B. & Marutzky, R. (1997). Nutzung von Holz aus Kurzumtriebsplantagen. *Holz-Zentralblatt*, 123(9), 141–142.

Dunky, M. & Niemz, P. (2002). *Holzwerkstoffe und Leime: Technologie und Einflussfaktoren.* Springer-Verlag.

Dym, C. (2004). *Principles of mathematical modeling.* Elsevier.

Džiugys, A. & Peters, B. (2001). An approach to simulate the motion of spherical and non-spherical fuel particles in combustion chambers. *Granular matter*, 3(4), 231–266.

Fahrni, F. (1957). Die Entwicklung der Holzspanplatte in dokumentarischer Sicht und der verfahrensmäßige Beitrag von Novopan. *Holz als Roh- und Werkstoff*, 15(1), 24–35.

Food and Agriculture Organization of the United Nations (11.04.2018). `http://www.fao.org/faostat/en/#data/FO`.

Frisch, U., d'Humieres, D., Hasslacher, B., Lallemand, P., Pomeau, Y., & Rivet, J.-P. (1986a). *Lattice Gas Hydrodynamics in Two and Three Dimensions*. Technical report, Los Alamos National Lab., NM (USA); Observatoire de Nice, 06 (France); Ecole Normale Superieure, 75-Paris (France).

Frisch, U., Hasslacher, B., & Pomeau, Y. (1986b). Lattice-gas automata for the Navier-Stokes equation. *Physical review letters*, 56(14), 1505.

Habenicht, G. (1986). *Kleben: Grundlagen, Technologie, Anwendungen*. Springer.

Hardy, J. & Pomeau, Y. (1972). Thermodynamics and hydrodynamics for a modeled fluid. *Journal of Mathematical Physics*, 13(7), 1042–1051.

Hardy, J., Pomeau, Y., & De Pazzis, O. (1973). Time evolution of a two-dimensional model system. I. Invariant states and time correlation functions. *Journal of Mathematical Physics*, 14(12), 1746–1759.

Jägersberg, O. (2004). *Max Himmelheber zum 100. Geburtstag*. Hirzel.

KRÜSS GmbH (08.11.2019). Drop Shape Analyzer - DSA30. `https://www.kruss-scientific.com/de/produkte/tropfenkontur/dsa30/drop-shape-analyzer-dsa30`.

Kutrib, M., Vollmar, R., & Worsch, T. (1997). Introduction to the special issue on cellular automata. *Parallel Computing*, 23(11), 1567–1576.

Lawler, G. F. & Limic, V. (2010). *Random Walk: A Modern Introduction*. Cambridge Studies in Advanced Mathematics. Cambridge University Press.

Lehmann, W. (1965). Improved particleboard through better resin efficiency. *Forest Prod. J*, 15(4), 155–161.

Macal, C. M. & North, M. J. (2005). Tutorial on agent-based modeling and simulation. In *Proceedings of the Winter Simulation Conference, 2005.* (pp. 14–pp).: IEEE.

Mahrdt, E., Stöckel, F., van Herwijnen, H. W., Müller, U., Kantner, W., Moser, J., & Gindl-Altmutter, W. (2015). Light microscopic detection of UF adhesive in industrial particle board. *Wood science and technology*, 49(3), 517–526.

Mantanis, G. I., Athanassiadou, E. T., Barbu, M. C., & Wijnendaele, K. (2018). Adhesive systems used in the European particleboard, MDF and OSB industries. *Wood material science & engineering*, 13(2), 104–116.

Marra, A. A. (1992). *Technology of wood bonding: principles in practice.* Van Nostrand Reinhold.

Martin, O., Odlyzko, A. M., & Wolfram, S. (1984). Algebraic properties of cellular automata. *Communications in mathematical physics*, 93(2), 219–258.

MATLAB (2018). *Version 9.5.0 (R2018b).* Natick, Massachusetts: The MathWorks Inc.

Meinecke, E. & Klauditz, W. (1962). *Über die physikalischen und technischen Vorgänge bei der Beleimung und Verleimung von Holzspänen bei der Herstellung von Holzspanplatten.* Westdeutscher Verlag/Köln und Opladen.

Metzger, M. T. (2007). *Naturnahe Bindemittel aus nachwachsenden Rohstoffen auf Proteinbasis zur Herstellung von Holzwerkstoffen.* PhD thesis, Technische Universität München.

Retsch Technology GmbH (11.11.2019). CAMSIZER. `https://www.retsch-technology.de`.

Riegler, M., Gindl-Altmutter, W., Hauptmann, M., & Müller, U. (2012). Detection of uf resin on wood particles and in particleboards: potential of selected methods for practice-oriented offline detection. *European Journal of Wood and Wood Products*, 70(6), 829–837.

Rivet, J.-P. & Boon, J.-P. (2001). Lattice gas hydrodynamics. *Cambridge nonlinear science series*, 11.

Rowell, R. M. (2012). *Handbook of Wood Chemistry and Wood Composites, Second Edition.* Taylor & Francis, Boca Raton, FL: CRC Press.

Schöpper, C. (2006). *Entwicklung eines naturnahen Bindemittels aus nachwachsenden Rohstoffen auf Proteinbasis zur Herstellung von Mitteldichten Faserplatten.* PhD thesis, Niedersächsische Staats- und Universitätsbibliothek Göttingen.

Smith, G. D. (2007). Direct observation of the tumbling of osb strands in an industrial scale coil blender. *Wood and fiber science*, 37(1), 147–159.

Spitzer, F. (1976). *Principles of random walk.* Graduate texts in mathematics. Springer-Verlag.

Sundin, M. (2007). Design of blow line resin injector for MDF production. Master's thesis, Luleå University of Technology.

Thömen, H. (2010). *Vom Holz zum Werkstoff - Grundlegende Untersuchungen zur Herstellung und Struktur von Holzwerkstoffen.* Schweiz.

Thömen, H. & Humphrey, P. E. (2007). Modeling the continuous pressing process for wood-based composites. *Wood and Fiber Science*, 35(3), 456–468.

Thormählen, T. (1977). Der Nutzwert der Nutzwertanalyse. *Wirtschaftsdienst*, 57(12), 638–644.

Türk, O. (2014). Stoffliche Nutzung nachwachsender Rohstoffe. *Grundlagen-Werkstoffe-Anwendungen, Wiesbaden.*

van Herwijnen, H., Fliedner, E., & Heep, W. (2010). Verwendung nachwachsender Rohstoffe in Bindemitteln für Holzwerkstoffe. *Chemie Ingenieur Technik*, 82(8), 1161–1168.

Verein Deutscher Ingenieure (1993). *VDI 2221: Methodik zum Entwickeln und Konstruieren technischer Systeme und Produkte.* Beuth.

Wagenführ, A. & Scholz, F. (2012). *Taschenbuch der Holztechnik.* Carl Hanser Verlag GmbH Co KG.

Winter, B. & Svehla, J. (2013). *Stand der Technik von Anlagen der Span- und Faserplattenindustrie.* Umweltbundesamt GmbH.

Wolf-Gladrow, D. A. (2004). *Lattice-gas cellular automata and lattice Boltzmann models: an introduction.* Springer.

Wolfram, S. (1983). Statistical mechanics of cellular automata. *Reviews of modern physics*, 55(3), 601.

Wolfram, S. (1986). Cellular automaton fluids 1: Basic theory. *Journal of statistical physics*, 45(3-4), 471–526.

Curriculum Vitae

Personal Information

Name:	Carina Rößler
Date of birth:	December 24, 1988
Place of birth:	Vöcklabruck
Nationality:	Austria
Adress:	Kugelgasse 5/3
	3100 St. Pölten

Education

since 01/2015	Technische Universität Wien
	Doctoral programme in Engineering Sciences Technical Mathematics
04/2011-10/2014	Technische Universität Wien
	Master programme Technical Mathematics
10/2007-04/2011	Technische Universität Wien
	Bachelor programme Technical Mathematics
09/1999-06/2007	Bundesgymnasium Vöcklabruck
	Secondary education

Work Experience

since 07/2019	Rail Cargo Austria AG
	Senior Specialist IT Business Analysis
08/2015-06/2019	Kompetenzzentrum Holz GmbH
	Area Wood Material Technologies
	Junior Researcher, PhD Student
03/2015-07/2015	Technische Universität Wien
	Institute of Analysis and Scientific Computing
	Project Assistant
02/2013-02/2015	Technische Universität Wien
	Institute of Analysis and Scientific Computing
	Project Assistant without Graduation

11/2012-05/2013   Austrian Institute of Technology
                   Energy Department
                   Student Apprentice

10/2011-02/2015   Technische Universität Wien
                   Institute of Analysis and Scientific Computing
                   Teaching Assistant